SOLID STATE SPECTROSCOPY

SPIN STATES OF Gd^{3+} IN $CeCl_3$, $PrCl_3$ AND $NdCl_3$

A thesis presented for the degree of
Master of Science in Physics
in the University of Canterbury,
Christchurch, New Zealand.

by

D.L. EVANS

1973

ACKNOWLEDGEMENTS

I wish to thank Professor McLellan for enabling me to carry out the research for this thesis.

Dr G.D. Jones I wish to thank for his supervision and I am also grateful to Dr K. Zdansky for a number of fruitful discussions. The technical assistance of Mr R. Ritchie in growing crystals, Mr D. Greig for his assistance in low temperature cryogenics and Mr F. Downing for preparation of glassware was much appreciated.

The cooperation of the Chemistry Department of the University of Canterbury in providing the use of their EPR spectrometer for the variable temperature work is noted here, thanks being due to Dr R.F.C. Claridge.

INDEX

INDEX TO FIGURES AND TABLES

ABSTRACT

The crystal fields of $CeCl_3$, $PrCl_3$ and $NdCl_3$ are investigated through electron spin resonance measurements on gadolinium ions introduced as impurities into these crystals. The crystal field parameters of the appropriate spin Hamiltonian were derived for all three crystals. Because the crystals all have paramagnetic host cations, the electron spin resonance lines were very broad and overlapped extensively. A study was made of possible mechanisms giving rise to such line widths and it is concluded that a motionally narrowed dipolar broadening mechanism can fairly satisfactorily account for the observed linewidths.

CHAPTER 1

INTRODUCTION

The electron spin resonance spectra of Gd^{3+} ions have been well studied in various crystal lattices by Bleaney[1], Elliott[2,3], Scovil[4], Trenam [5], Hutchinson, Judd & Pope[6], Abragam & Pryce[7], Boatner & Abraham[8], Low and Offenbacher[9], Low[10], Hutchings[11], Birgeneau, Hutchings & Wolf[12] and others.

In this thesis a description is given of the spectra of Gd^{3+} ions in the series $CeCl_3$, $PrCl_3$ and $NdCl_3$. These spectra are closely related to the spectra of Gd^{3+} in $LaCl_3$[6] and $EuCl_3$[12].

Comparison of the e.s.r. spectra for all five members of the series $LaCl_3$-$EuCl_3$ gives the variation in the crystal field at the cation site with the change in the unit cell dimensions along the series. Temperature dependence studies of the e.s.r. spectra give the crystal field changes due to the change in unit cell dimensions with temperature. In both cases, the Gd^{3+} ion serves as a probe for detecting such changes. Distortion of the cell by the Gd^{3+} is assumed negligible.

The resonance lines in the three crystals studied are markedly broader than for the case of $LaCl_3$. This is due to the magnetic interaction between the Gd ion and the paramagnetic neighbouring cations Ce, Pr and Nd. It will be shown that the contribution due to the line width due to static dipole interactions (as found by Al' Tschuler & Kozyrev[13]) is much larger than the observed line widths and it is necessary to include motional narrowing effects to give the

observed line widths. This is presented in Chapter 4.

The Ground State of Gd(IV)

In the usual spectroscopic notation the ground state of Gd^{3+} is $^8S_{7/2}$, a state of zero orbital angular momentum, in fact, an orbital singlet. 'Crystal fields cannot split the S state nor can spin orbit coupling by itself remove the eight-fold degeneracy but group theoretical considerations indicate that these degeneracies are removed in even cubic fields.' (Low[14]). Van Vleck and Penney[15] suggested that higher order perturbations involving simultaneously the crystal field and spin orbit coupling are necessary to split the S state.

Wybourne[16] has examined the splitting of the $^8S_{7/2}$ state in detail. He classifies the states according to their behaviour with respect to charge conjugation invariance and determines that coulombic, orbit-orbit and spin-spin interactions are only non-vanishing for states of the same class. Consequently the energy levels of a multiplet are not split in the Russell Saunders approximation and the first order crystal field matrix elements within the f^7 configuration all vanish. It is concluded that certain mechanisms mix into the ground state some of the character of certain excited states. Wybourne gives the following expressions indicating the admixing for J = 7/2 intermediate coupled states in Gd^{3+}.

$$|^8S_{7/2}\rangle = 0.987|^8S\rangle + 0.162|^6P\rangle - 0.012|^6D\rangle$$

$$|^6P_{7/2}\rangle = 0.85|^6P\rangle - 0.40|^6D\rangle + \text{small admixtures}$$

$$|^6D_{7/2}\rangle = 0.88|^6D\rangle - 0.42|^6P\rangle + \text{small admixtures.}$$

Recently Newman[17] has made a thorough discussion of lanthanide crystal fields. When discussing Wybourne's paper he points out that if any contributions to the crystal field exist which are in fact invariant under charge conjugation, they will be relatively more important for ions with half filled open shells. Two such mechanisms exist in the first, it being recognized that, in the ^6L_J states of Gd^{3+}, the spin unaligned electron has a different radial wavefunction from the spin aligned electron and hence is subject to a different crystal field. The second mechanism arises from the contributions of the correlation crystal field, this depending on two open shell electronic charges and thus symmetric under charge conjugation.

Newman further remarks that with the admixture of ^6D into the ground $^8S_{7/2}$ state being much smaller than the admixture of ^6P it is possible for the charge conjugation invariant field to dominate the b_2^m components of the ground state splitting without being obviously present in the excited states. Also as far as correlation is concerned it follows that the $n = 2$ terms in the spin Hamiltonian $H_{sp} = \sum_{n,m} b_n^m O_n^m$ express spin correlation between pairs of electrons, the $n = 4$ terms express 4-electron spin correlation and the $n = 6$ terms express 6-electron spin correlation. Higher order correlation effects being of lesser importance than 2-electron correlation, it dominates such higher order correlation effects.

Thus in a crystalline environment the ground state of Gd^{3+} is only nominally $^8S_{7/2}$ being, a multiplet, the degeneracy having been lifted by a number of mechanisms, predominantly those being invariant under charge conjugation.

The Hamiltonian

As a first approximation the Hamiltonian of an ion in a crystal can be written as

$$H = \left(\sum_{i=1}^{N} \left(\frac{-\hbar^2}{2m} \nabla_i^2 + U(r_i) \right) \right) + \left(\left(\sum_{i=1}^{N} \frac{-Ze^2}{r_i} - U(r_i) \right) \right) + \sum_{i<j} \frac{e^2}{r_{ij}}$$

$$= H_{\text{central field}} + H_{\text{elec.}}$$

This Hamiltonian is invariant under any simultaneous rotation of all spatial coordinates or any simultaneous rotation of all spin coordinates. Thus its symmetry group is the full rotation group. Eigenfunctions Q_{LS} can be constructed L,S being parameters of the irreducible representations of the full spatial rotation group and spin rotation group. Hund's rule predicts the ground state as ^8S; the first excited level is ^6P, and it is 32,000 cm^{-1} higher in energy.

Spin orbit, spin spin interactions split the ^6P multiplet but not the ^8S multiplet.

The Spin Hamiltonian Approach

As E.S.R. is conducted at temperatures where only the ground state levels are appreciably occupied this theory only concerns itself with the ground state Zeeman splittings.

The spin Hamiltonian method as originally propounded by Pryce[18] and Abragam and Pryce[7] was a perturbation technique utilising the concept of an effective spin S, the ground state being split into 2S+1 components. The spin Hamiltonian is a polynomial in the components of S, I the nuclear spin and H the magnetic field and acts on the states $|Mm\rangle$, the eigenstates of S_Z and I_Z. In order to determine the energy eigenvalues the

matrix having elements $\langle M'm|H_s|M\ m\rangle$ is diagonalised.

The simplest model for the crystal field is the point charge model, where the potentials are those of the neighbouring ions with these treated as point charges.

From Hutchings[11]

$$V(r,\theta,\phi) = \sum_j \frac{q_j}{|(\underline{R}_j - \underline{r})|}$$

and

$$\frac{1}{(\underline{R}-\underline{r})} = \sum_{n=0}^{\infty} \frac{r^n}{R^{n+1}} P_n^{\ 0}(\cos\omega)$$

ω being the angle between $\underline{R}$ and $\underline{r}$

$$V(r,\theta,\phi) = \sum_n \sum_{m=-n}^{n} r^n \gamma'_{nm} Y_n^m(\theta,\phi)$$

where

$$\gamma'_{nm} = \sum_j \frac{4\pi}{(2n+1)} \frac{q_j}{R_j^{(n+1)}} (-1)^m Y_n^{-m}(\theta_j,\phi_j)$$

For f electrons, matrix elements with $n > 6$ are all vanishing, the integrals being zero.

A convenient method of handling potentials (expressed in Cartesian coordinates) is the Stevens Method of "Operator Equivalents". Stevens[11] and Bleaney & Stevens[20]. The products of x,y,z in the Cartesian Hamiltonian $H_i = \sum_i |e|V(x_i,y_i,z_i)$ are replaced by combinations of all possible products of J_x, J_y, J_z, taking into account the commutation relations. For example

$$\sum_i (3z_i^2 - r_i^2) \equiv \alpha_J\langle r^2\rangle[3J_z^2 - J(J+1)] = \alpha_j\langle r^2\rangle O_2^0$$

$$\sum_i (x_i^2 - y_i^2) \equiv \alpha_J\langle r^2\rangle[J_x^2 - J_y^2] = \alpha_J\langle r^2\rangle O_2^2$$

$$\sum_i (x_i^4 - 6x_i^2y_i^2 + y_i^4) = \Sigma\{[(x_i + iy_i)^4 + (x_i - iy_i)^4]/2\}$$

$$\equiv \beta_J\langle r^4\rangle \tfrac{1}{2}[J_+^4 + J_-^4] = \beta_J\langle r^4\rangle O_4^4$$

where $J_{\pm} = J_x \pm iJ_y$.

Therefore the following can be said for an example of the matrix element of $\sum_i (3z_i^2 - r_i^2)$ between coupled states $|LSJJ_z\rangle$

$$\langle LSJJ_z' | \sum_i (3z_i^2 - r_i^2) | LSJJ_z \rangle$$

$$\equiv \alpha_J \langle r^2 \rangle \langle LSJJ_z' | [3J_z^2 - J(J+1)] | LSJJ_z \rangle$$

In Stevens notation then the spin Hamiltonian is written as

$$H_c = \sum_{nm} B_n^m O_n^m$$

The expressions for the O_n^m $n,m \leqslant 6$ are given in Table 1.

Table 1

$$O_2^0 = 3S_z^2 - S(S+1)$$

$$O_4^0 = 35S_z^4 - (30S(S+1)-25)S_z^2 - 6S(S+1) + 3S^2(S+1)^2$$

$$O_4^3 = \tfrac{1}{4}(S_z(S_+^3 + S_-^3) + (S_+^3 + S_-^3)S_z)$$

$$O_4^4 = \tfrac{1}{2}(S_+^4 + S_-^4)$$

$$O_6^0 = 23(S_z^6 - 105(3S(S+1)-7)S_z^4 + (105S^2(S+1)^2 - 525S(S+1) + 294)S_z^2 - 5S^3(S+1)^3 + 40S^2(S+1)^2 - 60S(S+1))$$

$$O_6^3 = \tfrac{1}{4}(11S_z^2 - 3S(S+1)S_z - 59S_z)(S_+^3 + S_-^3) + (S_+^3 + S_-^3)(11S_z^2 - 3S(S+1)S_z - 59S_z)$$

$$O_6^4 = \tfrac{1}{4}(11S_z - S(S+1) - 38)(S_+^4 + S_-^4) + (S_+^4 + S_-^4)(11S_z^2 - S(S+1) - 38)$$

$$O_6^6 = \tfrac{1}{2}(S_+^6 + S_-^6)$$

The B_n^m contain the radial dependence and other factors. The quantities b_n^m are often used where $b_2^m = 3B_2^m$

$$b_4^m = 60B_4^m$$

$$b_0^m = 1260B_6^m$$

The B_n^m (or b_n^m) are parameters measured experimentally.

In the case of C_{3h} symmetry

$$H_c = B_2^0 O_2^0 + B_4^0 O_4^0 + B_6^0 O_6^0 + B_6^6 O_6^6$$

In cubic symmetry

$$H_c = B_4 (O_4^0 + 5O_4^4) + B_6 (O_6^0 - 210 O_6^4)$$

The total spin Hamiltons therefore are

$$\begin{aligned} H_{s\ C_{3h}} = g\beta \underset{\sim}{H}.\underset{\sim}{S} &+ B_2^0 (3S_z^2 - S(S+1)) \\ &+ B_4^0 (35S_z^4 - 30S(S+1) - 25) S_z^2 - 6S(S+1) + 3S^2(S+1)^2 \\ &+ B_6^0 (231 S_z^6 - 105(3S(S+1) - 7) S_z^4 + 105 S^2 (S+1)^2 \\ &\quad - (525 S(S+1) - 294) S_z^2 - 5S^3 (S+1)^3 \\ &\quad + 40 S^2 (S+1)^2 - 60 S(S+1)) \\ &+ B_6^6 (\tfrac{1}{2}(S_+^6 + S_-^6)) \end{aligned}$$

$$\begin{aligned} H_{s\ cub.} = g\beta \underset{\sim}{H}.\underset{\sim}{S} &+ B_4^0 \ (35S_z^4 - (30S(S+1) - 25) S_z^2 - 6S(S+1) + 3S^2(S+1)^2 \\ &\quad + 5(\tfrac{1}{2} S_+^4 + S_-^4)) \\ &+ B_6^0 (231 S_z^6 - 105(3S(S+1) - 7) S_z^4 + 105 S^2 (S+1)^2 \\ &\quad - (525 S(S+1) - 294) S_z^2 - 5S^3 (S+1)^3 \\ &\quad + 40 S^2 (S+1)^2 - 60 S(S+1)) \\ &\quad - \frac{210}{4} ((11 S_z^2 - S(S+1) - 38)(S_+^4 + S_-^4) \\ &\quad + (S_+^4 + S_-^4)(11 S_z^2 - S(S+1) - 38)) \end{aligned}$$

Crystal Structure and Physical Properties

The lanthanide trichlorides $LaCl_3$, $CeCl_3$, $PrCl_3$, $NdCl_3$, $EuCl_3$ and $GdCl_3$ are isomorphic having a hexagonal crystal structure belonging to the Pb 3/M space group. The point symmetry of the lanthanide ion is C_{3h}. The structure below is reproduced from Shinagawa[11].

Figure 1

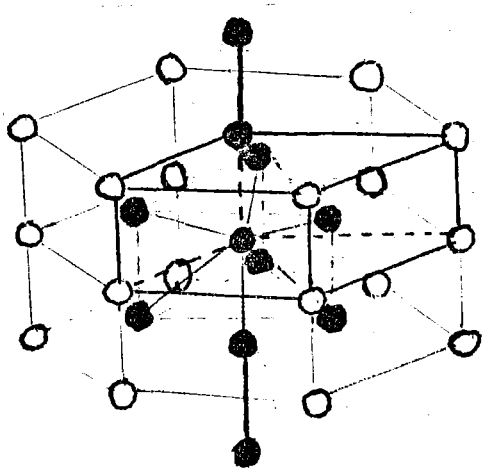

Each rare earth ion has three chlorine atoms above and below it (not shown in the diagram above).

The lattice dimensions and interionic distances are given in Table 2 along with the ionic radii of the rare earth ions. a_0 and c_0 are the unit cell dimensions, nn the nearest neighbour distance.

Table 2

	a_0	c_0	nn	nnn	nnnn	nnnnn	nnnnnn	Ionic radii
$LaCl_3$	7.483	4.364	4.364	4.839	7.483	8.662	8.728	1.061
$CeCl_3$	7.454	4.312	4.312	4.816	7.454	8.611	8.624	1.034
$PrCl_3$	7.423	4.272	4.272	4.788	7.423	8.564	8.544	1.013
$NdCl_3$	7.400	4.240	4.240	4.769	7.400	8.527	8.480	0.995
$EuCl_3$	7.375	4.134	4.134	4.733	7.375	8.455	8.268	0.938

This data was obtained from the Powder Diffraction File[22] and all distances are in Å.

The crystals are very hygroscopic rapidly forming the hexahydrate and must be protected from water vapour in the atmosphere.

They were protected by firstly dipping them in a solution of perspex (solvent chloroform) which dries quickly forming a thin transparent layer, and secondly in molten vaseline. The perspex cannot be rubbed off inadvertently and the vaseline seals any pinholes or cracks which may develop during handling. The expansion coefficients of perspex and the crystals being different, the crystals were recoated with vaseline whenever they had been subjected to any large change of temperature.

The cleavage planes of the crystals are illustrated in figure 2.

Figure 2

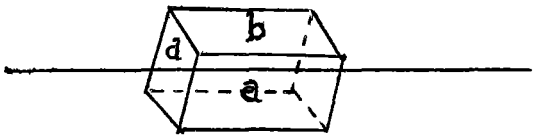

Two of the cleavage planes a and b are parallel to the c axis and the cleavage plane d is at an oblique angle to the c axis.

$LaCl_3$ and $CeCl_3$ are transparent crystals, $PrCl_3$ is green and $NdCl_3$ is purple. Under fluorescent lighting, $NdCl_3$ appears green.

Electronic Configurations of the Lanthanides La, Ce, Pr, Nd, Eu, Gd

The electronic configurations of the lanthanide series have as their base the Xenon structure. The additional configuration of the ions La^{3+}, Ce^{3+}, Pr^{3+}, Nd^{3+}, Eu^{3+}, Eu^{2+}, Gd^{3+} are given in Table 3.

Table 3

Ion	Atomic Number	Configuration	Ground State
La^{3+}	57	$4f^0$	$^1S_0$
Ce^{3+}	58	$4f^1$	$^2F_{5/2}$
Pr^{3+}	59	$4f^2$	$^3H_4$
Nd^{3+}	60	$4f^3$	$^4I_{9/2}$
Eu^{3+}	63	$4f^6$	$^7F_0$
Eu^{2+}	63	$4f^7$	$^8S_{7/2}$
Gd^{3+}	64	$4f^7$	$^8S_{7/2}$

Each of the ions has a partially filled 4f subshell which is partly shielded from external influences in particular neighbouring ions. Freeman and Watson[23] in 1962 calculated the radial parts of $\psi^*\psi$ for the orbitals. Figure 3 shows the peak of the 4f orbital lying well within the 5s, 5p and 6s orbitals.

Figure 3

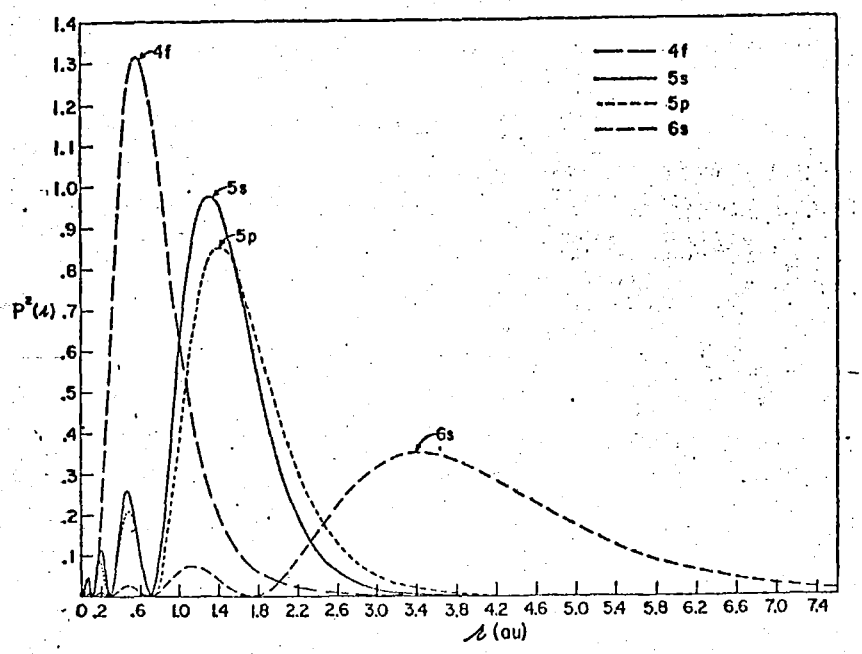

C H A P T E R 2

THEORY OF PARAMAGNETISM AND LINESHAPES

The Electron Spin Resonance Phenomenon

This is described quantum mechanically. A free ion with a 2J+1 fold degenerate (J being the total angular momentum operator) ground state has its degeneracy lifted by a magnetic field. Spin transitions occur between the 2J+1 levels. The spin quantum numbers m_J have the values J,J-1,...,-J and $\Delta m_J = 1$ is the selection rule for allowed transitions when the magnetic field is perpendicular to the microwave field.

The Zeeman Hamiltonian $H_{Zee} = g\beta \underset{\sim}{H}.\underset{\sim}{J}$ and the states are represented by the ket $|J\ M_J\rangle$. For $\underset{\sim}{H}$ parallel to z

$$H_{Zeeman}|J\ m_j\rangle = g\beta J_z.\underset{\sim}{H}|J\ m_j\rangle = m_j\ g\beta\underset{\sim}{H}|J\ m_j\rangle$$

i.e. $Em_j = m_j\ g\beta\underset{\sim}{H}$

Figure 4

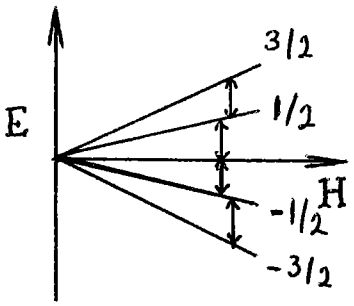

$$\Delta M_J = 1$$

$$\therefore\ \Delta E = \hbar\nu = g\beta\underset{\sim}{H}$$

The energy absorbed is transferred to the lattice and the rate at which this occurs is characterised by the spin lattice relaxation time. Resonance is observed if this relaxation is sufficiently rapid for net absorption to occur.

Line Shapes

The direct measurement of the power absorbed by a sample from the microwaves used in e.s.r. is impracticable. However, changes in the complex magnetic susceptibility of the sample alter the characteristics of the microwave cavity and the power reflected from the cavity is monitored. The method used involves the addition of a weak rf field to the steady magnetic field H_0.

$$\underset{\sim}{H} = \underset{\sim}{H}_0 + iH_1 \cos 2\pi\nu t \qquad i = \sqrt{-1}$$

Equations governing the magnetisation of a paramagnetic sample have been given by Bloch as

$$\frac{dM_z}{dt} = \gamma(\underset{\sim}{M}\times\underset{\sim}{H})_z + (M_0 - M_z)/T_1$$

$$\frac{dM_x}{dt} = \gamma(\underset{\sim}{M}\times\underset{\sim}{H})_x - M_x/T_2$$

$$\frac{dM_y}{dt} = \gamma(\underset{\sim}{M}\times\underset{\sim}{H})_y - M_y/T_2$$

where M is the magnetisation of the sample

H is the magnetic field

γ is the magnetogyric ratio

M_0 is the magnetisation at resonance

T_1 is the longitudinal relaxation time

T_2 is the transverse relaxation time

The steady state solution in the weak rf field approximation as used experimentally has been solved by Kittel (p508) [24] to yield values of the real and imaginary components of the magnetic susceptibility (χ' and χ''),

corresponding to dispersion and absorption

$$\chi' = \frac{\chi_0 \omega_0 (\omega_0 - \omega) T_2^2}{1+(\omega_0-\omega)^2 T_2^2}$$

$$\chi'' = \frac{\chi_0 \omega_0 T_2}{1+(\omega_0-\omega)^2 T_2^2}$$

where $\chi_0 = \frac{M_z}{H_0}$ is the static susceptibility.

The modulation of the magnetic field and use of a phase sensitive detector produces an output line shape of approximately the first derivative of the out of phase component of the magnetic susceptibility χ''. The form of χ'' is that of a Lorentzian function. Kittel and Abrahams* showed by an argument involving the moments of lineshapes that samples where the paramagnetic dopant fraction $f>0.1$ produce spectra with approximately Gaussian lineshapes, whereas those in which $f<0.01$ have approximately Lorentzian lineshapes. The Lorentzian line shape is used here, the dopant fraction being $f = 0.001$. The Gaussian line shape was also tested but did not simulate the observed lineshape quite as well as the corresponding Lorentzian line shape. An example of a Gaussian line shape simulation is given on page 50.

Topology of Lorentzian Functions

The Lorentzian function $\frac{1}{1+k^2x^2}$ is illustrated in figure 5 along with its derivative $\frac{-2k^2x}{(1+k^2x^2)^2}$

* C. Kittel and Elihu Abrahams Phys. Rev. 90 238 (1953).

Figure 5

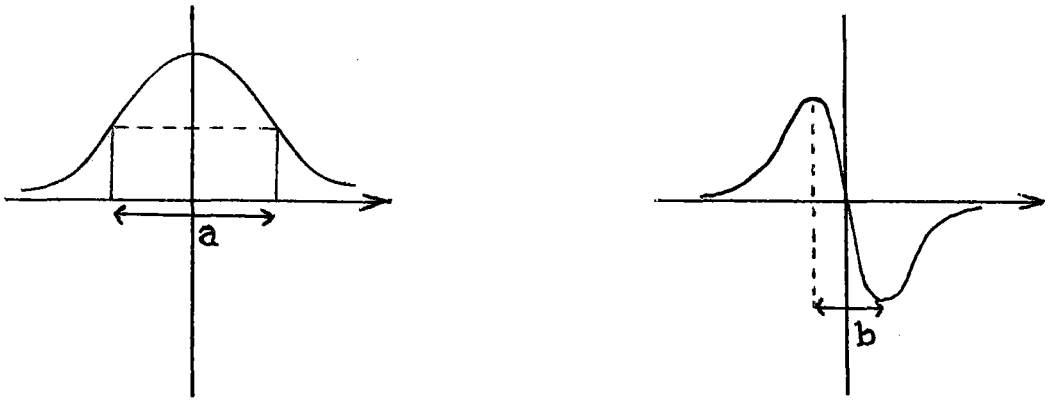

The value of the full width at half height = $\frac{2}{k}$. The full width shall hereafter be referred to as the width.

The value of b, the distance between the positions of maximum slope of $\frac{1}{1+k^2x^2}$, is $\frac{2}{\sqrt{3}k}$.

b is an easy value to measure experimentally while a is useful when a distribution is being used to simulate a spectrum, the width at half height of any symmetrical distribution being easy to determine.

Line Broadening Mechanisms

The line broadening mechanisms commonly encountered in paramagnetic resonance experiments are[13]; 1-dipolar interaction between like spins; 2-spin-lattice relaxation ; 3-interaction of spins with the radiation field; 4-exchange interactions; 5-motion of the unpaired spins in the microwave field; 6-diffusion of spin system excitation through the paramagnetic sample. Of these, the dipolar broadening mechanism is chosen here. The Ce^{3+}, Pr^{3+}, Nd^{3+} are paramagnetic ions whereas La^{3+} is diamagnetic. Because the electron spin resonance spectra linewidths have much broader lines in the case of the paramagnetic host ions, dipolar line broadening is expected to contribute to the linewidths.

The Dipolar Line Broadening Mechanism

The paramagnetism of neighbouring ions can be represented by a set of magnetic dipoles. The magnetic dipole field seen by a particular dipole i due to dipoles j is given by Kittel[14].

$$H_i = \sum_j \frac{3r_{ij}(\mu_j . r_{ij}) - \mu_j r_{ij}^2}{r_{ij}^5}$$

Taking $\underset{\sim}{\mu}_j = g_j \mu_\beta \underset{\sim}{S}_j$ and allowing $S = \pm\frac{1}{2}$, then

$$H_i = g_i \mu_\beta \sum_j \frac{3r_{ij}(\underset{\sim}{S} . \underset{\sim}{r}_{ij}) - \underset{\sim}{S}\, r_{ij}^2}{r_{ij}^5}$$

where $\underset{\sim}{r}_{ij}$ is the vector connecting dipoles i and j.

Static Dipolar Broadening

In the static model the dipoles interact with each other more strongly than with the lattice and the configuration of the dipoles surrounding a dopant ion remains the same while any spin transition is taking place. It is assumed in this model that all configurations of the dipoles are equally possible, the dipoles aligning themselves either parallel or antiparallel with the imposed magnetic field. The contribution that they make to the total magnetic field is taken to be the component of the resultant field H_i parallel to the imposed magnetic field.

Motional Narrowing of a Dipolar Broadened Line

In this model it is assumed that the interaction of a magnetic dipole with phonons in the lattice is much stronger than the interdipole interaction. Then each dipole flips up and down nearly independently of the others. This being the

case, the local field of the dopant ion may change randomly during a transition, and the spin precess an extra phase angle relative to its precession in the applied field[24]. Such motional narrowing will occur if the relaxation time of the paramagnetic host ions is comparable with the duration of the spin transition of the hosted ion.

CHAPTER 3

EXPERIMENTAL DETAILS AND SPECTRA

Crystal Preparation

The Cerium, Praseodymium and Neodymium trichloride crystals containing gadolinium were grown by Mr Ross Ritchie using the following method.

The appropriate rare earth oxide was dissolved in concentrated hydrochloric acid diluted with an equal volume of water. The Gd dopant was added in the form of the chloride at a molar concentration of 0.1%. The solution was then gradually evaporated to near dryness before being transferred to a vacuum oven where all remaining hydrochloric acid and water was removed by pumping over a period of 3-4 days while the temperature was raised above 100°C.

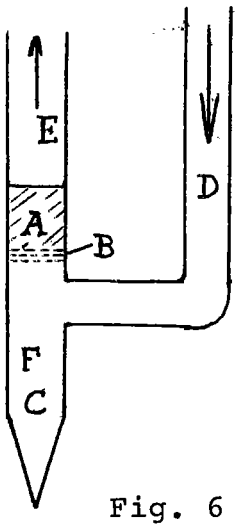

Fig. 6

The powdered chloride after drying was transferred to a quartz tube (A) containing a quartz perforated frit (B) and a side arm. Hydrogen chloride gas dried by sulphuric acid was passed in through the side arm D and through the chloride in A and out through E (see figure 6).

With the gas flowing the apparatus was placed in a cylindrical furnace and the chloride kept molten at ≈ 50°C above its melting point for a period of one hour in order to reduce any oxides present. Following this the gas flow was reversed forcing the chloride through the frit into the end of the tube (C) and the tube was

then sealed off at F. In order to obtain good crystals the capsule containing the chloride was passed through a 100°C temperature gradient centred on the melting point by lowering it through two vertically mounted furnaces 100°C different over a period of two days followed by approximately six hours slow cooling to room temperature. This produced reasonably good crystals which were suitable for cleaving to smaller dimensions.

It was found to be unnecessary to use a dry-box when cleaving the crystals as the hygroscopic character of the crystals did not manifest itself for a few minutes. Once crystals were cleaved they were coated with molten vaseline and if not required immediately stored beneath a depth of 5 cm vaseline. This proved a satisfactory procedure.

Alignment of Crystal by X-Ray Diffraction

When the crystals were cleaved the direction of the crystal axes, in particular the c axis, were in doubt, the crystals not necessarily cleaving perpendicular to axes. The crystals being hygroscopic had to be coated which precluded the use of the usual reflection techniques for orientation and the use of the polarising microscope to search for striations on the crystal surface which would indicate axis direction.

In order to avoid these problems X-ray diffraction was decided on. The system used was a Burger camera on a stereographic precessing mount where both sample and camera precess about the X-ray beam in such a way that a photo of the reciprocal lattice of the crystal is obtained[26]. Polaroid Land film was used and 15 minute exposures taken. A Molybdenum tube was used to produce the X-ray beam.

Figure 7

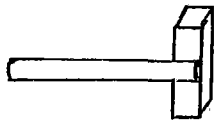

The crystal was mounted on a thin glass rod ~ 0.5 mm in diameter perpendicular to parallel faces of the crystal. This was mounted on a goniometer head on the camera with the beam directed along between the parallel faces, it being suspected that the c axis might lie along there. The crystal was positioned so that it obstructed at least 3/4 of the X-ray beam during all parts of its precessional motion by viewing it through the beam collimator, rotating the camera and adjusting its position with the goniometer.

The direct lattice viewed along the c axis consists of two arrays of parallel lines intersecting at 60° the intersections occurring on the photos as dots.

Initially the crystal will not be aligned, unless fortuitously, along the c axis. With the precession angle of the camera set to 15° a search can be made at 15° intervals around the crystal. Once the characteristic pattern is located finer adjustments can be made. There is a "circle" which appears which is off centre and must be centred on the centre of the photograph. (See fig. 8) The quantities $\alpha-\beta$ and $\gamma-\delta$ will then be 0. The non-zero values of $\alpha-\beta$ and $\gamma-\delta$ are obtained by measurement (mm) and the graph consulted to give the required angular adjustment in the vertical and horizontal planes.

An in the plane of the photo rotation, may also be desired, in order that the crystal planes are placed in a particular orientation. (See Appendix B1).

Figure 8

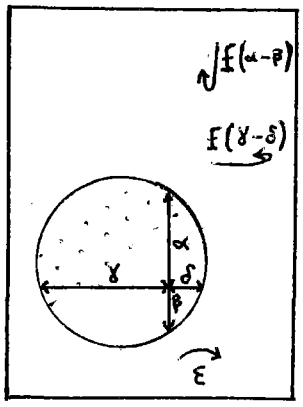

Figure 9

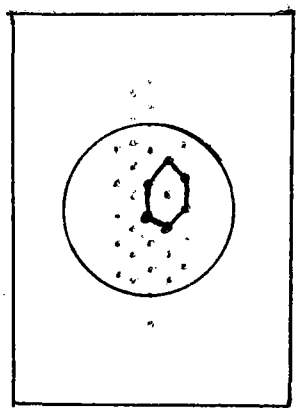

Figure 10

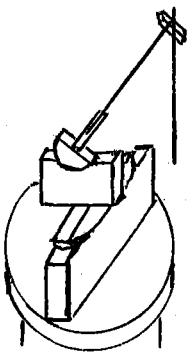

The reciprocal lattice lengths and interplanal angles were calculated using a computer program entitled MOLASZ[27] and the results are listed in Appendix B2. The distance between the points on the photo when looking down the c axis is 6.4 mm.

The c axis having been located, the mounting rod is in the wrong place so remounting is required. The goniometer head is removed from the precession camera and allowed to stand vertically on a bench.

A second glass fibre is glued to the crystal and allowed to hang vertically. When the glue has dried the new mount is placed on the goniometer head and a check exposure taken. If the new mount is satisfactorily placed the first mount can be snapped off ~1 mm from the crystal by holding it with tweezers adjacent to the crystal and carefully snapping the protruding rod.

When a sample is on the precession mounting it is mounted from the side. If the lattice photo is as in fig. 9 it must be remembered that when the sample is mounted for ESR spectroscopy it may be rotated through

Figure 11

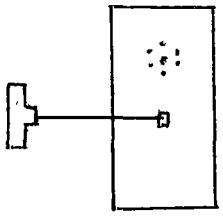

Figure 12

90^{o} and so the orientation of the unit cell relative to the magnetic field will be different, e.g. in the vertical mounting position, (see figure 12).

Two vertical mounting positions are of interest:  and  and crystals of each species were mounted in each of these positions.

Mounting of the Sample

In order to carry out low temperature work it was necessary to use the Chemistry Department's X-band spectrometer which has a cavity of high Q and in order to retain this all samples are mounted in quartz tubes of internal diameter 3 mm. For solutions this is a simple procedure. In order to place the sample in a known position at the bottom of the quartz tube a thin walled tube of external diameter 2.5 mm was used as a slider to carry the sample, the mounting rod being glued to the interior of the wall of the slider.

Figure 13

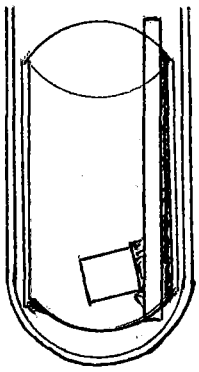

Spectroscopic Studies

For each of the host crystals $CeCl_3$, $PrCl_3$ and $NdCl_3$ the angular dependence of the Gd^{3+} spin resonance transitions was studied. These studies were carried out over a range of temperatures and with the crystals being rotated through the arcs indicated in figure 14.

Figure 14

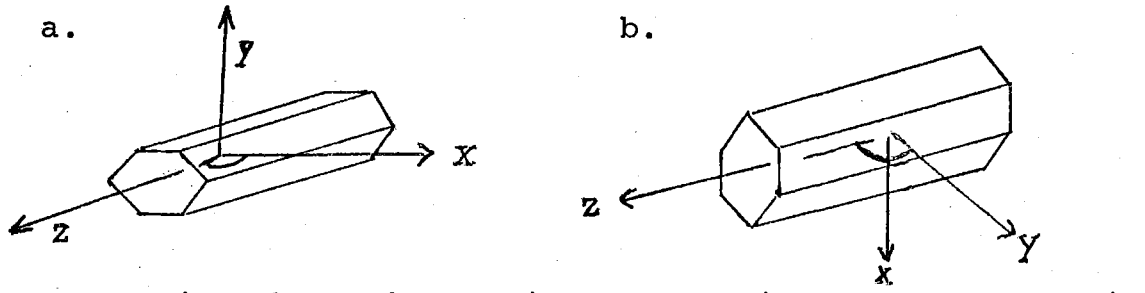

Rotation about the y axis

Rotation about the x axis

c.

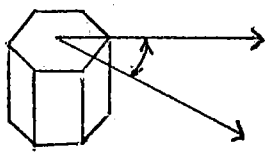

Rotation about the z axis

The X band spectrometer used was a Varian E-12 EPR spectrometer. ν = 9.16 GHz. A rectangular cavity was used and the sample rotated therein. The low temperature studies were carried out using cooled nitrogen gas. The nitrogen gas was dried, then passed through a heat exchange coil immersed in a bath of liquid nitrogen, after which it was heated to the desired temperature (using a Varian variable temperature controller) and passed into the microwave cavity where it cooled the tube containing the sample. The range of temperatures studied was 120°K-290°K, 120°K being the lowest temperature able to be reached.

In addition Gd^{3+} in $PrCl_3$ was studied at ~4°K using a liquid helium dewar and a Q band spectrometer ν = 35.2 GHz. The Q band spectrometer was built at the University of Canterbury with a Newport magnet control system. Its field was measured using a Varian FH-20 gaussmeter and considerable fluctuations occurred over a period of time so that the spectra were distorted. A cylindrical cavity was used and the magnet was rotated.

The Spectra

The spectra included here are listed in table 4. They have been reduced in linear dimensions to 36% of the size of the original recordings. In the analysis of these spectra they are simulated in order to determine the individual line positions and the values of the parameters b_2^0, b_4^0, b_6^0 of the Spin Hamiltonian. The recordings presented at this point indicate the features of the spectra obtained for each host under various conditions.

Table 4

Host	Rotation Axis	Temperature	Range of Magnetic Field Sound
$CeCl_3$	x	120°K	2750-3750 Gauss
$CeCl_3$	y	273°K	2750-3750 Gauss
$CeCl_3$	y	290°K	2750-3750 Gauss
$PrCl_3$	y	130°K	2750-3750 Gauss
$PrCl_3$	x	290°K	2750-3750 Gauss
$NdCl_3$	y	290°K	2250-4250 Gauss
$NdCl_3$	y	150°K	2250-4250 Gauss

$CeCl_3 + Gd^{3+}$

Rotation axis: x

Temperature: 120°K

Magnetic Field: 2750-3750 G

Attenuation: 30 dB

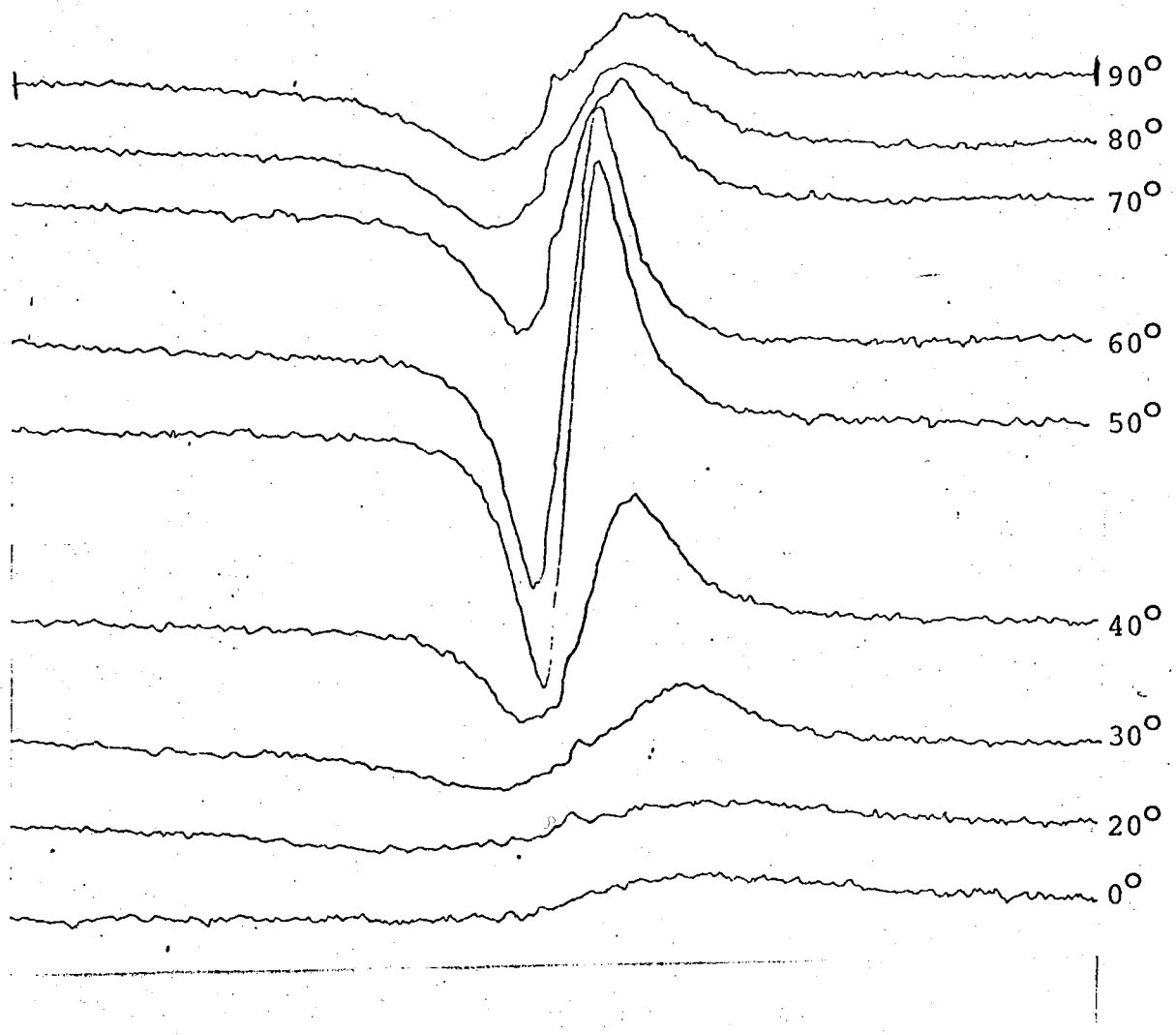

$CeCl_3 + Gd^{3+}$

Rotation axis: y

Temperature: 273°K

Magnetic Field: 2750-3750 G

Attenuation: 30 dB

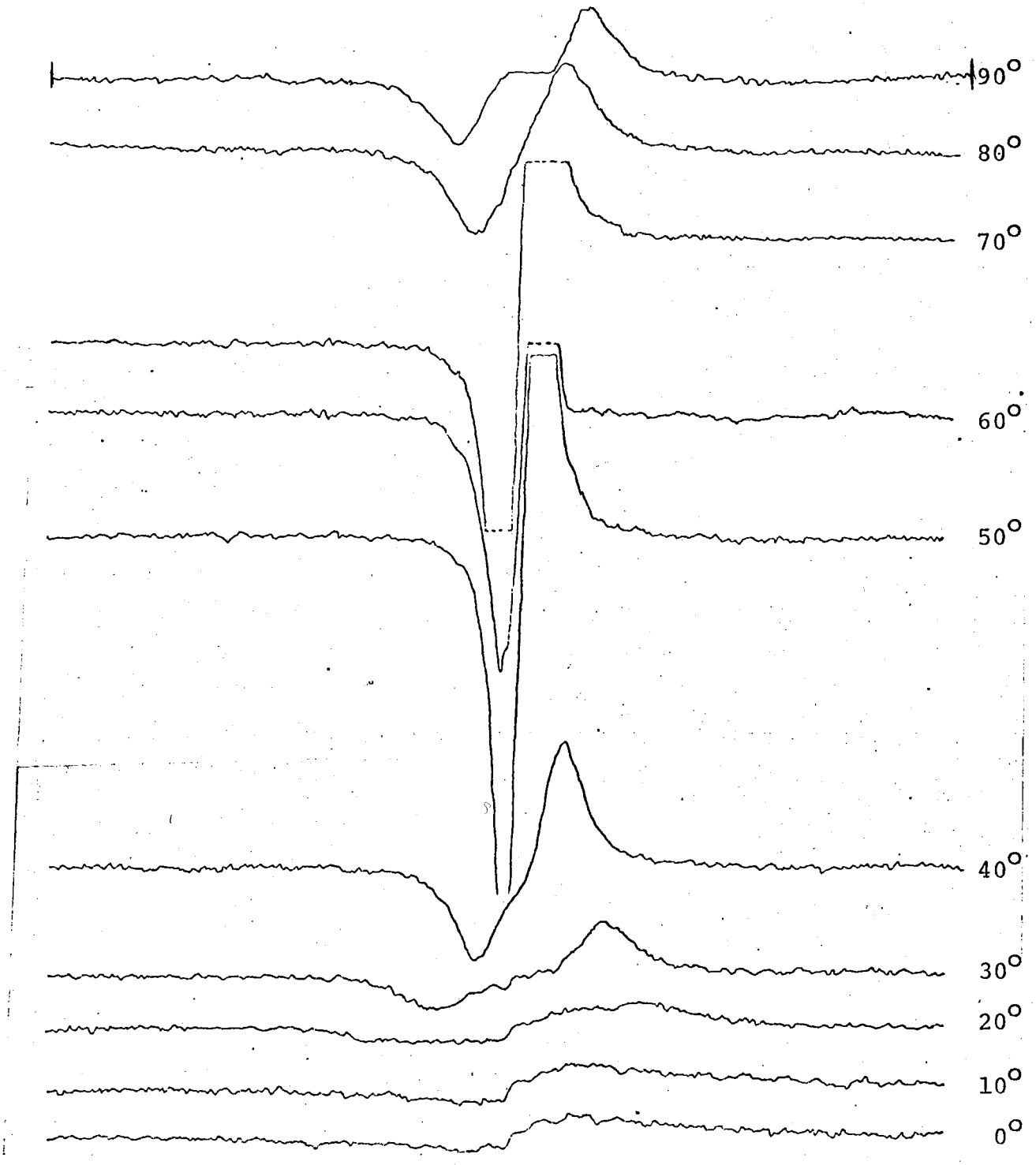

$CeCl_3 + Gd^{3+}$

Rotation axis: y

Temperature: 290°K

Magnetic Field: 2750-3750 G

Attenuation: 10 dB

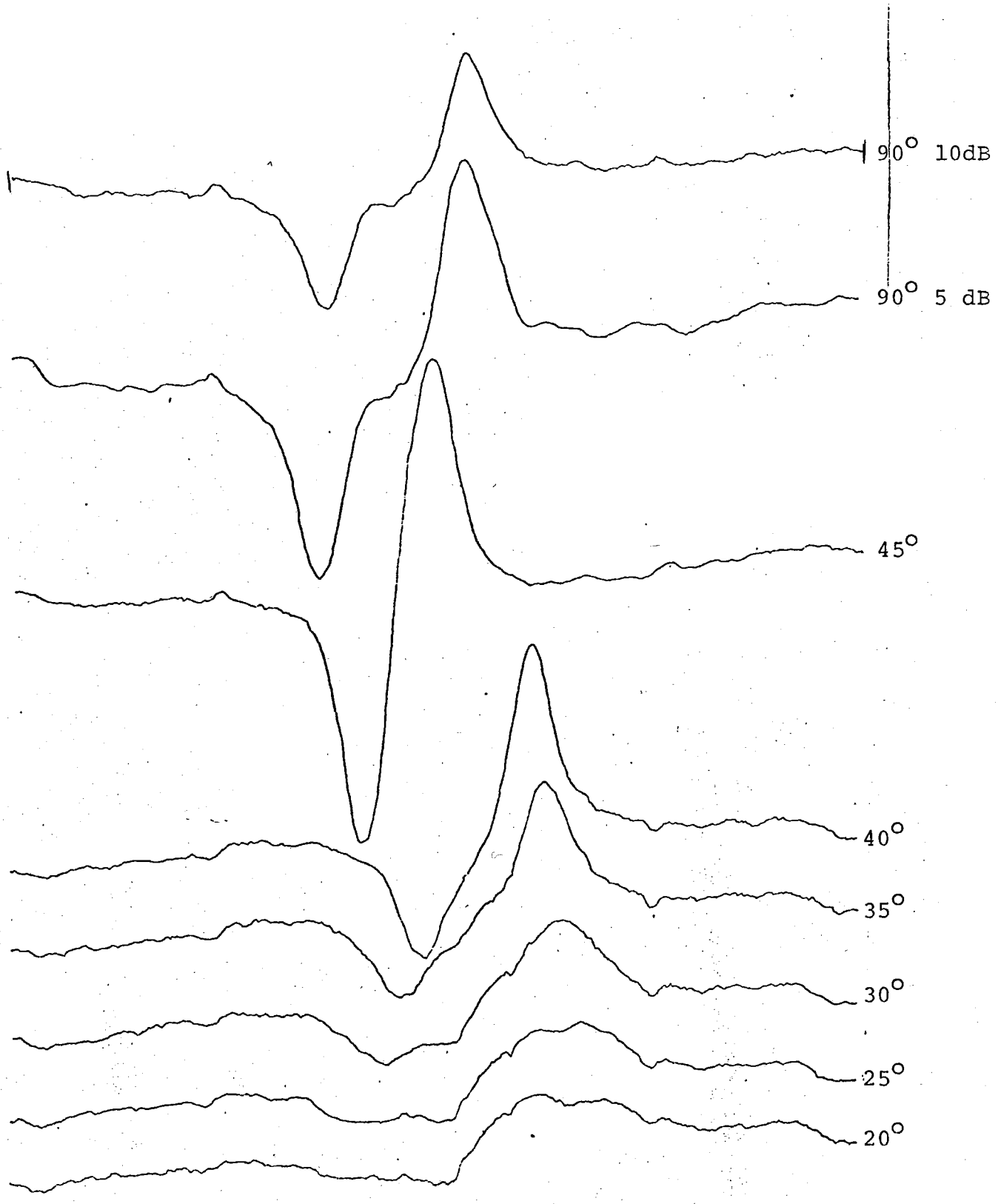

$PrCl_3 + Gd^{3+}$

Rotation axis: y

Temperature: 130°K

Magnetic Field: 2750-3750 G

Attenuation: 30 dB

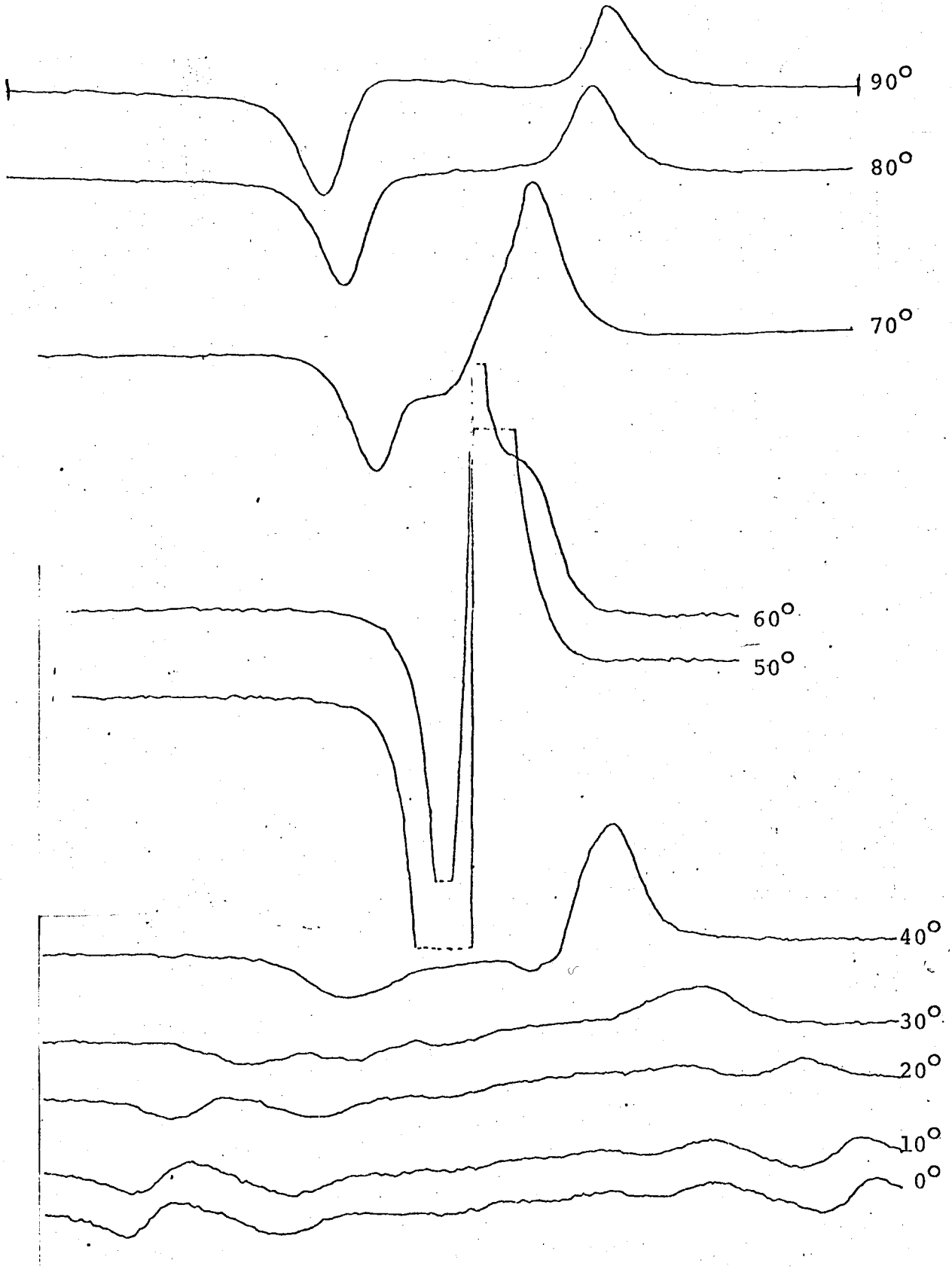

$PrCl_3 + Gd^{3+}$

Rotation Axis: x

Temperature: 290°K

Magnetic Field: 2750-3750 G

Attenuation: 30 dB

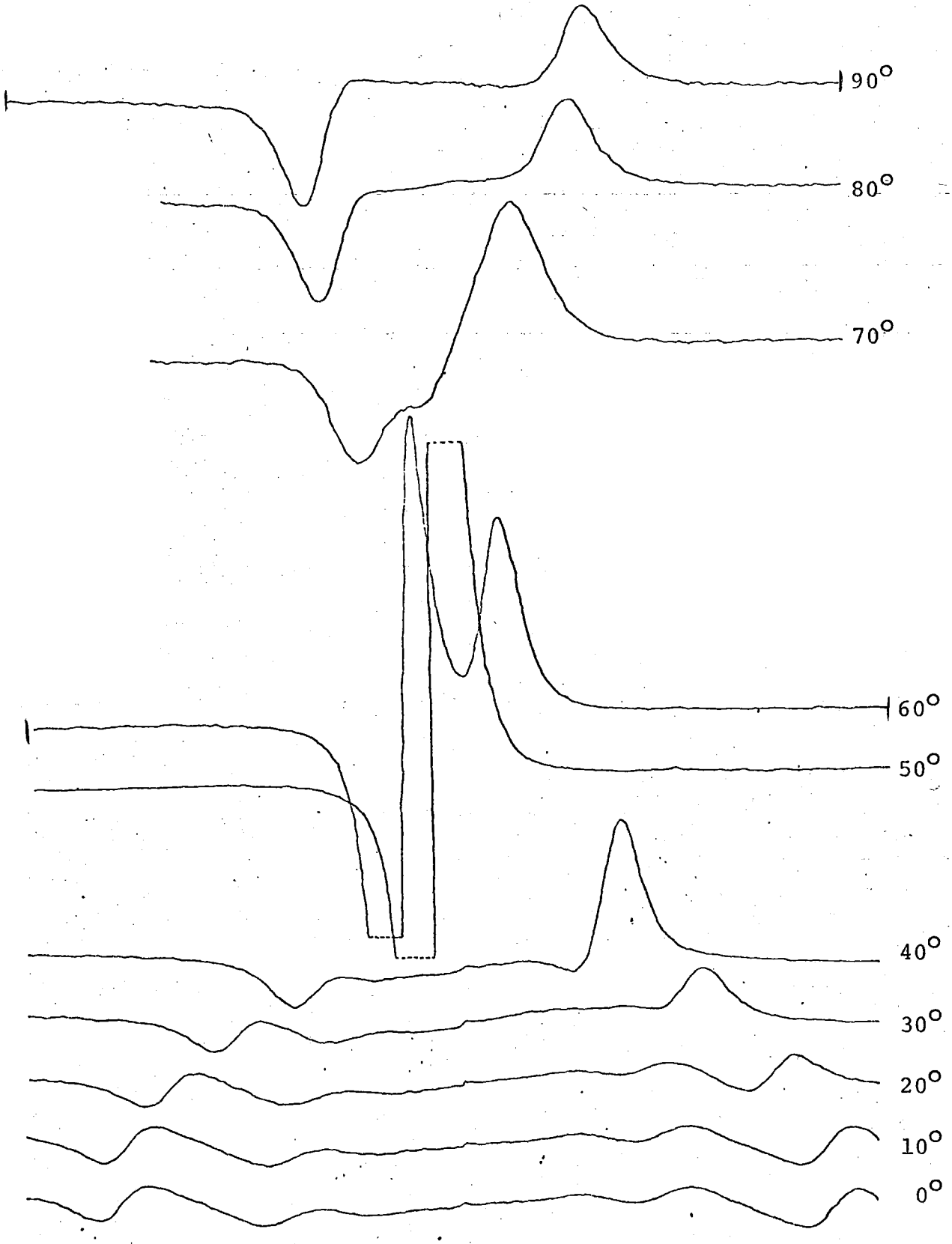

$NdCl_3 + Gd^{3+}$

Rotation axis: y

Temperature: 290°K

Magnetic Field: 2250-4250 G

Attenuation: 20 dB

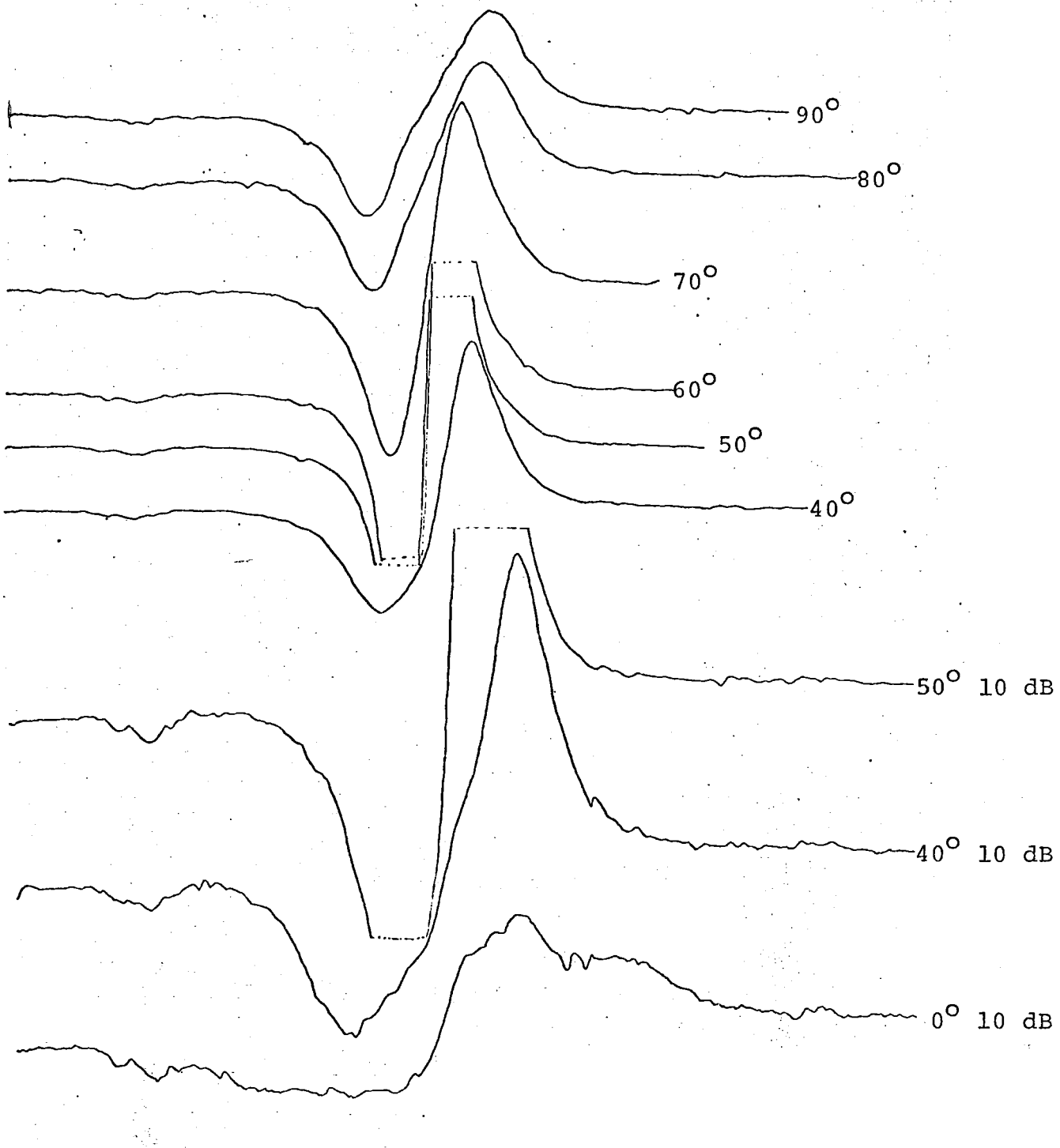

$NdCl_3 + Gd^{3+}$

Rotation Axis: y

Temperature: 150°K

Magnetic Field: 2250-4250 G

Attenuation: 30 dB

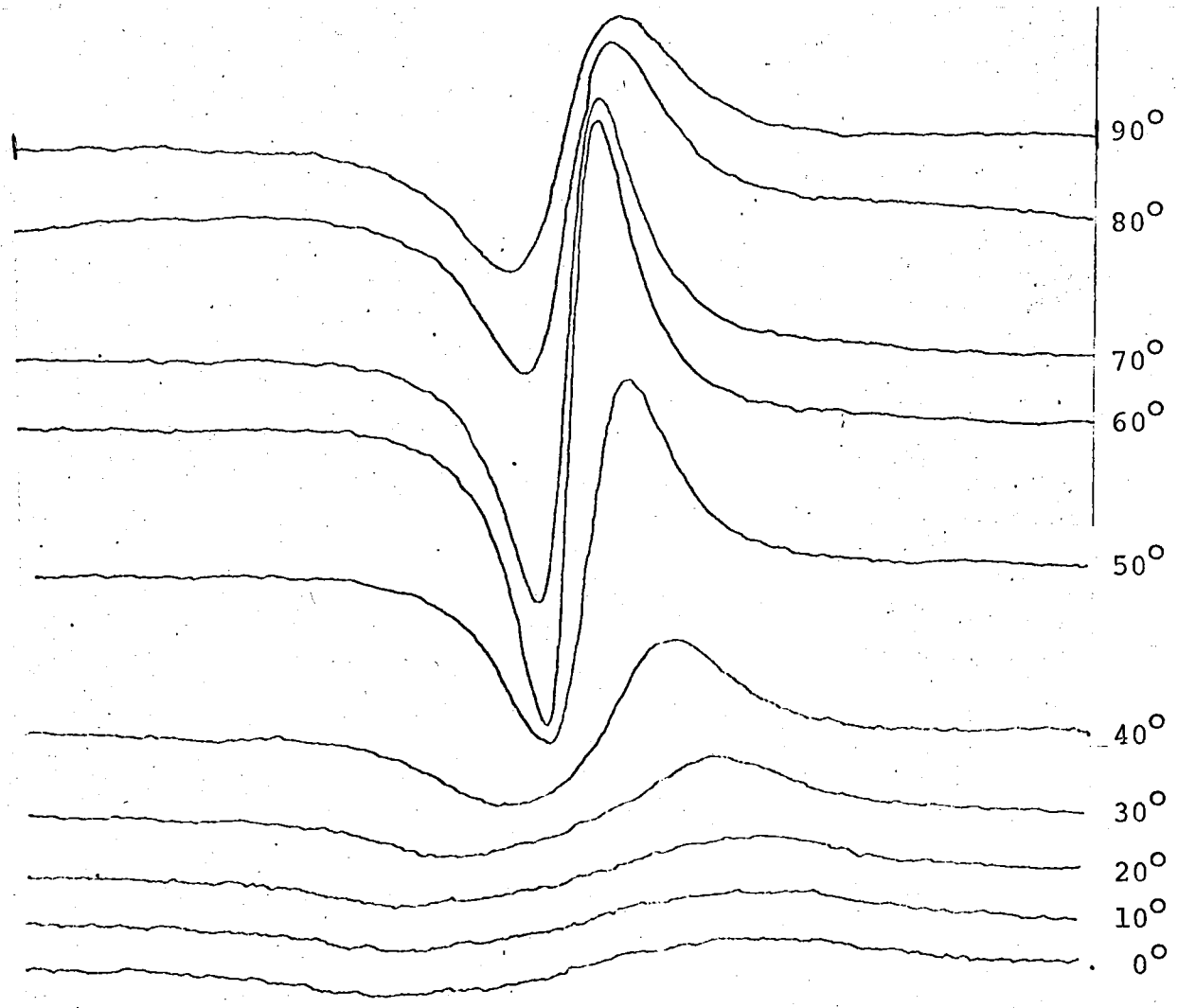

Curve Fitting Procedures

In the case of Gd^{3+} ($^8S_{7/2}$) seven spin transitions are expected to occur when the ground state levels are split by a magnetic field. One would normally expect each spin resonance line to have the shape of the first derivative of the Lorentzian function

$$f(x) = \frac{1}{1+k^2x^2}$$

$$f'(x) = \frac{-2k^2x}{(1+k^2x^2)^2}$$

To test this expectation the curve $g(x) = \sum_{i=1}^{7} \frac{A2k^2(x-a_i)}{(1+k^2(x-a_i)^2)^2}$ in which the values of a_i position each of the seven lines, was calculated and plotted by computer (PROGRAM A4). The height A was the same for each line. The lines were initially equally spaced and their widths varied methodically, a set of graphs being obtained as shown in figure 15. These indicate the plausibility of there being seven lines in the spectra when compared with actual spectra. Secondly, the lines were moved closer together, maintaining the equal spacing, and figure 16 shows that the curves produced resemble those obtained in different parts of the angular dependence studies.

In order to locate the line positions in the spectra the following technique was employed. The scale of the plot was set so that simulated spectra could be compared with the observed spectra by overlaying. The Hamiltonian program (Appendix A1) was coupled to the plotting program to calculate the values a_i. Initially values of the b_n^m for $Gd^{3+}/LaCl_3$ were inserted and scaled up by a factor of 4 (for the case of $PrCl_3$ as it was studied first), and the height A and line

Figure 15

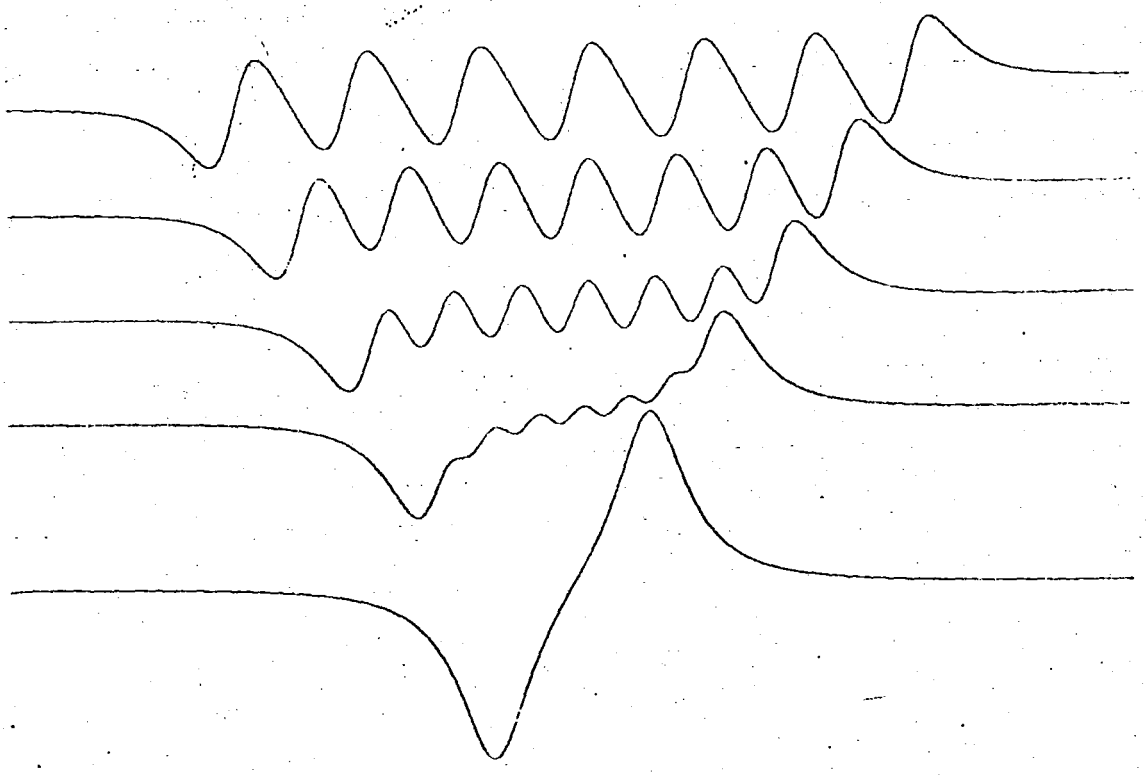

Figure 16

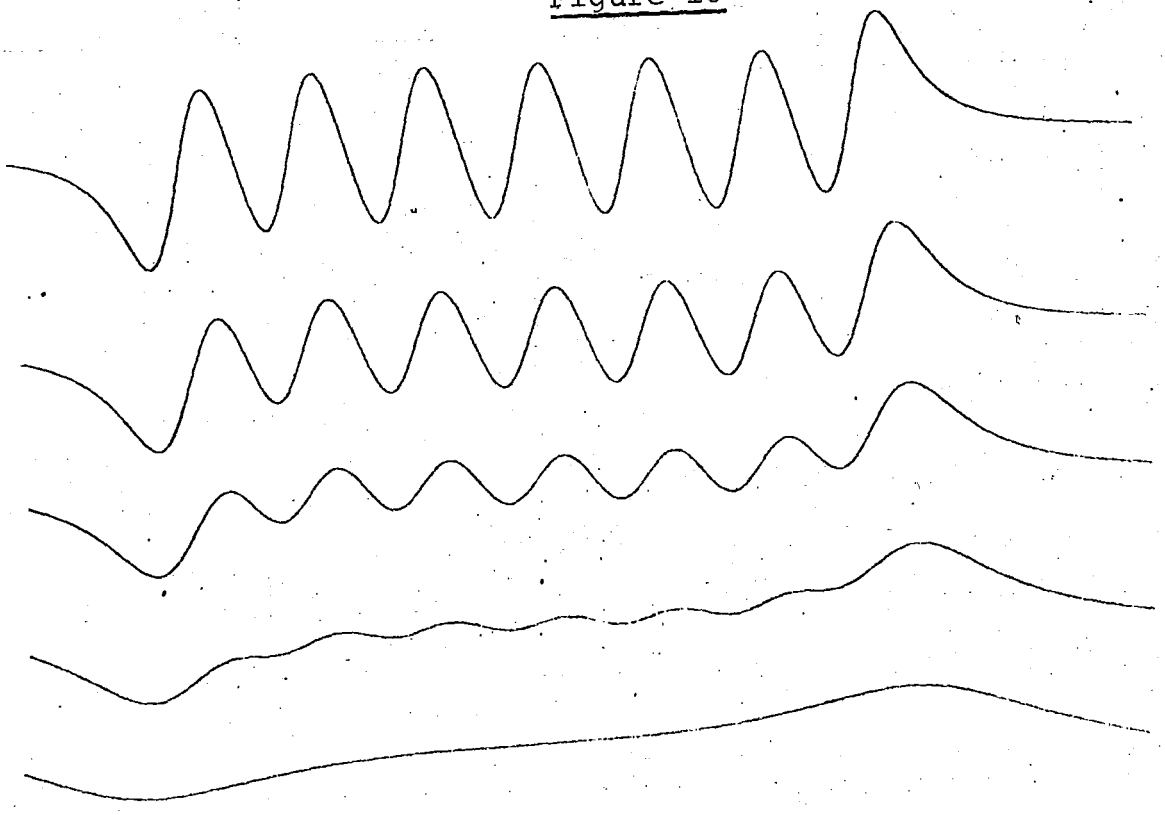

width factor k varied until the resulting curve bore a resemblance to the observed spectrum for $PrCl_3$ at $\theta = 0^\circ$. The values of the b_n^m were adjusted so that the spectrum was simulated correctly at both 0° and 90° (with the same b_n^m) and then tested at other orientations. This technique was further refined in order to conserve computer time by the use of a model spectrum. A set of linear expressions giving true positions was derived empirically using scaled values of b_2^0, b_4^0, b_6^0 for $LaCl_3$. This was compared with the set given by Boatner and Abraham[8] and verified that the Hamiltonian program was reliable. The parameters M and D (see p40 of this thesis) were initially set at 2 and 100 respectively and the value of O was determined by varying it in a range of values (350-450). Once O was determined M and D were varied methodically at 0° and 90° the model spectrum program being prefixed to the Hamiltonian to generate values of b_2^0, b_4^0, b_6^0 and the Hamiltonian program being required for the values at 90°. The best pair of M and D were picked and simulations at other orientations tested (at 10° intervals). These were found to agree with the experimentally observed spectra as far as line position was concerned but at angles $>30^\circ$ were broader and lower in height.

Curve Fitting for Broadened Lineshapes

In the model of dipolar broadening being used the total lineshape is pictured as a sum of Lorentzian derivatives each being due to a sum of transitions at a certain magnetic field.

A total spectrum representing this therefore consists of seven "lines", each a sum of smaller contributions (see figure 17).

Figure 17

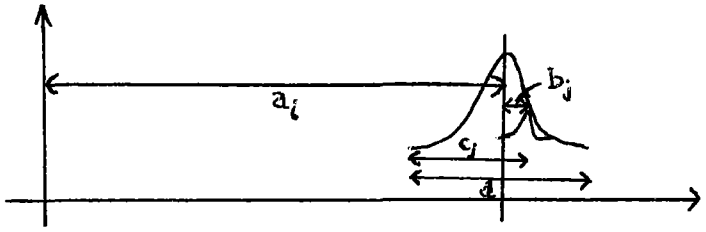

$$b_j = c_j - \frac{d}{2}$$

The contribution at x of line j with lineshape f(x) to "line" i of the total spectrum is

$$f(x-(a_i+b_j)) = f(x + \frac{d}{2} - (a_i+c_j)).$$

The total lineshape therefore is

$$y = \sum_{i=1}^{7} \sum_{j=1}^{d} f(x + \frac{d}{2} - (a_i+c_j))$$

$$y'(x) = \sum_{i=1}^{7} \sum_{j=1}^{d} \left| \frac{h_i h_j \; 2k^2 (x + \frac{d}{2} - (a_i+c_j))}{(1 + k^2 (x + \frac{d}{2} - (a_i+c_j))^2)^2} \right|$$

h_i = height of "line" h (i = 1, 7)

h_j = height of line j (j = 1, d)

This was explored to a certain extent using a Lorentzian function to determine the values h_i.

As far as using the actual distributions for dipolar broadening the line width required for the lines j was unrealistically large to simulate the spectrum. The main drawbacks of this method are that with the spectra being plotted over a domain of 1000 units the maximum value of j = 50 and this does not allow for a very smooth distribution function. On the practical side the number of contributions to be calculated = 1000 x i x j = 1000 x 7 x 50 = 350,000. Extending the domain of j becomes impracticable especially when k is to be determined

by trial.

The alternative to this approach is to utilise the width at half height; determine it for the calculated distribution and express k in terms of it, assuming that the resulting curve as described above is Lorentzian in character.

This was used satisfactorily when motional narrowing of the dipolar broadened lines was studied.

CHAPTER 4

ANALYSIS OF THE RESULTS

Introductory Note

The resonance results show broad lines indicative of dipolar broadening. The analysis was carried out in several stages as follows:

1. The Spin Hamiltonian was solved for energy eigenvalues.
2. The spectra were simulated utilising model spectra to locate the lines and evaluate the parameters b_2^0, b_4^0, b_6^0.
3. A model was developed to account for the linewidths, and the spectra re-simulated.

Spin Hamiltonian Analysis of the E.S.R. Spectrum

Following Hutchison et al.[6], and Boatner and Abraham[8] the spin Hamiltonian appropriate to a trivalent gadolinium ion substituting for the La^{3+} ion in the $LaCl_3$ lattice has the following form:

$$H = B_2^0 O_2^0 + B_4^0 O_4^0 + B_6^0 O_6^0 + B_6^6 O_6^6$$

the O_n^m being Stevens' 'Operator Equivalents' as discussed earlier and the B_n^m are the spin Hamiltonian parameters. This Hamiltonian is used to determine the energies of the various $|M_s\rangle$ states of the $^8S_{7/2}$ ground state of the gadolinium ion.

As a first approximation the O_6^6 term is neglected and for the case of the magnetic field along the z axis the Hamiltonian then yields the energies of the various $|M_s\rangle$ states as:

$$E_{\pm 7/2} = (\pm\tfrac{7}{2})g\beta H + 7b_2^0 + 7b_4^0 + b_6^0$$

$$E_{\pm 5/2} = (\pm\tfrac{5}{2})g\beta H + b_2^0 - 13b_4^0 - 5b_6^0$$

$$E_{\pm 3/2} = (\pm\tfrac{3}{2})g\beta H - 3b_2^0 - 3b_4^0 + 9b_6^0$$

$$E_{\pm 1/2} = (\pm\tfrac{1}{2})g\beta H - 5b_2^0 + 9b_4^0 - 5b_6^0$$

where $E_{\pm M_s}$ is the energy of the $|\pm M_s\rangle$ state,

$b_2^0 = 3B_2^0$ $b_4^0 = 60B_4^0$ and $b_6^0 = 1260B_6^0$.

There are seven $M_s = \pm 1$ allowed transitions between these levels, viz.:

$$|+\tfrac{7}{2}\rangle \rightarrow |+\tfrac{5}{2}\rangle : h\nu = g\beta H + 6b_2^0 + 20b_4^0 + 6b_6^0$$

$$|+\tfrac{5}{2}\rangle \rightarrow |+\tfrac{3}{2}\rangle : h\nu = g\beta H + 4b_2^0 - 10b_4^0 - 14b_6^0$$

$$|+\tfrac{3}{2}\rangle \rightarrow |+\tfrac{1}{2}\rangle : h\nu = g\beta H + 2b_2^0 - 12b_4^0 + 14b_6^0$$

$$|+\tfrac{1}{2}\rangle \rightarrow |-\tfrac{1}{2}\rangle : h\nu = g\beta H$$

$$|-\tfrac{1}{2}\rangle \rightarrow |-\tfrac{3}{2}\rangle : h\nu = g\beta H - 2b_2^0 + 12b_4^0 - 14b_6^0$$

$$|-\tfrac{3}{2}\rangle \rightarrow |-\tfrac{5}{2}\rangle : h\nu = g\beta H - 4b_2^0 + 10b_4^0 + 14b_6^0$$

$$|-\tfrac{5}{2}\rangle \rightarrow |-\tfrac{7}{2}\rangle : h\nu = g\beta H - 6b_2^0 - 20b_4^0 - 6b_6^0$$

which gives rise to a seven line resonance spectrum which may be diagrammatically represented as follows:

Figure 18

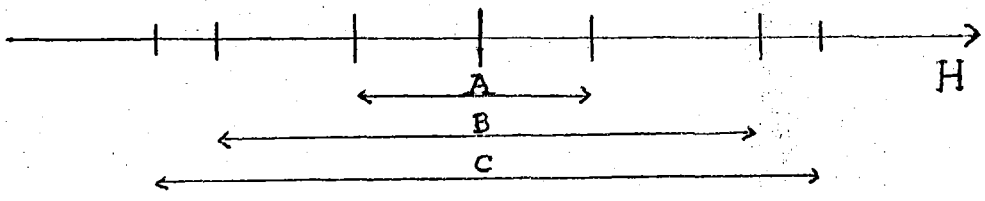

The intervals A, B and C expressed in terms of the spin Hamiltonian parameters b_2^0, b_4^0 and b_6^0 must satisfy:

$$\begin{aligned} A &= 4b_2^0 - 24b_4^0 + 28b_6^0 \\ B &= 8b_2^0 - 20b_4^0 - 28b_6^0 \\ C &= 12b_2^0 + 40b_4^0 + 12b_6^0 \end{aligned} \qquad (1)$$

Bleaney et al.[1] have shown that by using these intervals A, B, C the second order terms arising from the neglected O_6^6 term of the spin Hamiltonian are eliminated.

Rearranging (1) yields

$$\begin{aligned} b_2^0 &= \frac{1}{168}(7C + 8B + 5A) \\ b_4^0 &= \frac{1}{616}(7C - 6B - 9A) \\ b_6^0 &= \frac{1}{264}(C - 4B + 5A) \end{aligned} \qquad (2)$$

Boatner and Abraham emphasise the importance of considering all possible magnitudes and signs for A, B and C. Using (2), it is possible to evaluate the spin Hamiltonian parameters b_2^0 b_4^0 and b_6^0 from the observed resonance pattern for the case of the magnetic field along the z axis of the crystal.

Solution of the Spin Hamiltonian

The spin Hamiltonian is of the form

$$H_{spin} = g\beta \underset{\sim}{H}.\underset{\sim}{S} + \sum B_n^m O_n^m$$

and for the case of Gd^{3+} at a site of C_{3h} symmetry this may be written as

$$H_{spin} = g\beta(H_z S_z + H_x S_x + H_y S_y) + \sum_{\substack{m=0 \\ n=2,4,6}} [B_n^m O_n^m(S_z,S)]$$

$$+ B_6^6(S_+^6 + iS_-^6)$$

In order to determine the energy eigenvalues the matrix elements $\langle M_s|H|M_s'\rangle$ are calculated and the matrix diagonalised. The matrix elements can be classified as diagonal and off-diagonal. They can be calculated using the relations

$$\langle M|S_z|M'\rangle = M\delta_{MM'}$$

$$\langle M|S_+|M'\rangle = \sqrt{M(M\pm1) + S(S+1)}\ \delta_{MM'+1}$$

The diagonal elements are represented by $F(M_s,M_s)$.

$$F(M_s,M_s) = gHM_s\cos\theta + \frac{hc}{\beta}B_2^0(3M_s^2 - S(S+1))$$

$$+ \frac{hc}{\beta}B_4^0(35M_s^4 - ((30S(S+1) - 25)M_s^2 + 6S(S+1) + 3S^2(S+1)^2)$$

$$+ \frac{hc}{\beta}B_6^0((231M_s^6 + M_s^2(105S^2(S+1)^2 - 525S(S+1) + 294)$$

$$+ 40S^2(S+1)^2) - 105M_s^4(3S(S+1) - 7) + 5S^3(S+1)^3 + 60S(S+1))$$

The first off-diagonal elements are represented by $F(M_s,M_s-1)$

$$F(M_s,M_s-1) = gH\sin\theta\ (\sqrt{S(S+1) - M_s(M_s+1)}\ )$$

The remaining off-diagonal elements are $F(M_s,M_s-6)$.

$$F(M_s,M_s-6) = \frac{hc}{\beta}B_6^6\ 720\sqrt{7}.$$

In determining the matrix elements it is convenient to divide the Hamiltonian by β. The following constants were used.

$$\frac{hc}{\beta} = 2.11; \qquad \frac{h\nu}{\beta} = 6555; \qquad \nu = 9.16\ \text{GHz}.$$ (Measured with the frequency meter on the instrument used.)

The matrix is symmetric. For gadolinium M_s is given by $-\frac{7}{2} \leq M_s \leq \frac{7}{2}$. The energy eigenvalues were obtained by computer diagonalisation of this matrix using the Jacobian method of pivotal elements.

Experimentally the magnetic field is varied and absorption at a particular energy detected at various magnetic fields. Consequently it is necessary to solve for the energy eigenvalues at a series of magnetic fields until magnetic fields corresponding to each of the possible transitions have been located.

The detailed steps involved in the computing are given in Appendix A1.

Model Spectra and the Parameters b_2^0, b_4^0, b_6^0

In order to simulate the spectra values of the b_n^0 were taken as scaled values of the b_n^0 for $LaCl_3$. In the computer program therefore B20 = $\alpha b_2^0(LaCl_3)$, B40 = $\beta b_4^0(LaCl_3)$, B60 = $\gamma b_6^0(LaCl_3)$. In order to check the Hamiltonian program the values α, β, γ were varied between 1 and 5 and transitions were found to occur as follows:

$\pm \frac{7}{2} \rightarrow \pm \frac{5}{2}$ $\quad 3292 \pm (54\alpha + 36\beta + 3\frac{1}{2}\gamma)$

$\pm \frac{5}{2} \rightarrow \pm \frac{3}{2}$ $\quad 3292 \pm (36\alpha - 18\beta - 9\frac{1}{2}\gamma)$

$\pm \frac{3}{2} \rightarrow \pm \frac{1}{2}$ $\quad 3292 \pm (18\alpha - 21\beta + 9\frac{1}{2}\gamma)$

$\pm \frac{1}{2} \rightarrow - \frac{1}{2}$ $\quad 3292$

Note: these are given for $\theta = 0^o$ (i.e. H parallel to the z axis). Boatner and Abraham, for instance, give

$$\pm \frac{7}{2} \rightarrow \pm \frac{5}{2} \quad g\beta H \pm 6b_2^0 + 20b_4^0 + 6b_6^0$$

$$\pm \frac{5}{2} \rightarrow \pm \frac{3}{2} \quad g\beta H \pm 4b_2^0 - 10b_4^0 - 14b_6^0$$

$$\pm \frac{3}{2} \rightarrow \pm \tfrac{1}{2} \quad g\beta H \pm 2b_2^0 - 12b_4^0 + 14b_6^0$$

The ratio of the coefficients of the b_2^0's in each case are identical as is the case for the b_4^0's and the b_6^0's and the signs are all identical. Various model spectra can be employed and the one constructed here is shown in figure 19.

Figure 19

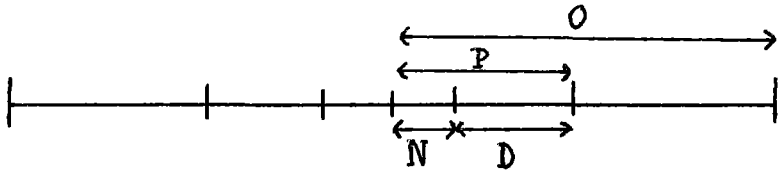

The parameters used are O, M, D, $M = \frac{P}{N}$. This enables a search for O to be carried out initially, followed by a simultaneous determination of the inner two line positions. This method was used as the distance D could be measured without knowing N, P exactly in the case of $PrCl_3$. (Maxima are not at line centres.)

Solving for α, β, γ

$$\alpha = \frac{O(M-1)370.5 + 3D(138.5M + 93.0)}{740.5(M-1)54}$$

$$\beta = \frac{O(M-1)85.5 - 3D(25M + 35.5)}{740.5(M-1)9}$$

$$\gamma = \frac{O(M-1)8 - 3D(11M-14)}{740.5(M-1)}$$

Once the model spectrum had been used at 0° the values of B20, B40, B60 were used for simulation at other orientations using the Hamiltonian program.

Table 5

Host	Temperature	Rotation axis	$b_2^0 \times 10^{-4} cm^{-1}$	$b_4^0 \times 10^{-4} cm^{-1}$	$b_6^0 \times 10^{-4} cm^{-1}$	$b_6^6 \times 10^{-4} cm^{-1}$
Lanthanum trichloride	77°K		16.1	2.13	0.23	1.4
	290°K		8.36	1.68	0.64	
Cerium trichloride	290°K	y	13.96	0.53	-0.05	
Praseodymium trichloride	130°K	y	54.67	3.02	-0.22	
	290°K	y	45.62	2.75	0.46	
Neodymium trichloride	170°K	y	30.68	2.08	0.67	
Europium trichloride	77°K		101.0	1.47	0.31	3.0

The values of the Spin Hamiltonian parameters b_2^0, b_4^0, b_6^0 obtained are given in table 5 along with those for $LaCl_3$ and $EuCl_3$ acting as hosts to Gd^{3+}. The effect of b_6^6 cancels out when one considers model spectra and when it is included its effect on the transition energies is indeterminate when the line widths are as broad as they are in $CeCl_3$, $PrCl_2$ and $NdCl_3$.

The graphs of the angular dependence of the line positions which follow (p43-45) were plotted from the computed line positions used in the line simulations. They may be compared with those for $LaCl_3$, $EuCl_3$ (p42).

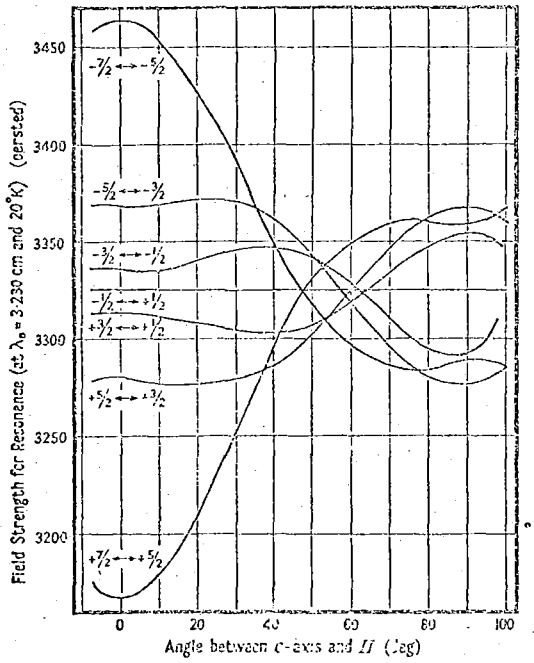

Figure 20 Gd^{3+} in $LaCl_3$

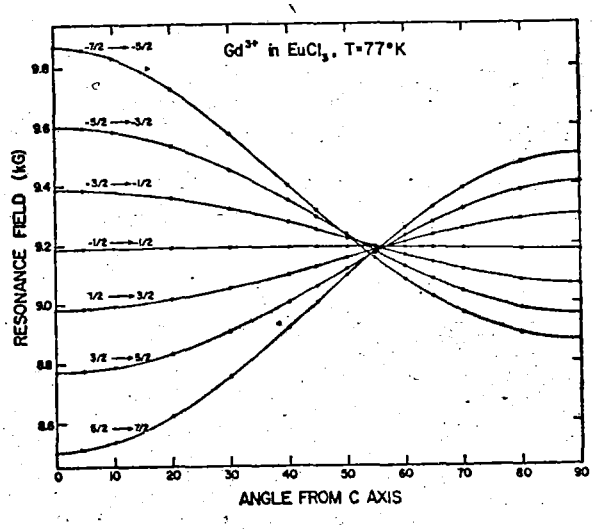

Figure 21 Gd^{3+} in $EuCl_3$

Figure 22

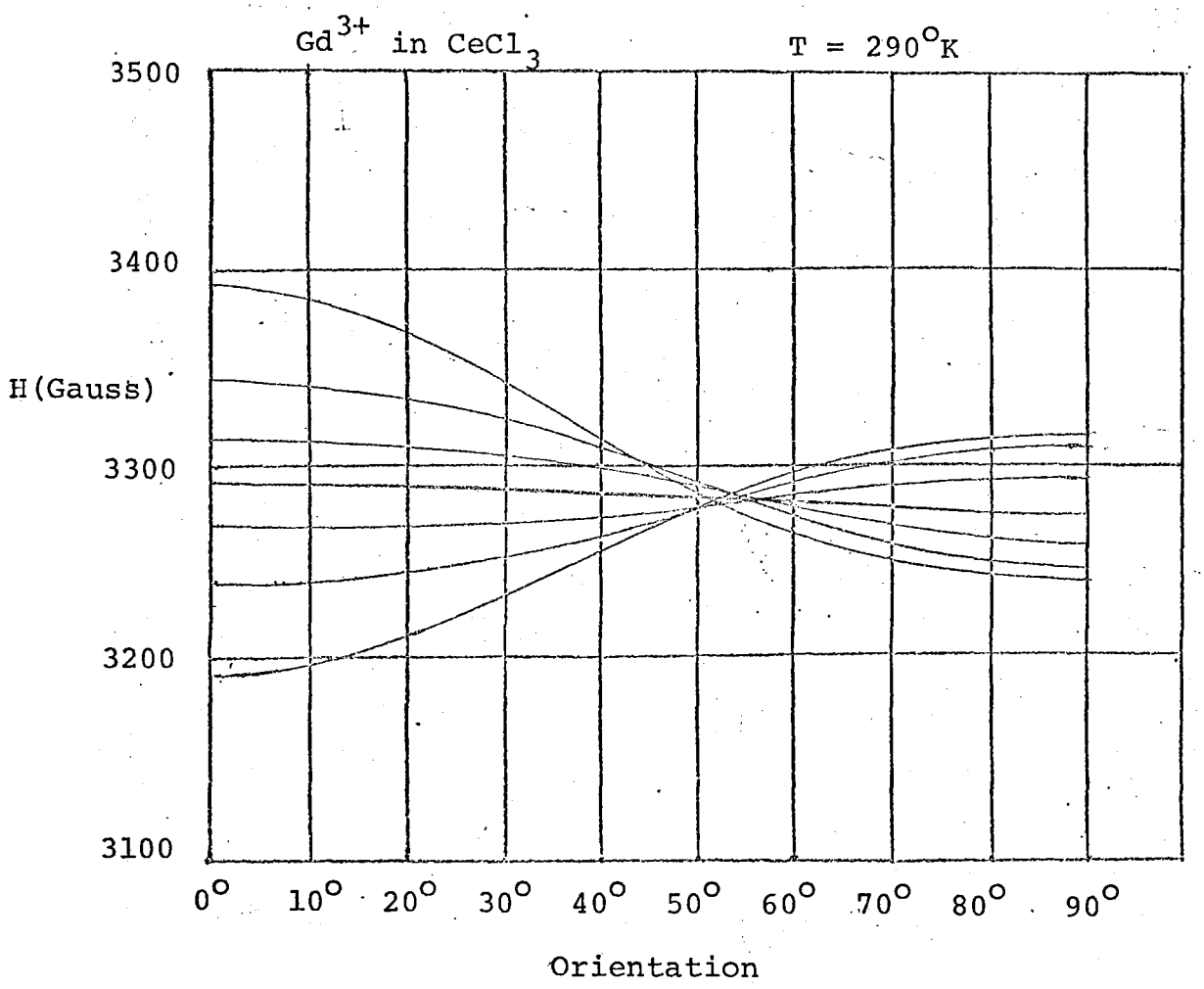
Gd3+ in CeCl3
T = 290°K
3500
3400
3300
3200
3100
H(Gauss)
0°
10°
20°
30°
40°
50°
60°
70°
80°
90°
Orientation

Figure 23

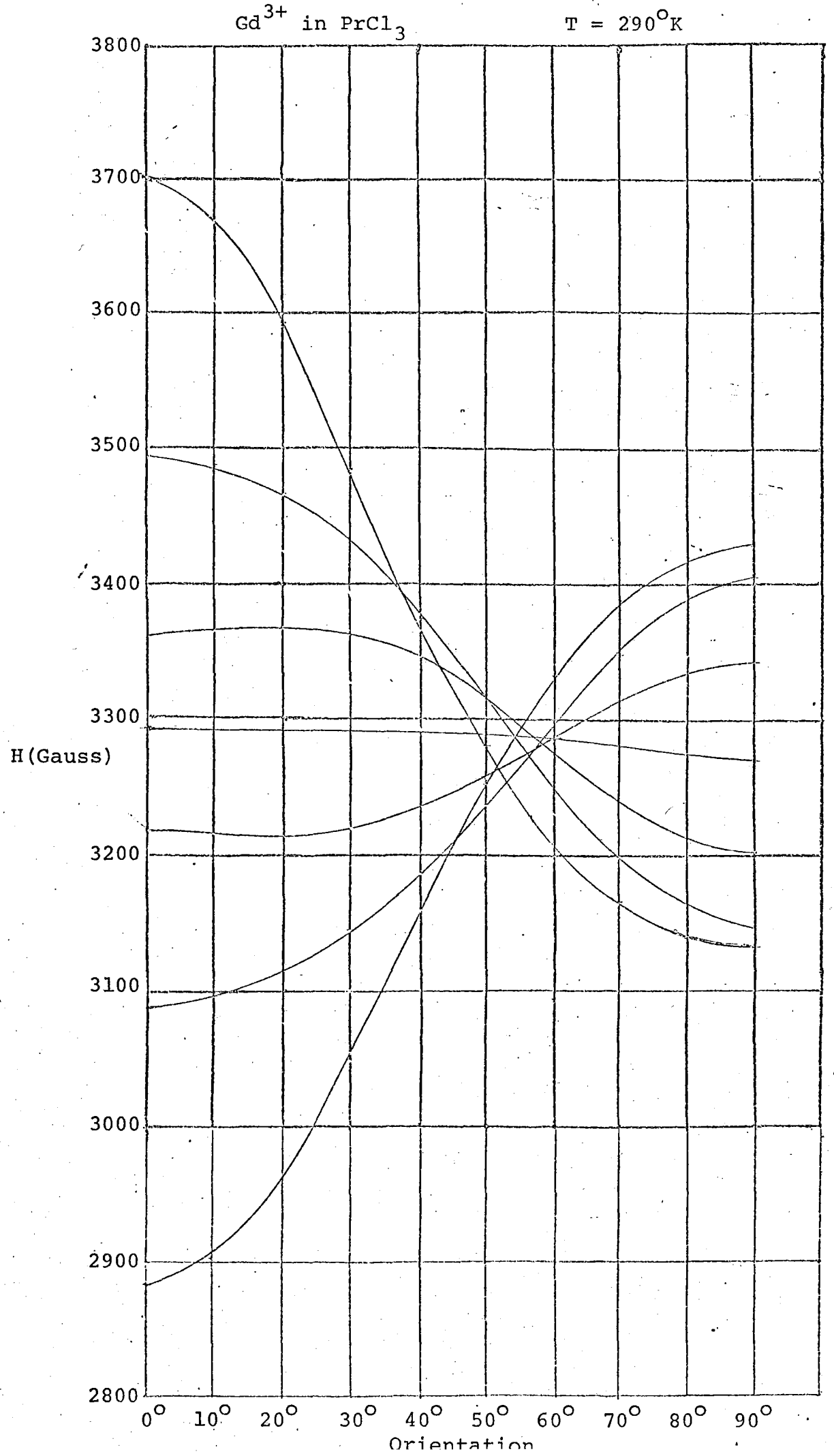
Gd^{3+} in $PrCl_3$
T = 290°K
3800
3700
3600
3500
3400
3300
3200
3100
3000
2900
2800
H(Gauss)
0°
10°
20°
30°
40°
50°
60°
70°
80°
90°
Orientation

Figure 24

Gd^{3+} in $NdCl_3$ T = 153°K

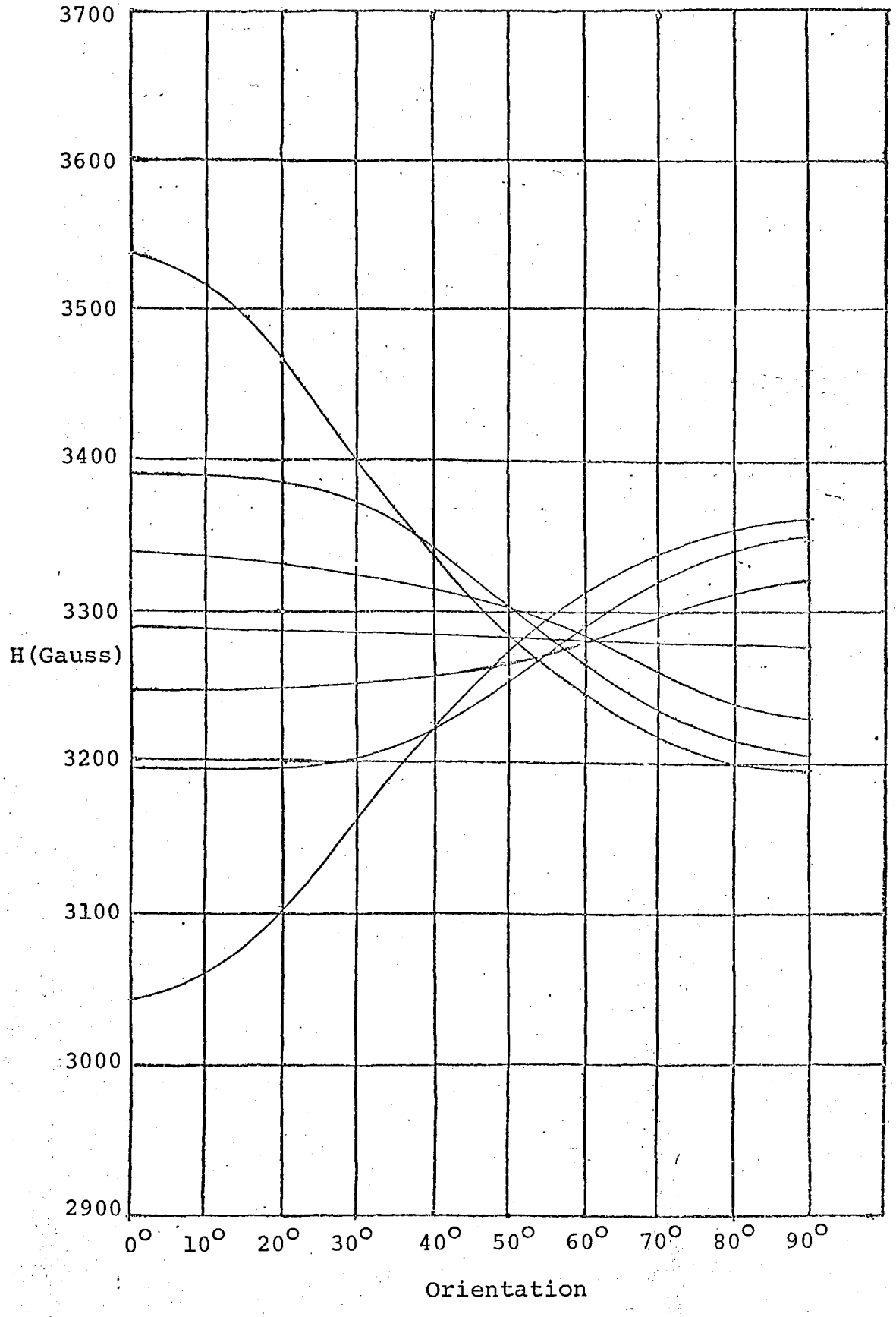

Simulated Spectra

The simulated spectra included at this point (table 6) show certain features in common. In each case the broad lines overlap. At angles >30° the lines are broader and lower in height than the recorded spectra. This indicates that the linewidths are a function of orientation.

Table 6

Simulated Spectra

Host	Rotation axis	Temperature	Magnetic field	Line height
$CeCl_3$	y	290°K	2800-3800G	8000
$PrCl_3$	y	290°K	2800-3800G	13000
$PrCl_3$	(Gaussian line shape)	290°K	2800-3800G	13000
$PrCl_3$	y	130°K	2800-3800G	80000
$NdCl_3$	y	153°K	2300-4300G	15000

$CeCl_3 + Gd^{3+}$

Rotation axis: y
Temperature: 290°K
Magnetic Field: 2800-3800G
Line Height: 8000

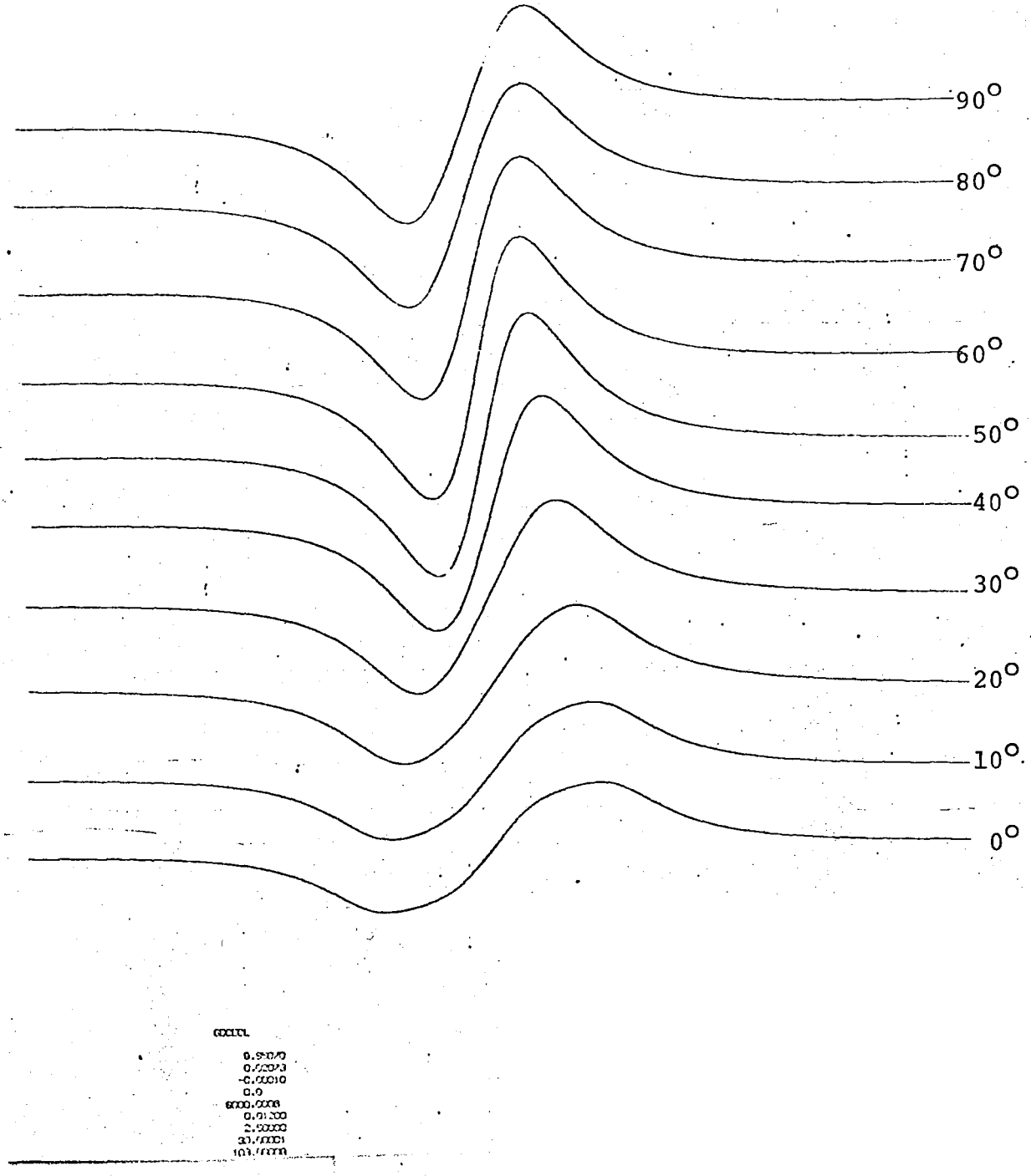

$PrCl_3 + Gd^{3+}$

Rotation axis: y
Temperature: 290°K
Magnetic field: 2800-3800G
Line Height: 13000

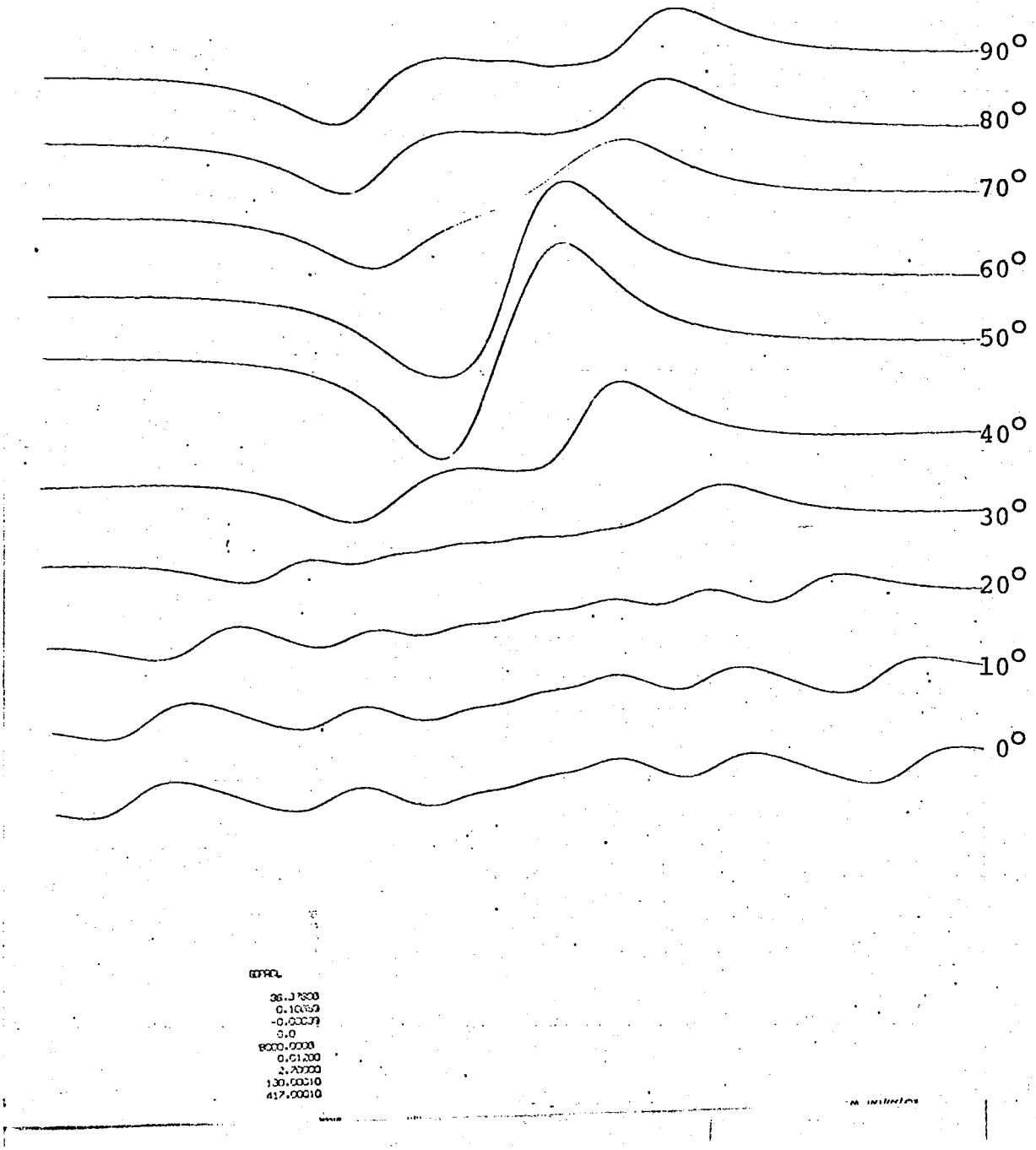

$PrCl_3 + Gd^{3+}$

Gaussian Lineshapes Used
Temperature: 290°K
Magnetic field: 2800-3800G
Line Height: 13000

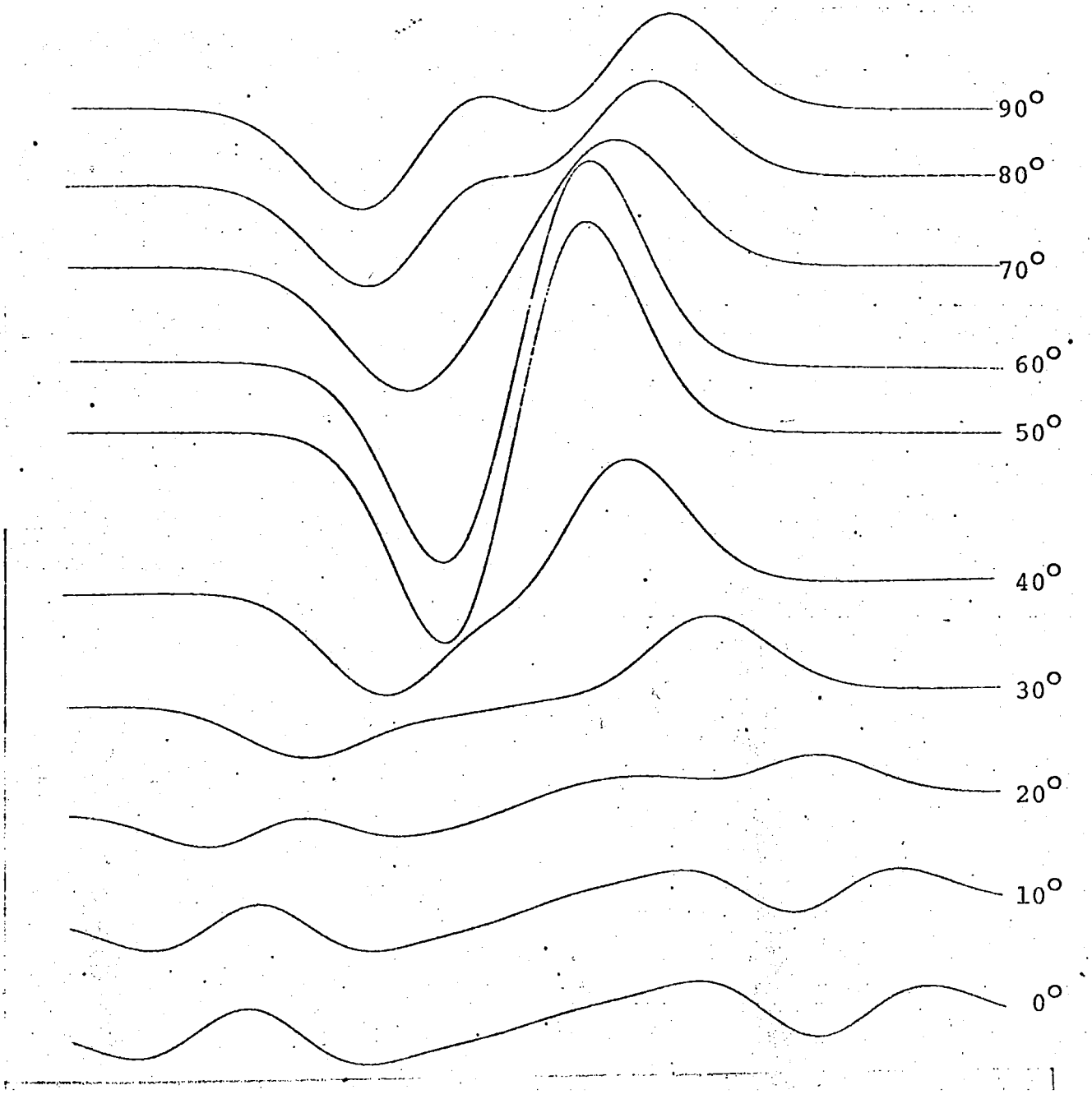

$PrCl_3 + Gd^{3+}$

Rotation axis: y
Temperature: 130°K
Magnetic field: 2800-3800G
Line Height: 8000

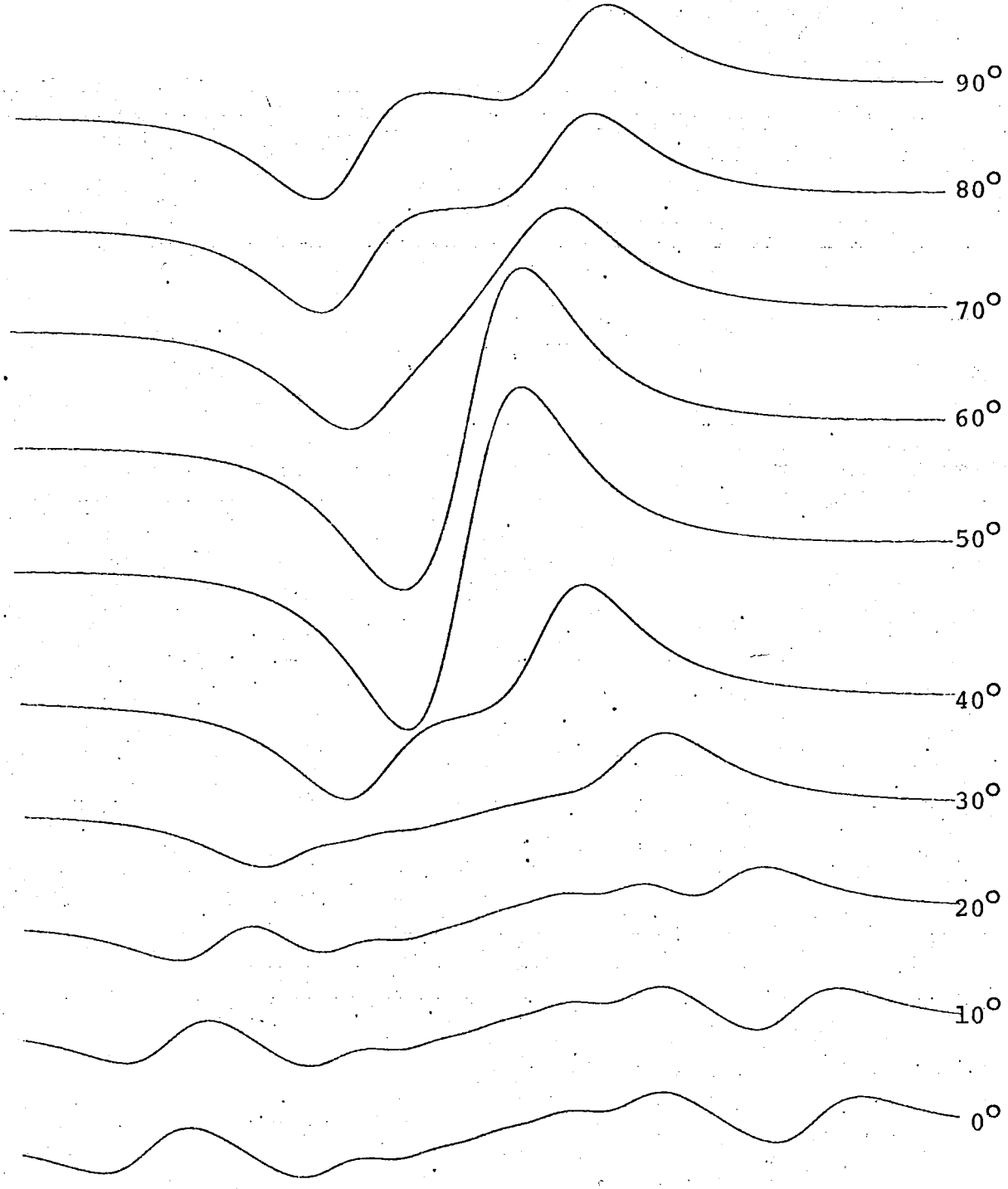

$NdCl_3 + Gd^{3+}$

Rotation axis: y
Temperature: 153°K
Magnetic field: 2300-4300G
Line height: 15000

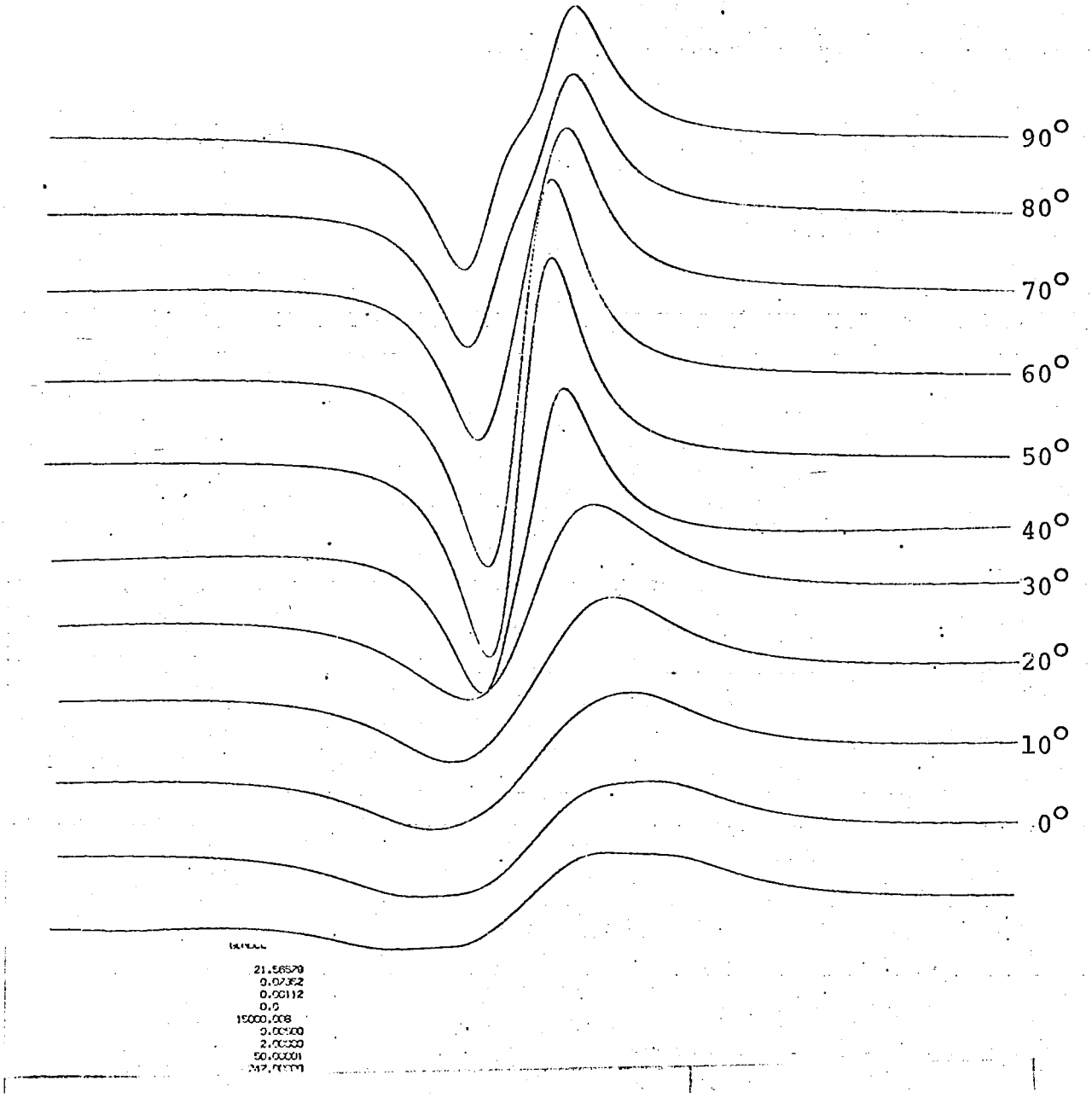

Calculation of the Dipolar Magnetic Field Contributions

In the close environment of the Gd^{3+} ion there are 14 paramagnetic host ions, in the case of $CeCl_3$, $PrCl_3$, $NdCl_3$ within 7.500Å and 28 within 8.750Å. The spin of each of these neighbours is assumed to be either parallel or antiparallel to the external magnetic field. The number of different ways of obtaining a local field is 2^n. From the computational point of view $2^{14} \approx 16{,}000$ is a much more manageable figure than $2^{28} \approx 256{,}000{,}000$ as 16,000 configurations can be calculated in about 5 minutes on an IBM 360/44 computer.

The local field was calculated in a component-wise fashion (see appendix A.2).

For the purposes of analysis the component of the resultant local field parallel to the imposed magnetic field is considered. It can be obtained as indicated in figure 25.

Figure 25

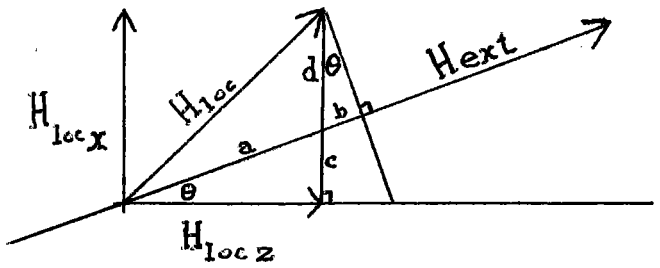

$$H_{loc} = g_j U_\beta \sum_{j=1}^{14} \frac{3\underset{\sim}{r}_{ij}(\underset{\sim}{S}.\underset{\sim}{r}_{ij}) - \underset{\sim}{S}\underset{\sim}{r}_{ij}^{2}}{r_{ij}^{5}}$$

$$H_{loc_{//}} = a + b$$

$$= \frac{H_{loc_z}}{\cos\theta} + (d + c - c)\sin\theta$$

$$= \frac{H_{loc_z}}{\cos\theta} + (H_{loc_x} - H_{loc_z} \tan\theta) \sin\theta$$

$$= H_{loc_z} \cos\theta + H_{loc_x} \sin\theta$$

Computed Distributions for the Static Dipolar Mechanism

These are calculated for each of the hosts $CeCl_3$, $PrCl_3$, $NdCl_3$ at intervals of 10^o corresponding to the orientations at which observations were made. The range covered in each instance is -1500 → +1500 Gauss and is divided into 60 intervals each of 50 Gauss. The actual distributions are given in figures 26, 27, 28. The widths at half height are given in table 7.

Table 7

	Dipolar Broadening Model: Widths at half height: a									
θ	0	10	20	30	40	50	60	70	80	90
$CeCl_3$	1800	1650	1450	1450	1050	850	500	300	250	150
$PrCl_3$	450	450	450	350	300	250	150	100	100	50
$NdCl_3$	2050	1700	1650	1050	1050	700	600	550	450	550

The corresponding values of $\frac{2}{K}$ are given in table 8.

Table 8

	Dipolar Broadening Model: Values of $\frac{2}{K}$ at half height									
θ	0	10	20	30	40	50	60	70	80	90
$CeCl_3$	0.0011	0.0012	0.0014	0.0014	0.0019	0.0024	0.0040	0.0066	0.0080	0.0144
$PrCl_3$	0.0048	0.0048	0.0048	0.0057	0.0066	0.0080	0.0144	0.0200	0.0200	0.0400
$NdCl_3$	0.0010	0.0012	0.0012	0.0019	0.0019	0.0029	0.0033	0.0036	0.0044	0.0036

The values which were used in order to simulate the spectra, as far as line position is concerned, (i.e. not simulating intensity accurately) are given in table 9.

Table 9

Values of k for line width

θ	0	10	20	30	40	50	60	70	80	90
$CeCl_3$	0.012	0.012	0.012	0.012	0.012	0.012	0.012	0.012	0.012	0.012
$PrCl_3$	0.014	0.014	0.014	0.014	0.014	0.014	0.014	0.014	0.014	0.014
$NdCl_3$	0.005	0.005	0.005	0.010	0.010	0.010	0.010	0.010	0.010	0.010

Figure 26

Static Dipolar Broadening Distribution for $CeCl_3$

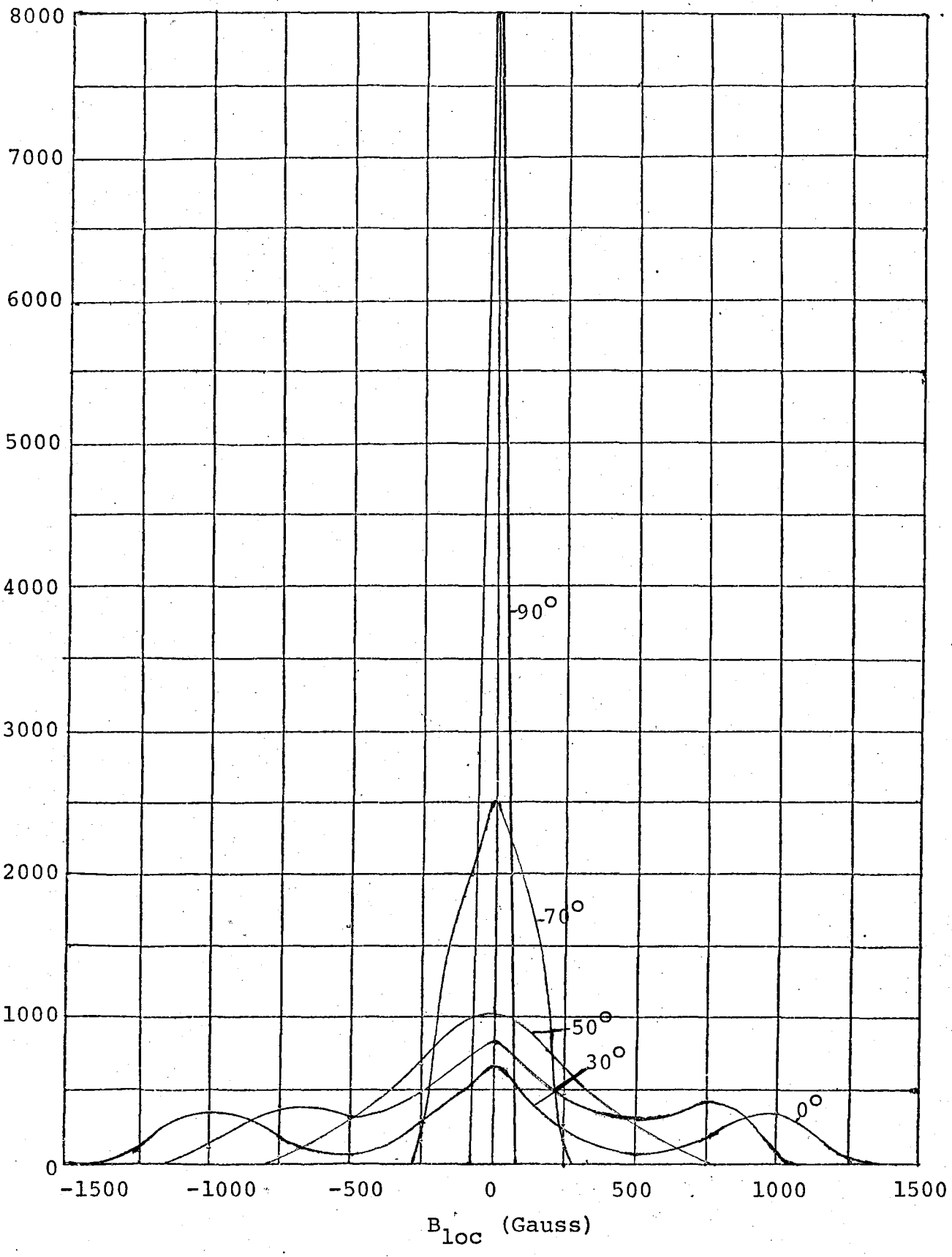

Figure 27

Static Dipolar Broadening Distribution for $PrCl_3$

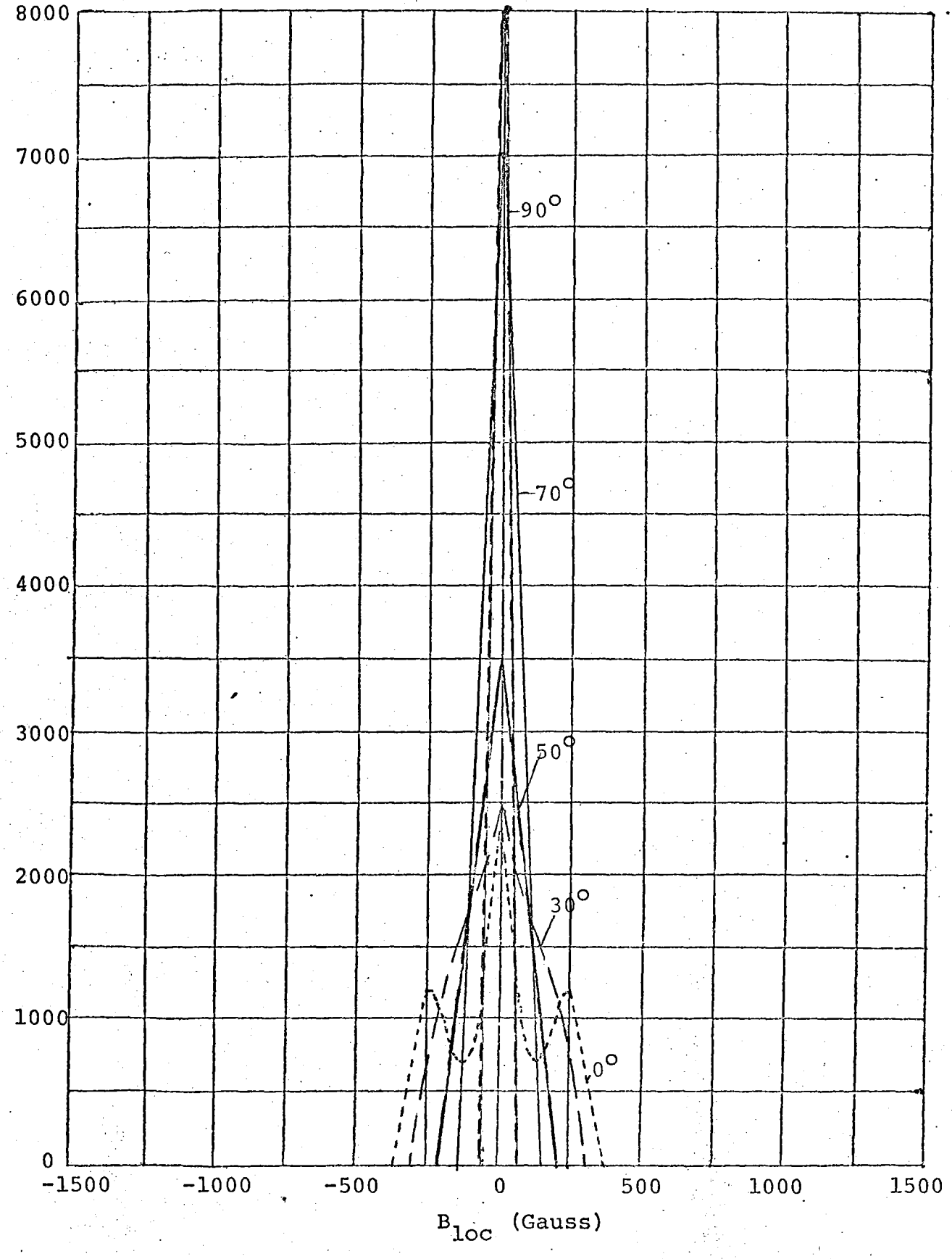

Figure 28

Static Dipolar Broadening Distribution for $NdCl_3$

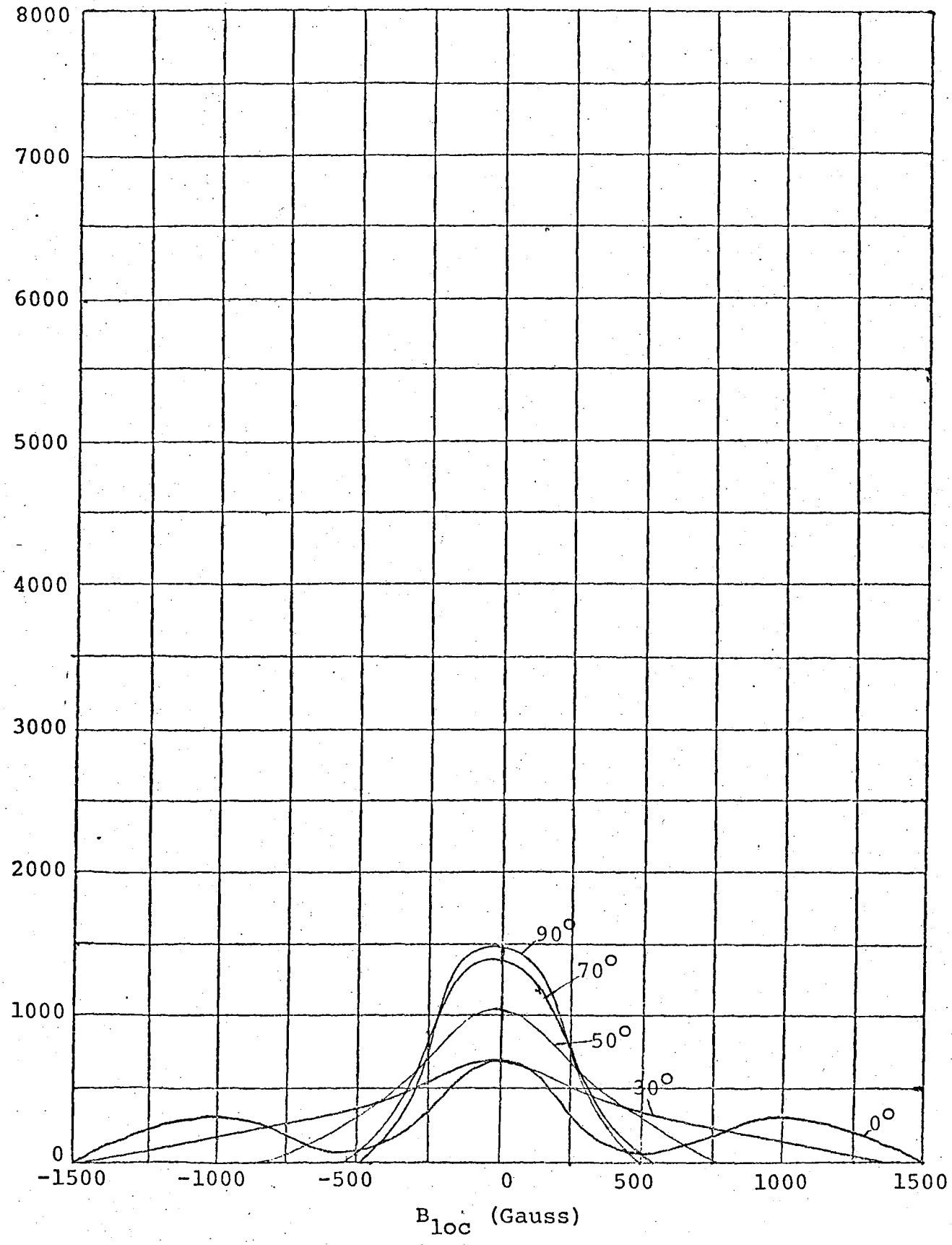

Motional Narrowing

When a dopant ion has a number of close neighbours each contributing to a local dipolar magnetic field such fields have a distribution of values. If the interaction of the magnetic dipoles with the lattice phonons is much stronger than the interdipole interaction the dipoles flip up and down (the magnetic field). The average fields experienced during transitions produces a distribution of effective local fields narrower in width than in the static case.

The rate at which the dipoles flip compared with the rate at which the microwave fields oscillate determines the extent of the averaging of the local magnetic field which occurs and the resultant width of the distribution. For any particular host crystal there will be an average flipping rate at a given temperature independent of the direction of the external magnetic field. As phonons can only propagate along rows of atoms, there is a non-uniform distribution of intensity, in the disturbance caused by phonons, as a function of angle. Consequently when the external magnetic field is aligned in certain directions the probability of changes in the local magnetic fields may be greater than in other directions. Thus the motional narrowing can be characterised by two parameters, one describing an overall effect and the other the detailed angular dependence.

Let it be assumed that on average the local magnetic field changes n times during the time of observation T ($T \approx \frac{1}{f}$ where f is the microwave frequency being used for electron spin resonance). To calculate the average magnetic field experienced during the time T the initial, intermediate and final states must be considered.

$$H_{av} = \frac{H_i + \sum_{int=1}^{n-2} H_{int} + H_f}{n}$$

Figure 29 shows a possible path involving four intermediate states.

Figure 29

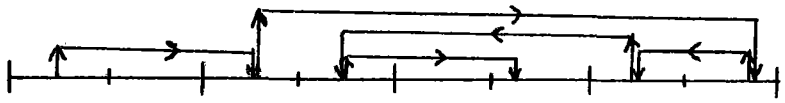

$$H_{av} = 150 \text{ Gauss} \quad \left(\frac{H_i + H_f}{2} = -250 \text{ Gauss}\right)$$

The greater the number of steps which are made, the nearer the average field experienced will tend to zero, there being an equal number of states possible either side of zero.

In a crystalline sample many identical configurations of dipoles producing a given local magnetic field H_i may change to the identical configurations having magnetic field H_f. If these changes are by random intermediate paths then the average of the average fields at which transitions can occur is given by

$$\bar{H}_{av} = \frac{\sum_{\text{all sites}} H_i + \sum H_{int} + H_j}{\text{no. sites} \times N^{n-2}}$$

$$= \frac{H_i + H_j}{n} + \frac{\sum_{\text{all sites}} \sum H_{int}}{\text{no. sites} \times N}$$

$$= \frac{H_i + H_j}{n}$$

as $\sum_{\text{all sites}} \sum_{int=1}^{n-2} H_{int} = (n-2) \sum_{\text{all sites}} H_{int} = 0.$

Such averaging as this can occur during the response time of the electronics of the detection equipment, the signal detected being a sum of signals detected, noise being averaged out.

On the detailed level consider a configuration of dipoles surrounding a dopant ion in which i spins are up (an i type configuration). Each such configuration has an associated magnetic field. The same is true for a j type configuration. If the initial magnetic field is of an i type configuration the final field can be another i type configuration or a j type configuration.

The change from an i to a j type configuration ($i < j$) may take place in several steps, via a number of intermediate states, however the net effect is that at the end j-i more spins are up than at the beginning. If k of the spins originally up have turned down then $(j-i)+k$ of the spins down must have turned up. k, which shall be called the path number, is restricted in that it is clearly less than i, and the number of spins down initially must be greater than or equal to the number of spins which turn up.

i.e. $k \leqslant i$ and $(j-i)+k \leqslant n-i$

i.e. $k \leqslant i$ and $k \leqslant n-j$

where n is the number of neighbours being considered, it being assumed that each number has one spin of value $M_S = \pm\frac{1}{2}$. A typical change in configuration is illustrated in Figure 30.

Figure 30

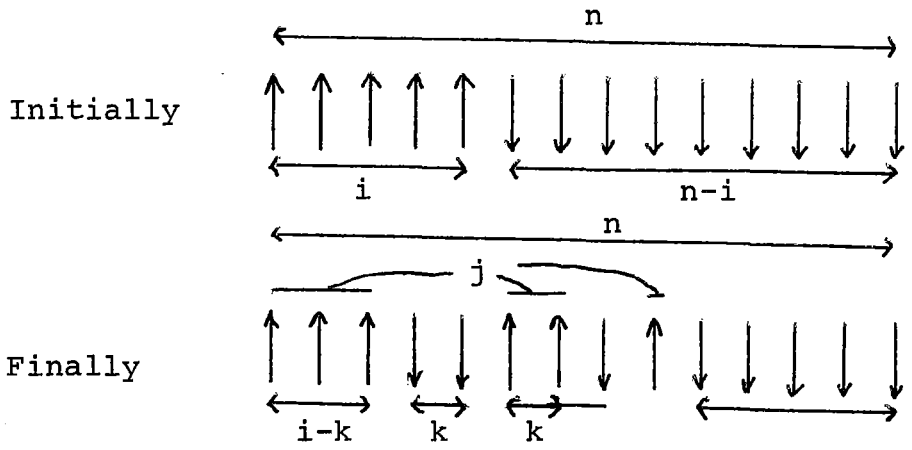

The number of type j configurations a type i configuration can change to, via pathway k, is given by the product of the number of ways in which k spins out of i can turn down, $\frac{i!}{k!(i-k)!}$, and the number of ways in which (j-i)+k out of the n-i spins down can turn up, $\frac{(n-i)!}{((j-i)+k)!(n-(j+k))!}$ $(k \leqslant i, n-j)$

$$N_{ij}(k) = \frac{i!}{k!(i-k)!} \frac{(n-i)!}{((j-i)+k)!(n-(j+k))!}$$

Let the probability that the overall spin change is 1 be p then the probability $p_{ij}(k)$ for 2k+(j-i) changes is $p^{2k+(j-i)}$ and the contribution of pathway k is $p_{ij}(k)N_{ij}(k)$. For example, if p is small the contributions of pathways of large k are reduced. In other words small p characterises the situation where the rate of flipping caused by phonons is low.

The effect of using all different pathways k can be represented by the average probability

$$P_{ij} = \frac{\sum_k p_{ij}(k)N_{ij}(k)}{\sum_K N_{ij}(k)} .$$

A set of values P_{ij} $(1 \leqslant i \leqslant j \leqslant n)$ with $p = 0.92$ is given in table 11.

The contribution to the distribution of averaged local fields can now be re-expressed as

$$H_{av_{ij}} = \frac{H_i + H_j P_{ij}}{(1+P_{ij})N}$$

Variation of the parameter p will clearly alter the width of the distribution. As p is varied the proportions of P_{ij} contributed by different pathways k varies. When p is small terms involving p^2, p^4 are clearly less significant than when p is larger.

The configurations of type i have associated with them a set of local magnetic fields, as have the configurations of type j.

Let the frequency of occurrence of field H in configurations of type i be $N(H_{\ell_i})$ and that of H_m in configurations of type j be $N(H_{m_j})$. When configurations change the average field is $H_{av_{ij}}$ and the contribution to the distribution at $H_{av_{ij}}$ is the number of opportunities that exist for the averaging to take place.

$$\text{i.e. } f_{\ell_i, m_j}(H_{av_{ij}}) = N(H_{\ell_i})\, N(H_{m_j})$$

The total distribution function for the motional narrowing is therefore

$$M(H) = \sum_{i,j,\alpha,\beta} f_{\alpha_i,\beta_j}(\delta_{H_{av_{i,j}}}; H_{av_{\alpha,\beta}})$$

The narrowed distributions are given in figures 31, 32, 33. The development of this model to account for the line broadening allows the resimulation of the spectra. Examples of resimulated spectra are given in table 10.

Computed Distributions for the Motionally Narrowed Dipolar Broadened Lines

The two parameters N, p determine the width of the distribution of averaged local magnetic fields. Variation of p alone produces changes in the width, the maximum narrowing being from W_0 to $\frac{2}{3} W_0$ (p = 0.92). Variation of N effects an N fold narrowing of the distribution.

In order to simulate the spectra the values of N, p indicated in Table 10 were used and the half widths obtained are given there also. The distributions obtained for $CeCl_3$, $PrCl_3$, $NdCl_3$ at = 0^o, 30^o, 60^o, 90^o are graphed in figures 31, 32 and 33.

Table 10

Host	N	P	Widths at Half Height			
Orientation			0^o	30^o	60^o	90^o
$CeCl_3$	7.0	0.92	190	150	60	20
$PrCl_3$	4.0	0.92	170	130	75	30
$NdCl_3$	3.0	0.92	450	340	170	140

When the spectra are resimulated at the orientations of Table 10 and using the predicted widths, N, p, as indicated in the case of $CeCl_3$ the spectrum of 90^o has lines which are too narrow. They can be broadened sufficiently by altering p such that the width increases to 30 which can be achieved with p = 0.1. In the case of $PrCl_3$ the value of p has to be altered for the angles 60^o and 90^o to improve the width such that unobserved peaks do not appear in the spectra. That this is

the case is due to the value of $g_\perp$ (see table 18) being so small. In the case of $NdCl_3$ the one value of p is sufficient.

Resimulations of the spectra are given on pages 69-71

Table 11

p = 0.92

p_{ij}	i	j
0.85	1	1
0.79	1	2
0.75	2	2
0.74	1	3
0.71	2	3
0.67	3	3
0.69	1	4
0.67	2	4
0.64	3	4
0.62	4	4
0.64	1	5
0.63	2	5
0.61	3	5
0.60	4	5
0.59	5	5
0.60	1	6
0.59	2	6
0.59	3	6
0.58	4	6
0.57	5	6
0.57	6	6
0.55	1	7
0.56	2	7
0.56	3	7
0.56	4	7
0.56	5	7
0.56	6	7
0.56	7	7
0.52	1	8
0.52	2	8
0.53	3	8
0.54	4	8
0.55	5	8
0.55	6	8
0.56	7	8
0.57	8	8
0.48	1	9
0.49	2	9
0.51	3	9
0.52	4	9
0.53	5	9
0.55	6	9
0.56	7	9
0.57	8	9
0.59	9	9
0.45	1	10
0.46	2	10
0.48	3	10
0.50	4	10
0.52	5	10
0.54	6	10
0.56	7	10
0.58	8	10
0.60	9	10
0.62	10	10
0.42	1	11
0.44	2	11
0.46	3	11
0.48	4	11
0.51	5	11
0.53	6	11
0.56	7	11
0.59	8	11
0.61	9	11
0.64	10	11
0.67	11	11
0.39	1	12
0.41	2	12
0.44	3	12
0.46	4	12
0.49	5	12
0.52	6	12
0.56	7	12
0.59	8	12
0.63	9	12
0.67	10	12
0.71	11	12
0.75	12	12
0.36	1	13
0.39	2	13
0.42	3	13
0.45	4	13
0.48	5	13
0.52	6	13
0.55	7	13
0.60	8	13
0.64	9	13
0.69	10	13
0.74	11	13
0.79	12	13
0.85	13	13
0.33	1	14
0.36	2	14
0.39	3	14
0.43	4	14
0.47	5	14
0.51	6	14
0.55	7	14
0.60	8	14
0.65	9	14
0.71	10	14
0.77	11	14
0.84	12	14
0.92	13	14
1.00	14	14

Figure 31

Motionally Narrowed Dipolar Broadening Distribution for $CeCl_3$

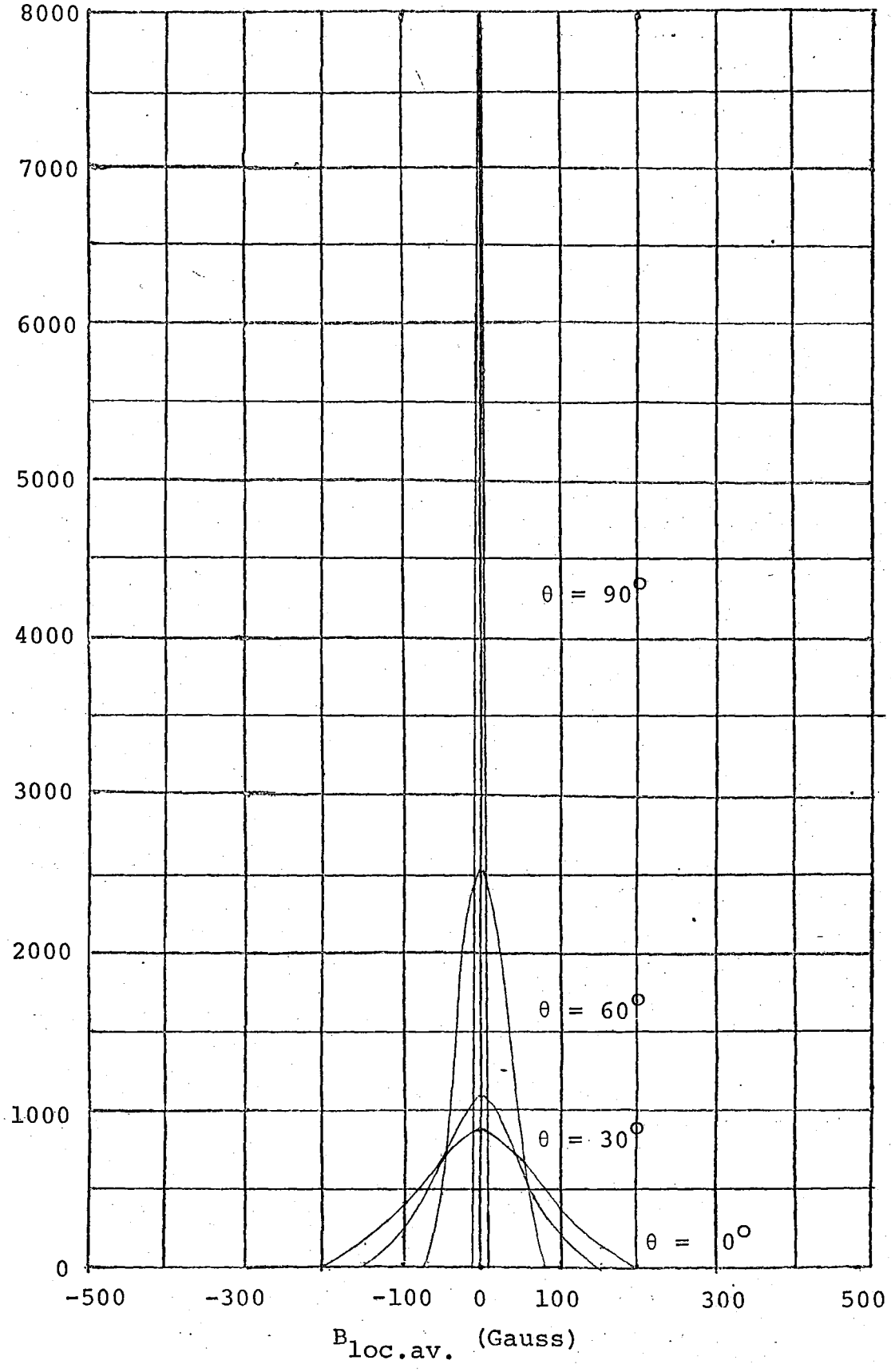

Figure 32

Motionally Narrowed Dipolar Broadening Distribution for $PrCl_3$

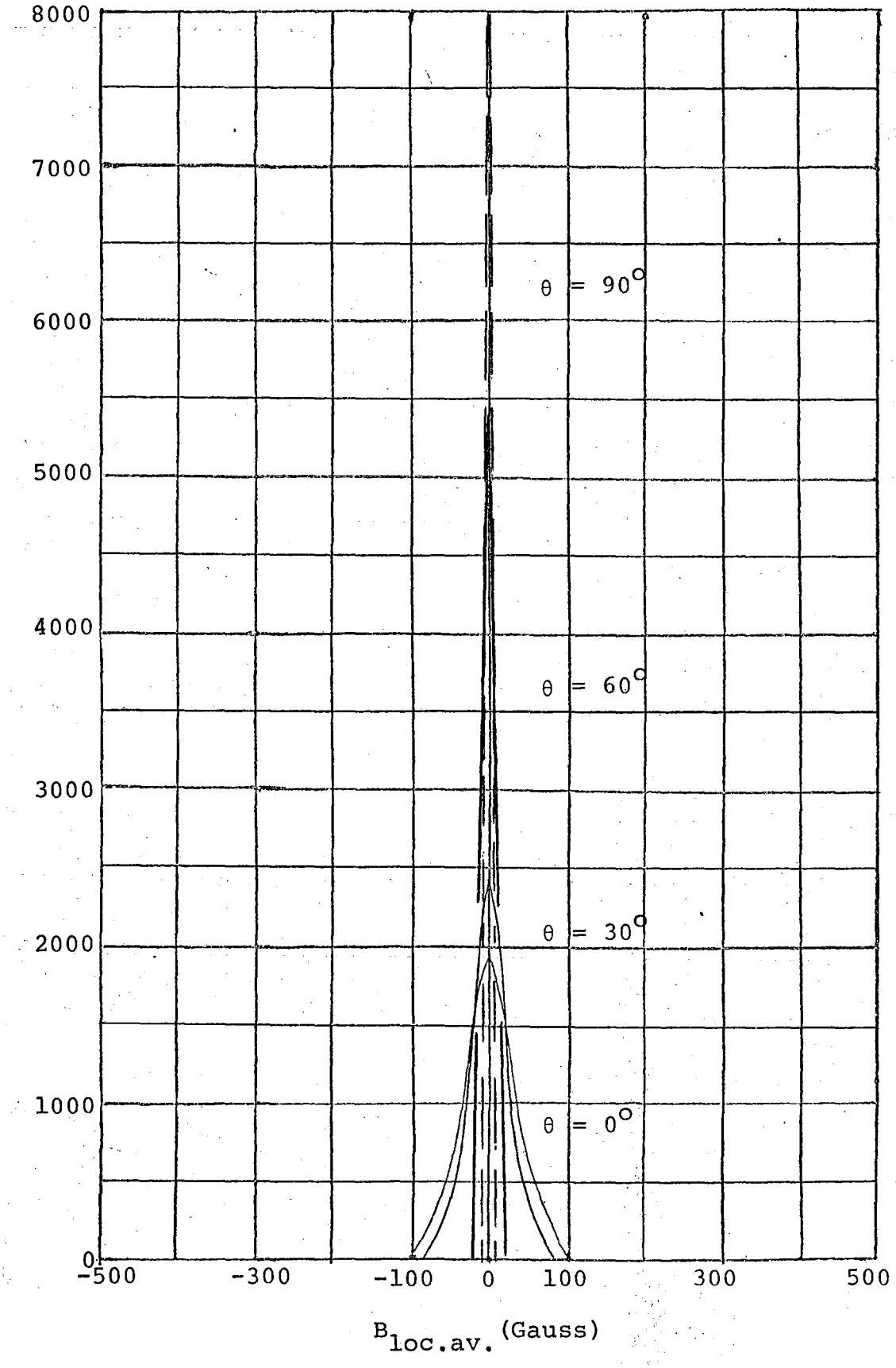

Figure 33

Motionally Narrowed Dipolar Broadening Distribution for NdCl.

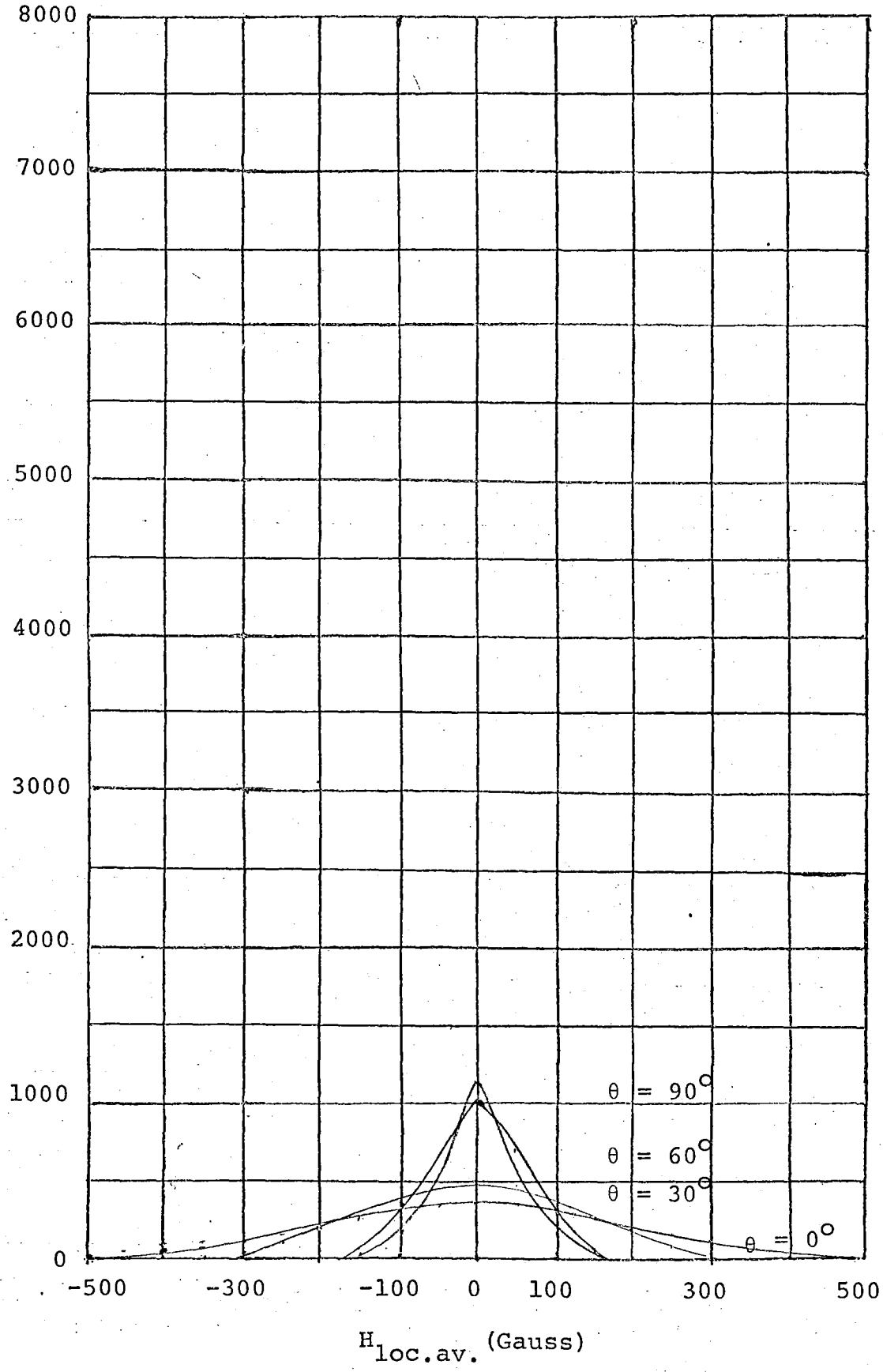

Resimulated Spectra of $CeCl_3$

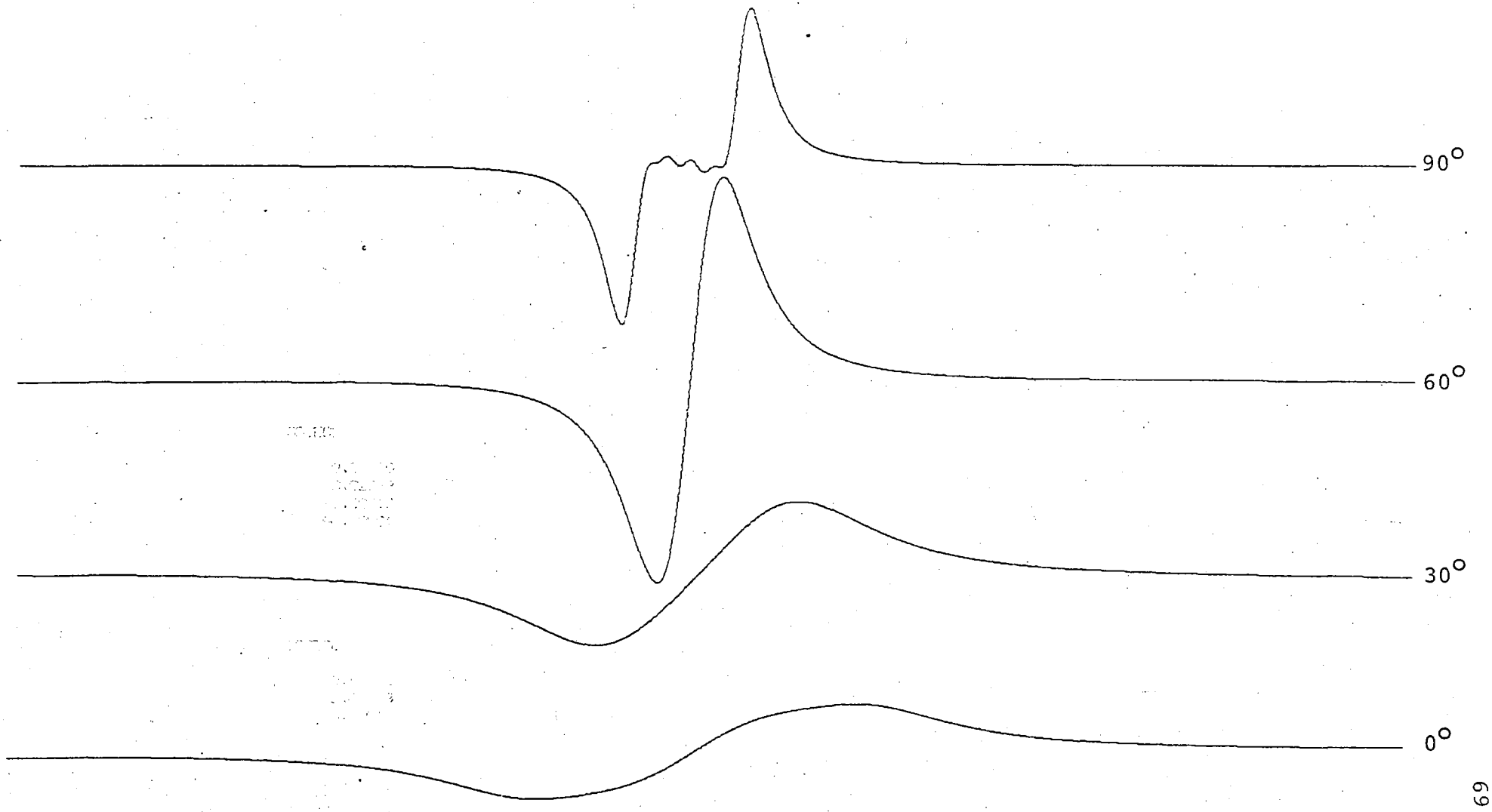

Resimulated Spectra of $PrCl_3$

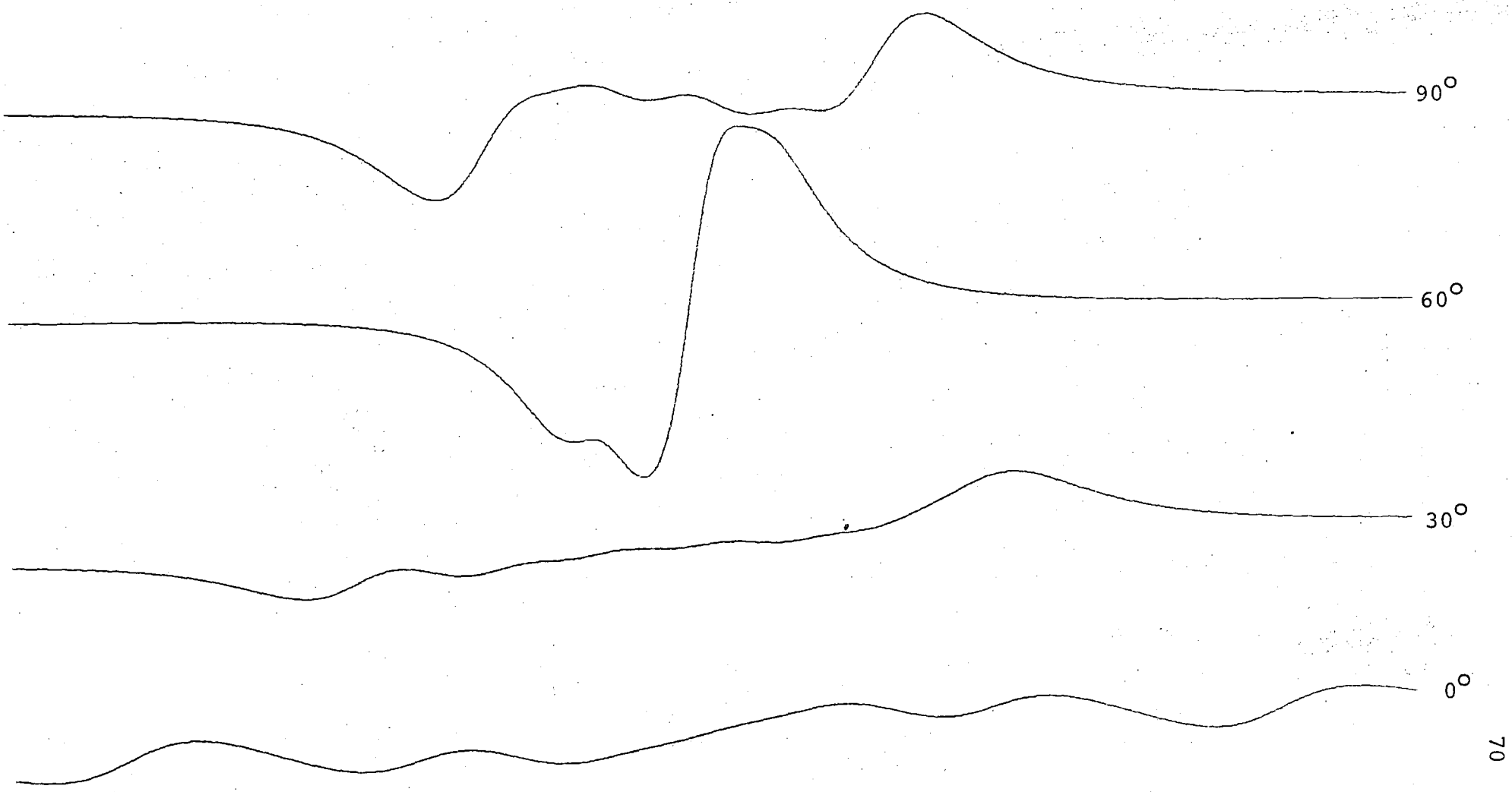

Resimulated Spectra of $NdCl_3$

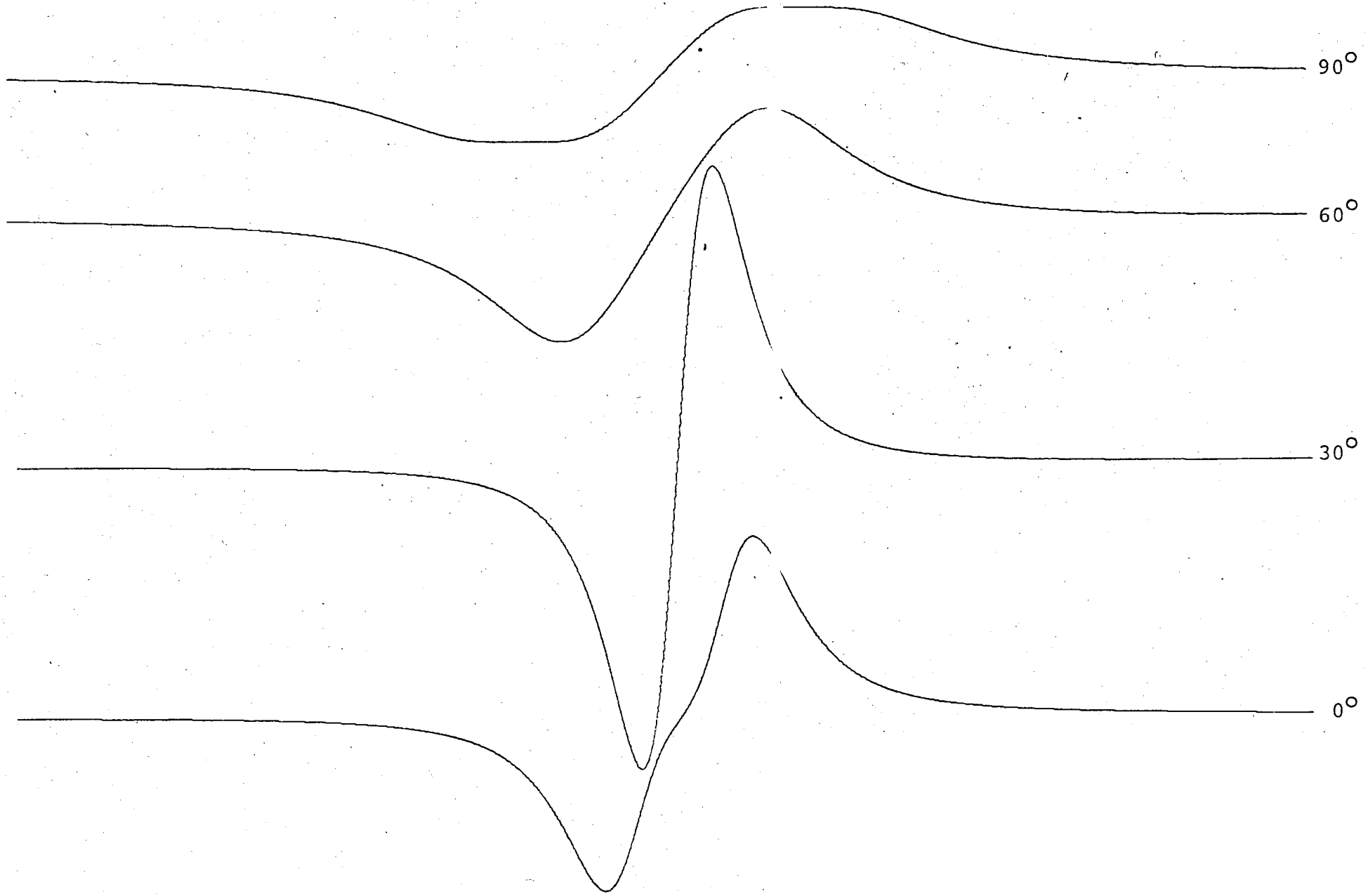

CHAPTER 5

DISCUSSION OF THE RESULTS

The parameters b_2^0, b_4^0, b_6^0

The values b_2^0, b_4^0, b_6^0 obtained have been determined by comparing simulated spectra with the actual spectra. The seven lines whose presence they characterise are not visible individually in any instance. The best example is that of Gd^{3+} in $PrCl_3$ where the lines are the most clearly resolved being furthest apart in this instance.

Let us consider what the parameters b_n^m represent in the Hamiltonian. In the free ion state (which is equivalent to having removed all neighbouring atoms to infinity) the $b_n^m = 0$, the effective potential in which the electrons exist having spherical symmetry. When neighbours are present certain of the b_n^m are non-zero, depending on the point symmetry of crystal which in turn dictates the angular properties of the crystal field potential. The radial properties of that part of the spin Hamiltonian describing the environmental effects are represented by the b_n^m and these can be pictured as representing the deviation of the effective electric field from that which would prevail in the free ion state. Bearing this in mind any effect which moves the neighbours relative to the dopant ion will produce charges in the values of the b_n^m. The methods available to effect such changes are (a) change of temperature, (b) stress, (c) change of host ions.

The effect of an increase in temperature is to move the neighbours away from the dopant ion and to lessen the "distortion" of the electric field, the magnitude of the large b_n^m decreasing.

When changes of host are considered the changes in lattice dimensions are nonlinear and the magnitude of the effective crystal field (which depends on a large number of mechanisms) will vary from host ion to host ion. The change in lattice dimensions occurring with change in host is thus not the only influence affecting the value of the b_n^m. Consequently although the $b_n^m \to 0$ as the lattice spacing $\to \infty$ the rates at which corresponding b_n^m, associated with isomorphic host lattices, decrease, can be expected to differ.

In this study methods (a) and (c) were used. As the temperature increased the value of b_2^0 which is large compared to b_4^0 and b_6^0 decreased, the spectrum contracting in width as expected. The changes in the b_n^m can be examined in table 5 . Over the range of temperatures examined in each case the contraction in the width of the spectrum was linear with increase in temperature.

The variation in the value of b_2^0 between hosts at the same temperature is indicated in table (5). In general as the host lattice dimensions decrease as one goes from host to host the value of b_2^0 increases. The exception to this is $NdCl_3$, the value of b_2^0 not having increased beyond that of $CeCl_3$ as much as its predecessor $PrCl_3$.

Width of the Resonance Lines

The observed spectra have lines much broader than in the case of Gd^{3+} in $LaCl_3$. The ions cerium, praseodymium and neodymium are paramagnetic and a model of dipolar broadening is used here to account for the width of the lines observed. Each local field H_i in the distribution of local fields has the form

$$H_i = g_{host}\,\mu_B \sum_{neighbours} \frac{3(\underset{\sim}{S}.\underset{\sim}{r}_{ij})\underset{\sim}{r}_{ij} - \underset{\sim}{S}\underset{\sim}{r}_{ij}^{\,2}}{r_{ij}^{\,5}}$$

The value of H_i in all instances increases as g increases and as r_{ij} decreases. The g values for the hosts employed are given in table 12, as given by Low[10].

Table 12

Host	Lattice constants a_0	c_0	$g_{\parallel}$	$g_{\perp}$	$g_{\parallel}/g_{\perp}$
$CeCl_3$	7.454Å	4.312Å	4.036	0.17	23.74
$PrCl_3$	7.423Å	4.272Å	1.035	0.1	10.35
$NdCl_3$	7.400Å	4.240Å	3.996	1.763	2.27

It is immediately obvious from the g values that with dipolar broadening the best $PrCl_3$ could be expected to have the clearest spectrum, and this is indeed the case. This correspondence adds weight to the choice of the dipolar broadening mechanism. There are two features of the local field distributions calculated using the static model which indicate that it is inadequate. For small angles the distributions consist of triplets the height of the central peak being $\simeq$ 2 x height of the outer peaks. These represent the situations where (a) most spins are parallel or anti-parallel to the external field and (b) approximately half the spins are pointing in opposite directions. This feature is not present in the observed spectra. The second feature is that the widths at half height of the calculated distributions are several times those observed, and significantly different from host to host.

The effect of motional narrowing is to average out the triplets and to narrow the distributions down as desired. The rates at which the local magnetic fields change are low compared to those observed in solutions, ions in a solid being more restrained in their movement. The parameters p, N are sufficient to describe the variation in line width. They appear to be fairly insensitive to changes in temperature - at least within the temperature range studied.

Study of Gd^{3+} in $PrCl_3$ at Liquid Helium Temperatures

The angular distributions of the spectra were much the same as at higher temperatures and the shape of the resonance curves very similar, the line widths being such that much overlap occurred. The magnetic field used was not very steady so simulation of the spectra was not worthwhile.

CHAPTER 6

Conclusions

This study has involved the use of a range of techniques; the simulation of the spectra by computer which enabled the seven lines of the spectrum to be located in a complex set of spectra, the precise orientation by X-ray diffraction, the double coating of the crystals was developed.

The spectral patterns correspond in their angular dependence to those obtained in the isomorphic hosts $LaCl_3$ and $EuCl_3$ when the same spin Hamiltonian is used.

The parameters b_2^0, b_4^0, b_6^0 determined lie between those of $CaCl_3$ and $EuCl_3$, however the increase in b_2^0 La → Eu is not monotonic, the value for $NdCl_3$ being less than that for $PrCl_3$. The effect of a decrease of temperature on b_2^0 is to increase its value, and when b_2^0 is viewed as characterising a distortion of the symmetry of the electric field from spherical, in the free ion state, contraction of the lattice as the temperature decreases can be expected to increase such a distortion.

The line widths have been accounted for by using a model of dipolar broadening where the dipoles flip randomly, interactions with the lattice being greater than intradipole interactions. The overall rate of flipping during the observation period is characterised by the parameter N while the influence of the different pathways for the flipping in different orientations are characterised by the factor p. Phonons propagate along rows of atoms in crystal lattices and so are directional in nature, and the disturbance caused by them to a set of dipoles aligned along the direction of an external magnetic field depends on the direction of the magnetic field. The parameter p varies for this reason and

has been defined as the probability that a host ion 'flips' its spin while a spin transition is taking place on a gadolinium ion.

The use of computer facilities enabled the simulation of the spectra, an otherwise formidable task, and the subsequent determination of the parameters b_2^0, b_4^0, b_6^0, N, p used to describe the line positions and line widths.

Future Work

The theory of motional narrowing could be applied to other cases where paramagnetic hosts broaden the E.S.R. spectra. An interesting study could be carried out at the melting point of such a crystal to observe the increase in motion as the lattice is destroyed, motional narrowing being commonly encountered in ligands. The effect on line width of the excitation of particular phonon modes while resonance studies were being carried out would be of interest. The changes in lattice dimension under stress and changes of temperature could be studied quantitatively and variations in the b_n^m related to variations in the cell dimensions.

REFERENCES

1. B. Bleaney, Phil. Mag. 42 (1951) 1062.
2. R.J. Elliott and K.W.H. Stevens, Roy. Soc. A219 (195) 387.
3. R.J. Elliott, Phil. Mag. 42 (1951) 1062.
4. H.E.D. Scovil, Phil. Mag. 42 (1951) 1062.
5. R.S. Trenam, Phil. Mag. 42 (1951) 1062.
6. C.A. Hutchinson, B.R. Judd and D.F.D. Pope, Proc. Phys. Soc. B70 (1957) 514.
7. A. Abragam and M.H.L. Pryce, Proc. Roy. Soc. A205 (1951) 135.
8. L.A. Boatner and M.M. Abraham, Phys. Rev. 163 (1967) 213-216.
9. W. Low and E.L. Offenbacher, Solid State Physics Series 17 (1965) 135-216.
10. W. Low, Solid State Physics Series Supplement 2 (1960).
11. M.T. Hutchings, Solid State Physics Series 16 (1964) 227-273.
12. R.J. Birgeneau, M.T. Hutchings and W.P. Wolf, Phys. Rev. 179 (1969) 275-288.
13. S.A. Al'tshuler and B.M. Kozyrev, Electron Paramagnetic Resonance, Academic Press (1964) 237.
14. W. Low, Solid State Physics Series Supplement 2 (1960) 113-136.
15. J.H. Van Vleck and W.G. Penney, Solid State Physics Series Supplement 2 (1960) 113.
16. B.G. Wybourne, Phys. Rev. 148 (1966) 317-327.
17. D.J. Newman, Adv. in Phys. Vol. 20, No. 84 (1971) 197.
18. M.L. Pryce, Proc. Phys. Soc. A63 (1950) 25.
19. K.W.H. Stevens, Proc. Phys. Soc. A65 (1952) 209.

20. B. Bleaney and K.W.H. Stevens, Rep. Progr. Phys. 16 (1953) 109-160, 150.

21. K. Shinagawa, Phys. Soc. of Japan Vol. 23, No. 5 (1967) 1057-1062.

22. The Powder Diffraction File: The American Society for Testing and Materials.

23. A.J. Freeman and R.E. Watson, Phys. Rev. 127 (1962) 2058.

24. C. Kittel, Introduction to Solid State Physics (Wiley 1967).

25. R. Ritchie, Crystal Growth Technician - University of Canterbury (Dept of Physics).

26. G.H. Stout & L.H. Jensen, X-ray Structure Determination (MacMillan 1968), 122.

27. Molasz. Computer program held in Dept of Chem., University

APPENDIX A

Computer Programs

This appendix contains the computer programs written in the course of this study. They have been documented with appropriate comments indicating the variables used and detailing the steps being performed. The programs are:

A1 The Hamiltonian Program

A2 The Plotting Program

A3 The Line Broadening Program.

A1 and A2 are presented as one unit as they were linked together in practice.

Following the programs a summary of the comments documenting the program A3 is also given.

```
0001            REAL MULT
0002            REAL*4 MTXA
0003            DIMENSION RED(9)
0004            DIMENSION AP(7)
0005            DIMENSION MTXA(36),RSLTA(64)
0006            DIMENSION ENGA(1000,7)
0007            DIMENSION Y(1565)
          C         ************ THE HAMILTONIAN PROGRAM ************
          C         SUMMARY.
          C         THIS PROGRAM SOLVES THE HAMILTONIAN BY DIAGONALISING THE MATRIX, AND
          C         FINDING THE ENERGY EIGENVALUES AT A GIVEN MAGNETIC FIELD THE
          C         PARAMETERS B_n^m HAVING BEEN SPECIFIED. IT REPEATS THIS AT A SEQUENCE
          C         OF MAGNETIC FIELDS, COMPARING THE TRANSITION ENERGIES OBTAINED
          C         WITH THE VALUE OF THE MICROWAVE ENERGY USED IN THE EXPERIMENT.
          C         IT FURTHER, INTERPOLATES BETWEEN MAGNETIC FIELDS NEARLY
          C         CORRESPONDING TO THE TRANSITION FIELD IN ORDER TO DETERMINE THE
          C         FIELD OF TRANSITION. THIS ENTIRE PROCESS IS REPEATED FOR DIFFERENT
          C         VALUES OF θ (THE ORIENTATION ANGLE)
          C         THE FIRST SECTION POSITIONS LINES ACCORDING TO THE MODEL
          C         SPECTRUM ( θ= 0 )
0008            KDEL = 20.0
0009            MULT = 2.7
          C         DIFF = D
0010            DIFF = 130
          C         OUTSD = O
0011            OUTSD = 417
          C         ALP = α
0012            ALP = (OUTSD*(MULT-1.0)*370.5 + 3.0*DIFF*(138.5*MULT + 93.0))
               */(740.5*(MULT-1.0)*54.0)
0013            SAJ = ALP
          C         BET = β
0014            BET = (OUTSD*(MULT-1.0)*85.5 - 3.0*DIFF*(25.0*MULT + 35.5))
               */(740.5*(MULT - 1.0)*9.0)
0015            TAJ = BET
          C         GAM = γ
0016            GAM = (OUTSD*(MULT-1.0)*8.0 - 3.0*DIFF*(11.0*MULT-14.0))
               */(740.5*(MULT-1.0))
0017            UAJ = GAM
0018            WRITE (6,4327) ALP ,BET ,GAM
0019         4327 FORMAT (1H ,3F20.8)
          C         THE PARAMETERS B_n^m ARE INTRODUCED
          C         B20 = b_02
          C         B40 = b_00
          C         B60 = b_06
0020            B20 = 2.11*2.78*SAJ
0021            B40 = 2.11*(2.8E-2)*TAJ
0022            B60 = 2.11*(5.08E-4)*UAJ
0023            B66 = 2.11*(3.0E-4)
          C         THE ORIENTATION IS SPECIFIED NT = θ
0024            NT = 90
0025            TN = NT
          C         TX =  θ (RADIANS)
0026            TX= 3.14159*TN/180.0
          C         THE MAGNETIC FIELD IS SPECIFIED AT 20GAUSS INTERVALS KDEL = Δ H
0027            DO 4001 KA = 20,1000,KDEL
0028            AK = KA
          C         BHA = H
0029            BHA = 2800 + AK
          C         THE NEXT SECTION DEALS WITH THE CALCULATION OF THE MATRIX
          C         ELEMENTS.
          C         GE = g_Gd
0030            GE = 1.991
0031            JA = 0
0032            DO 1002 JP = 1,15,2
0033            PJ = JP
          C         AW = M_s
0034            AW = (8.0-PJ)/2.0
          C         B = M_2
0035            B = AW**2
          C         C = M_4
0036            C = B**2
0037            Q = B**3
          C         Z = S(S+1)
0038            Z = 63.0/4.0
          C         F = S^2(S+1)^2
0039            F = Z**2
          C         S = S^3(S+1)^3
0040            S = Z**3
0041            NMO =  (JP+1)/2
          C         JA, JB, JC,...JH ARE USED TO PLACE THE MATRIX ELEMENTS IN THE
          C         MATRIX WHICH FOR THE COMPUTER IS REPRESENTED AS A SINGLE COLUMN ARRAY
          C         THE IBM ROUTINE EIGEN IS USED TO DIAGOLALISE THE MATRIX AND
          C         BEING SUITABLE FOR SYMMETRIC MATRICES ONLY REQUIRES THE UPPER
          C         TRIANGLE. THESE ARE NUMBERED AS INDICATED BELOW.
          C
          C          1  2  4  7 11 16 22 29
          C             3  5  8 12 17 23 30
          C                6  9 13 18 24 31
          C                  10 14 19 25 32
          C                     15 20 26 33
          C                        21 27 34
          C                           28 35
          C                              36
          C
          C         THE DIAGONAL ELEMENTS JA CAN BE PLACED BY NOTING THAT
          C         1, 3 ,6, 10,... CAN BE GENERATED BY THE CUMULATIVE ADDITION
          C         OF THE INTEGERS 1, 2, 3, ... THE SET, JB = 2, 5, 9, 14,...
          C         = (3-1), (6-1), (10-1),...
```

```
C          THUS THE LOOP CONTAINING JA = JA + NMO GENERATES THE POSITIONS
C          OF THE ELEMENTS. THE IF STATEMENTS INDICATE WHEN MATRIX ELEMENTS
C          ARE TO BE CALCULATED AND PLACES THEM AFTER THEY HAVE BEEN
C          CALCULATED.          MTXA(JA) = MATRIX ELEMENT
0042            JA = JA + NMO
0043            JB = JA-1
0044            JC = JA-2
0045            JD = JA-3
0046            JE = JA-4
0047            JF = JA-5
0048            JG = JA-6
0049            JH = JA-7
0050            IF (JH .GT. 21) MTXA(JH) = 0.0
0051            IF (JG .GT. 25) MTXA(30) = B66*720.0*SQRT(7.0)
0052            IF (JG .GT. 15) MTXA(22) = B66*720.0*SQRT(7.0)
0053            IF (JF .GT. 10) MTXA(JF) = 0.0
0054            IF (JE .GT.  6) MTXA(JE) = 0.0
0055            IF (JD .GT.  3) MTXA(JD) = 0.0
0056            IF (JC .GT.  1) MTXA(JC) = 0.0
0057            IF (JB .GT.  0) MTXA(JB) = BHA*SIN(TX)*(SQRT(Z-(B+AW)))
0058            P1 = GE*BHA*AW*COS(TX) + B20*(3.0*B-Z)
0059            P2 = B40*(35.0*C-((30.0*Z-25.0)*B+6.0*Z)+3.0*F)
0060            P3 = B60*(231.0*Q+B*(105.0*F-525.0*Z+294.0)+40.0*F)
0061            P4 = -(105.0*C*(3.0*Z-7.0) + 5.0*S+60.0*Z)*B60
0062            IF (JA .GT. 0) MTXA(JA) = P1 + P2 + P3 + P4
0063         1002 CONTINUE
C          END OF ELEMENTS
C          THE MATRIX IS DIAGONALISED... CALL EIGEN
0064            CALL EIGEN(MTXA,RSLTA,8,0)
C          THE EIGENVALUES ARE PRESENTED IN A COLUMN ARRAY.. CALL LOC
0065            DO 61 J = 1,8
0066            CALL LOC(J,J,JJ,8,8,1)
0067            DO 61 K = 1,8
0068            CALL LOC(J,K,JK,8,8,0)
0069           61 CONTINUE
0070            J = 0
0071            K=1
C          THE EIGHT ENERGY EIGENVALUES ARE STORED IN THE DIAGONAL POSITIONS
C           OF THE ARRAY BEING THOSE LABELLED BY 1, 3, 6, 10, 15, 21, 28, 36.
0072            DO 1003 L = 1,7
C          THE TRANSITION ENERGIES ALLOWED ARE THOSE BETWEEN CONSECUTIVE STATES.
C          THE POSITIONS OF THE EIGENVALUES REQUIRED, IN THE ARRAY, ARE GIVEN
C          BY J = J+L , K = K + L + 1 WHERE L LABELS THE TRANSITIONS
C          (L = 1,7)
0073            J = J + L
0074            K=K+L+1
C          THE TRANSITION ENERGY AT THE MAGNETIC FIELD CORRESPONDING
C          TO KA IS ENGA(KA,L)
0075            ENGA(KA,L) = MTXA(J) - MTXA(K)
0076            AAA = ABS(ENGA(KA,L) - 6555.0)
C          THE TRANSITION ENERGIES ARE NEXT COMPARED WITH THE MICROWAVE ENERGY.
C          IF A TRANSITION ENERGY IS CLOSE TO THE MICROWAVE ENERGY AN
C          INTERPOLATION IS CARRIED OUT TO FIND THE MAGNETIC FIELD
C          CORRESPONDING TO THE TRANSITION.
C
C
C
C            6555
C     ENGA(KA,L)
C
C
C     ENGA(MKA,L)
C
C
C
C
C
C
C
```

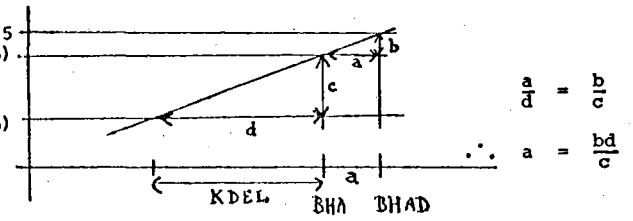

$$\frac{a}{d} = \frac{b}{c}$$

$$\therefore\ a = \frac{bd}{c}$$

```
0077            IF (AAA .GT. KDEL) GO TO 4321
0078            MKA = KA - KDEL
C               BHAD = BHA + a
C                  = (6555 -ENGA(KA,L))KDEL/(ENGA(KA,L) - ENGA(MKA,L))
C               THEREFORE BHAD = BHA + (6555-ENGA(KA,L))KDEL/(ENGA(KA,L)-ENGA(MKA,L))
C               BHAD = MAGNETIC FIELDS AT WHICH TRANSITIONS OCCUR
0079            BHAD = (6555.0-ENGA(KA,L))*KDEL/(ENGA(KA,L) - ENGA(MKA,L)) + BHA
C               FINALLY THE QUANTITIES BHA, BHAD, TN, J, K ARE PRINTED OUT
0080            WRITE (6,1605) BHA ,BHAD ,TN ,J ,K
0081         1605 FORMAT (1H ,3F20.8 ,2I5)
0082            AP(L) = BHAD
0083         4321 CONTINUE
0084         1003 CONTINUE
0085         4001 CONTINUE

C          ************ THE PLOTTING PROGRAM ************
C           THIS IS COUPLED TO THE HAMILTONIAN PROGRAM AND FOLLOWS IT.
C          SUMMARY
C          THIS PROGRAM CALCULATES THE LINE SHAPE OF THE SPECTRUM BEING
C          SIMULATED, AND CAUSES CERTAIN TITLES AND DATA TO BE RECORDED
C          ON PUNCHED CARDS. THE PUNCHED CARDS ARE USED AS DATA FOR THE
C          PDP/11 PLOTTER
C          THE LINE HEIGHT AND WIDTH ARE SET T = LINE HEIGHT
0086            T = 8000.0
0087         1235 DO 1245 NWDT = 12,15
C               JPX  = X COORDINATE
0088            DO 8002 JPX = 1,1564
C               Y(JPX) = Y COORDINATE
0089            Y(JPX) = 0.0
0090         8002 CONTINUE
```

```
C       . U = LINE WIDTH FACTOR = 1/K
0091          U = 0.001 + C.001*NWDT
0092          V = U**2
0093          DO 5051 JPX = 1,1564
C               THE GRAPH BEGINS AT 2800 GAUSS AND EXTENDS THROUGH 1000 GAUSS
C               OVER A DISTANCE OF 40CM. ZX = 2800 + JPX*1000.0/1564
0094          ZX = 2800.0 + JPX*1000.0/1564.0
0095          DO 1111 KAP = 1,7
C               CTA =  (x - a_i)
0096          CTA = ZX - AP(KAP)
0097          CTAA = V*CTA**2
C               THE CONTRIBUTION TO EACH OF THE SEVEN LINES ARE SUMMED
0098          Y(JPX) = Y(JPX) + T*V*CTA/((1.0 + CTAA)**2)
0099         1111 CONTINUE
0100         5051 CONTINUE
0101          CALL AINIT(1800)
0102          LOGICAL*1 LABEL1(6)/'GDPRCL'/
0103          CALL ALAB(400,200,LABEL1,6,1,2)
0104          DIMENSION T1(3)
C               THE VALUES OF B20  B40  B60, θ, 1/k, LINE HEIGHT, WIDTH, M, D,
C               O ARE PRINTED OUT
0105          RED(1) = B20
0106          RED(2) = B40
0107          RED(3) = B60
0108          RED(4) = NT
0109          RED(5) = T
0110          RED(6) = U
0111          RED(7) = MULT
0112          RED(8) = DIFF
0113          RED(9) = OUTSD
0114          DO 789 IPY = 1,9
0115          T1(1) = RED(IPY)
0116          CALL FMT('F',12,5,T1)
0117         789 CALL ALAB(400,180-20*IPY,T1,12,1,2)
C               THE SUBROUTINE ALINEX INSTRUCTS THE PLOTTER HOW TO POSITION THE GRAPH.
0118          CALL ALINEX(100,1,Y,1564,-500.0,100.0)
0119          CALL AEND
0120         1245 CONTINUE
0121         9000 CONTINUE
0122         4568 CONTINUE
0123         4566 CONTINUE
0124         5598 CONTINUE
0125         4444 CONTINUE
0126         4567 CONTINUE
0127          STOP
0128          END
```

```
            C     BEGINNING OF EIGEN
C001              SUBROUTINE EIGEN(A,R,N,MV)
C002              DIMENSION A(1),R(1)
C003            5 RANGE=1.0E-12
C004              IF(MV-1) 10,25,10
C005           10 IQ = -N
C006              DO 20 J = 1,N
C007              IQ=IQ+N
C008              DO 20 I=1,N
0009              IJ = IQ+I
0010              R(IJ) = 0.0
0011              IF(I-J) 20,15,20
0012           15 R(IJ) = 1.0
0013           20 CONTINUE
0014           25 ANORM = 0.0
0015              DO 35 I=1,N
C016              DO 35 J=1,N
0017              IF(I-J) 30,35,30
0018           30 IA=I+(J*J-J)/2
0019              ANORM = ANORM + A(IA)*A(IA)
0020           35 CONTINUE
0021              IF(ANORM) 165,165,40
C022           40 ANORM = 1.414*SQRT(ANORM)
0023              ANRMX=ANORM*RANGE/FLOAT(N)
0024              IND = 0
0025              THR = ANORM
0026           45 THR = THR/FLOAT(N)
0027           50 L=1
0028           55 M=L+1
0029           60 MQ=(M*M-M)/2
C030              LQ = (L*L-L)/2
0031              LM=L+MQ
0032           62 IF(ABS(A(LM))-THR) 130,65,65
0033           65 IND=1
0034              LL = L+LQ
0035              MM= M+MQ
0036              X=0.5*(A(LL)-A(MM))
0037           68 Y=-A(LM)/SQRT(A(LM)*A(LM)+X*X)
0038              IF(X) 70,75,75
0039           70 Y = -Y
C040           75 SINX=Y/SQRT(2.0*(1.0+(SQRT(1.0-Y*Y))))
0041              SINX2 = SINX*SINX
0042           78 COSX = SQRT(1.0-SINX2)
0043              COSX2 = COSX*COSX
0044              SINCS = SINX*COSX
0045              ILQ= N*(L-1)
0046              IMQ = N*(M-1)
0047              DO 125 I= 1,N
0048              IQ=(I*I-I)/2
0049              IF(I-L) 80,115,80
0050           80 IF(I-M) 85,115,90
0051           85 IM= I+ MQ
0052              GO TO 95
0053           90 IM= M+IQ
0054           95 IF(I-L) 100,105,105
0055          100 IL = I+LQ
0056              GO TO 110
0057          105 IL = L+IQ
0058          110 X=A(IL)*COSX-A(IM)*SINX
0059              A(IM)= A(IL)*SINX+A(IM)*COSX
0060              A(IL)=X
0061          115 IF(MV-1) 120,125,120
0062          120 ILR=ILQ+I
0063              IMR = IMQ+I
0064              X=R(ILR)*COSX-R(IMR)*SINX
0065              R(IMR) = R(ILR)*SINX+R(IMR)*COSX
0066              R(ILR) =X
0067          125 CONTINUE
0068              X = 2.0*A(LM)*SINCS
0069              Y=A(LL)*COSX2+A(MM)*SINX2-X
0070              X=A(LL)*SINX2+A(MM)*COSX2+X
0071              A(LM)=(A(LL)-A(MM))*SINCS+A(LM)*(COSX2-SINX2)
0072              A(LL)=Y
0073              A(MM)=X
0074          130 IF(M-N) 135,140,135
0075          135 M=M+1
0076              GO TO 60
0077          140 IF(L-(N-1)) 145,150,145
0078          145 L=L+1
0079              GO TO 55
0080          150 IF(IND-1) 160,155,160
0081          155 IND=0
0082              GO TO 50
0083          160 IF(THR-ANRMX) 165,165,45
0084          165 IQ=-N
0085              DO 185 I=1,N
0086              IQ=IQ+N
0087              LL=I+(I*I-I)/2
0088              JQ=N*(I-2)
0089              DO 185 J=I,N
0090              JQ=JQ+N
0091              MM=J+(J*J-J)/2
0092              IF(A(LL)-A(MM)) 170,185,185
0093          170 X=A(LL)
0094               A(LL)=A(MM)
0095              A(MM)=X
0096              IF(MV-1) 175,185,175
0097          175 DO 180 K=1,N
```

```
0098            ILR=IQ+K
0099            IMR=JQ+K
0100            X = R(ILR)
0101            R(ILR)=R(IMR)
0102          180 R(IMR)=X
0103          185 CONTINUE
0104            RETURN
0105            END
```



```
0001            SUBROUTINE LOC(I,J,IR,N,M,MS)
0002            IX=I
0003            JX=J
0004            IF(MS-1) 10,20,30
0005           10 IRX=N*(JX-1)+IX
0006              GO TO 36
0007           20 IF(IX-JX) 22,24,24
0008           22 IRX = IX+(JX*JX-JX)/2
0009              GO TO 36
0010           24 IRX=JX+(IX*IX-IX)/2
0011              GO TO 36
0012           30 IRX=0
0013              IF(IX-JX) 36,32,36
0014           32 IRX = IX
0015           36 IR=IRX
0016              RETURN
0017              END
```

Example of Computer Output of Results

B20	B40	B60		
1.6	0.3	-0.0		
Approximate Magnetic Field for Transition	Interpolated Magnetic Field	Orientation (degrees)	Eigenvalue Identifiers for Transitions	
3200.0	3191.1	0.0	1	1
3240.0	3238.3	0.0	3	6
3280.0	3270.9	0.0	6	10
3300.0	3292.3	0.0	10	15
3320.0	3313.6	0.0	15	21
3340.0	3346.3	0.0	21	28
3400.0	3393.5	0.0	28	36
3240.0	3231.5	30.0	1	3
3260.0	3252.0	30.0	3	6
3280.0	3270.2	30.0	6	10
3280.0	3288.9	30.0	10	15
3300.0	3307.5	30.0	15	21
3320.0	3325.0	30.0	21	28
3340.0	3343.0	30.0	28	36
3260.0	3265.6	60.0	28	36
3280.0	3286.5	60.0	3	6
3280.0	3282.9	60.0	6	10
3280.0	3281.5	60.0	10	15
3280.0	3279.7	60.0	15	21
3280.0	3275.0	60.0	21	28
3300.0	3295.3	60.0	1	3
3240.0	3244.7	90.0	21	28
3240.0	3238.4	90.0	28	36
3260.0	3260.7	90.0	15	21
3280.0	3277.1	90.0	10	15
3300.0	3293.9	90.0	6	10
3320.0	3316.9	90.0	1	3
3320.0	3310.4	90.0	3	6

```
C001              IMPLICIT INTEGER (C-R),REAL(M)
C002              DIMENSION EEMN(1200)
C003              DIMENSION SMNKA(14,14)
C004              DIMENSION SMNPG(14,14)
C005              DIMENSION GMN(14,14,14)
C006              DIMENSION MN(14,14,14)
C007              DIMENSION BAB(300)
C008              DIMENSION BBB(60)
C009              DIMENSION A(3000,13)
0010              DIMENSION SSMNPG(14,14)
0011              DIMENSION BB(300,13)
C012              REAL KMNF,IMKMNF,JMIPKF,NMJPKF,JMNF,NMIF,NMNF
C013              DIMENSION X(3,28)
C014              DIMENSION SUM(3)
C015              DIMENSION M(3)
C016              DIMENSION VECOFA(28)
C017              DIMENSION VECOFB(28)
C018              DIMENSION BC(3,14)
C019              DIMENSION PRESM(14)
C020              DIMENSION S5(28)
C021              DIMENSION S3(28)
0022              DIMENSION SA(28)
C023              DIMENSION R(27,28)
C024              DIMENSION SUMA(3)
C025              DIMENSION SUM7(3)
C026              DIMENSION SUM8(3)
C027              DIMENSION SUM9(3)
C028              DIMENSION SUM10(3)
C029              DIMENSION SUM11(3)
C030              DIMENSION SUM12(3)
C031              DIMENSION SUM13(3)
C032              DIMENSION SUM14(3)
0033              DIMENSION SUM15(3)
C034              DIMENSION SUM16(3)
C035              DIMENSION SUM17(3)
C036              DIMENSION SUM18(3)
C037              DIMENSION SUM19(3)
C038              DIMENSION SUM20(3)
C039              DIMENSION ZFF(15)
C040              DIMENSION SMNK(14,14)
0041              DIMENSION SISMNK(14)
C042              DIMENSION HMN(14,14)
C043              DIMENSION HHMN(14,14)
C044              DIMENSION EMN(3000)
                  C          ************LINE BROADENING PROGRAM************
                  C            SUMMARY
                  C            THIS PROGRAM CALCULATES ALL THE POSSIBLE LOCAL MAGNETIC
                  C            FIELDS DUE TO 14 NEIGHBOURING IONS THEREBY PRODUCING
                  C            THE DISTRIBUTION OF LOCAL FIELDS FOR STATIC DIPOLAR
                  C            BROADENING. IT ALSO CALCULATES THE DISTRIBUTION WHEN MOTIONAL
                  C            NARROWING IS TAKEN INTO CONDIDERATION USING THE FIELDS
                  C            CALCULATED IN THE FIRST PART AS A BASIS FOR THIS FURTHER
                  C            CALCULATION.
                  C            THE PROGRAM BEGINS BY SPECIFYING THE CRYSTAL LATTICE
                  C            DIMENSIONS AND ION POSITIONS AND CALCULATES THE INTERIONIC
                  C            DISTANCES REQUIRED
                  C            AR = a0
C045              AR = 4.272
                  C            DR = c0
C046              DR = 7.423
C047              AM = 9270.0
0048              ARR = AR/2.0
C049              DRR = DR/2.0
C050              DRRR = DR/(SQRT(3.0))
C051              DRRRR = DR/(2.0*SQRT(3.0))
                  C            X(I,J) IS THE ITH COMPONENT OF THE POSITION OF THE JTH
                  C            NEIGHBOURING ION.
C052              X(1,1)=0.0
C053              X(1,2)=0.0
C054              X(1,3)=DRR
C055              X(1,4)=-DRR
C056              X(1,5)=0.0
C057              X(1,6)=DRR
0058              X(1,7)=-DRR
C059              X(1,8)=0.0
C060              X(2,1)=0.0
C061              X(2,2)=DRRR
0062              X(2,3)=-DRRRR
C063              X(2,4)=-DRRRR
C064              X(2,5)=DRRR
C065              X(2,6)=-DRRRR
C066              X(2,7)=-DRRRR
C067              X(2,8)=0.0
C068              X(3,1)=AR
C069              X(3,2)=ARR
C070              X(3,3)=ARR
C071              X(3,4)=ARR
C072              X(3,5)=-ARR
0073              X(3,6)=-ARR
C074              X(3,7)=-ARR
C075              X(3,8)=-AR
C076              DO 320 K=9,14
C077              X(3,K)=0.0
C078            320 CONTINUE
C079              DO 324 K=9,9
C080              X(1,K)=DRR
C081              X(2,K)=DR*SQRT(3.0)/2.0
C082            324 CONTINUE
```

```
C083              DO 325 K=10,10
C084              X(1,K)=DR
C085              X(2,K)=0.0
C086            325 CONTINUE
C087              DO 326 K=11,11
C088              X(1,K)=DRR
C089              X(2,K)=-DR*SQRT(3.0)/2.0
C090            326 CONTINUE
C091              DO 327 K=12,12
C092              X(1,K)=-DRR
C093              X(2,K)=-DR*SQRT(3.0)/2.0
C094            327 CONTINUE
C095              DO 328 K=13,13
C096              X(1,K)=-DR
C097              X(2,K)=0.0
C098            328 CONTINUE
C099              DO 329 K=14,14
C100              X(1,K)=-DRR
C101              X(2,K)=DR*SQRT(3.0)/2.0
C102            329 CONTINUE
                C         THE PARAMETERS FOR NARROWING  ARE SPECIFIED
                C         WDTFAC = N
C103              WDTFAC = 2.0
                C         PMN = p
C104              PMN = 0.92
C105              WRITE(6,9736) PMN
C106           9736 FORMAT (2H ,1E20.5)
                C         THE FACTORIALS 1! TO 14! ARE CALCULATED ZFF(NNNNM)=FACTORIAL OF NNNNM
C107              DO 961 NNNNM=1,14
C108              ZFF(NNNNM)=0.0
C109            961 CONTINUE
C110              SSMN=1.0
C111              DO 930 NNNNM=1,14
C112              ZNN=NNNNM
C113              SSMN=SSMN*ZNN
C114              ZFF(NNNNM)=SSMN
C115            930 CONTINUE
                C         JMN = j
C116              DO 901 JMN=1,14
                C         IMN = i
C117              DO 902 IMN=1,JMN
C118              LMN=IMN+1
C119              NNM=15-JMN
C120              NNNM=14-JMN
C121              IF(IMN.LE.NNNM) GO TO 981
C122              DO 918 KMNA=1,NNM
C123              NMN=14
                C         KMN = k
C124              KMN=KMNA-1
                C         IMK = i-k
C125              IMK=IMN-KMN
                C         JMIPK = (j-i)+k
C126              JMIPK=(JMN-IMN)+KMN
                C         NMJPK = n-(j+k)
C127              NMJPK=NMN-(JMN+KMN)
C128              IF(IMK.LE.0) IMKMNF=1
C129              IF(IMK.GT.0) IMKMNF=ZFF(IMK)
C130              IF(NMJPK.LE.0) NMJPKF=1
C131              IF(NMJPK.GT.0) NMJPKF=ZFF(NMJPK)
C132              IF(JMIPK.LE.0) JMIPKF=1
C133              IF(JMIPK.GT.0) JMIPKF=ZFF(JMIPK)
C134              IF(KMN.LE.0) KMNF=1
C135              IF(KMN.GT.0) KMNF=ZFF(KMN)
C136              NMNF=ZFF(NMN)
C137              IMNF=ZFF(IMN)
                C         NMI = n-i
C138              NMI=NMN-IMN
                C         AS 0! IS AN INVALID INDEX IT IS NECESSARY TO MANIPULATE k IN
                C         ORDER THAT IT IS REPRESENTED AS NONZERO IN ALL  INSTANCES
                C         AND ALSO TO DEFINE 0! AS 1
C139              IF(NMI.GT.0) NMIF=ZFF(NMI)
C140              IF(NMI.LE.0) NMIF=1
                C         THIS SECTION CALCULATES THE PROBABILITIES FOR CONFIGURATION
                C         TYPE CHANGES. THE CALCULATION OF MN IS DONE IN 2 PARTS AS IT
                C         HAS 2 RESTRICTIONS APPLYING TO IT
C141              MN(IMN,JMN,KMNA)=IMNF*NMIF/(KMNF*IMKMNF*JMIPKF*NMJPKF)
C142            918 CONTINUE
                C         THE SUMMATION OVER k IS NEXT CARRIED OUT IN TWO STEPS
                C         1. IMN ≤ JMN, 2. IMN > JMN
                C         MN(IMN,JMN,KMNA) = N_ij(k)
C143              IF(IMN.GT.NNNM) GO TO 985
C144            981 DO 903 KMNA=1,LMN
C145              NMN=14
C146              KMN=KMNA-1
C147              IMK=IMN-KMN
C148              JMIPK=(JMN-IMN)+KMN
C149              NMJPK=NMN-(JMN+KMN)
C150              IF(IMK.LE.0) IMKMNF=1
C151              IF(IMK.GT.0) IMKMNF=ZFF(IMK)
C152              IF (NMJPK.LE.0) NMJPKF=1
C153              IF(NMJPK.GT.0) NMJPKF=ZFF(NMJPK)
C154              IF(JMIPK.LE.0) JMIPKF=1
C155              IF(JMIPK.GT.0) JMIPKF=ZFF(JMIPK)
C156              IF(KMN.LE.0) KMNF=1
C157              IF(KMN.GT.0) KMNF=ZFF(KMN)
C158              NMNF=ZFF(NMN)
C159              IMNF=ZFF(IMN)
C160              NMI=NMN-IMN
```

```
C161              IF(NMI.GT.0) NMIF=ZFF(NMI)
C162              IF(NMI.LE.0) NMIF=1
C163              MN(IMN,JMN,KMNA)=MNF*NMIF/(KMNF*IMKMNF*JMIPKF*NMJPKF)
C164            902 CONTINUE
C165            985 CONTINUE
C166            902 CONTINUE
C167            901 CONTINUE
C168              DO 904 JMN=1,14
C169              DO 905 IMN=1,JMN
C170              LMN=IMN+1
C171              NNM=15-JMN
C172              NNNM=14-JMN
C173              MNK=0.0
C174              IF(IMN.LE.NNNM) GO TO 984
C175              DO 916 KMNA=1,NNM
C176              MNK=MNK+MN(IMN,JMN,KMNA)
C177            916 CONTINUE
C178              IF(IMN.GT.NNNM) GO TO 982
C179            984 DO 906 KMNA=1,LMN
C180              MNK=MNK+MN(IMN,JMN,KMNA)
C181            906 CONTINUE
C182            982 CONTINUE
                C       SMNK(IMN,JMN) =   Σ   MN(IMN,JMN,KMNA)   =  Σ  N_ij(k)
C183                    SMNK(IMN,JMN)=MNK    KMNA                    k
C184              NMN=14
C185              NMI=NMN-IMN
C186            905 CONTINUE
C187            904 CONTINUE
                C       THE NEXT SECTION IS THAT OF CALCULATING GMN(IMN,JMN,KMNA)
                C       GMN(IMN,JMN,KMNA) = N_ij(k) / Σ N_ij(k)
                C                                    KMNA
                C       AND AGAIN IS DONE IN TWO PARTS KMNA BEING SUBJECT TO THE TWO
                C       CONDITIONS AS BEFORE.
C188              DO 9112 JMN=1,14
C189              DO 9113 IMN=1,JMN
C190              LMN=IMN+1
C191              NNM=15-JMN
C192              NNNM=14-JMN
C193              IF(IMN.LE.NNNM) GO TO 9116
C194              DO 9114 KMNA=1,NNM
C195              GMN(IMN,JMN,KMNA)=MN(IMN,JMN,KMNA)/SMNK(IMN,JMN)
C196            9114 CONTINUE
C197              IF(IMN.GT.NNNM) GO TO 9131
C198            9116 DO 9117 KMNA=1,LMN
C199              GMN(IMN,JMN,KMNA)=MN(IMN,JMN,KMNA)/SMNK(IMN,JMN)
C200            9117 CONTINUE
C201            9131 CONTINUE
C202            9113 CONTINUE
C203            9112 CONTINUE
                C       THE NEXT SECTION CALCULATES THE AVERAGE PROBABILITY.
C204              DO 9121 JMN=1,14
C205              DO 9122 IMN=1,JMN
C206              LMN=IMN+1
C207              NNM=15-JMN
C208              NNNM=14-JMN
C209              SMNP=0.0
C210              IF(IMN.LE.NNNM) GO TO 9123
C211              DO 9125 KMNA=1,NNM
C212              KMN=KMNA-1
C213              SMNP=SMNP+GMN(IMN,JMN,KMNA)*(PMN**((JMN-IMN)+2*KMN))
C214            9125 CONTINUE
C215              IF(IMN.GT.NNNM) GO TO 9127
C216            9123 DO 9128 KMNA=1,LMN
C217              KMN=KMNA-1
C218              SMNP=SMNP+GMN(IMN,JMN,KMNA)*(PMN**((JMN-IMN)+2*KMN))
C219            9128 CONTINUE
C220            9127 CONTINUE
                C       THE VALUES OF SMNPG(IMN,JMN) = P_ij   = Σ p_ij(k) x GMN ARE
                C       CALCULATED FOR ALL i,j (1≤i≤j≤n)^ij    k
C221              SMNPG(IMN,JMN)=SMNP
                C       FINALLY THE DIVISOR IN THE AVERAGE PROBABILITY IS CALCULATED
                C       AND ALSO MULTIPLIED BY N.
                C       SSMNPG(IMN,JMN) = (1.0 + P  )N
C222              SSMNPG(IMN,JMN) = (1.0 + SMNP)*WDTFAC
                C       THE VALUES OF SMNPG(IMN,JMN), IMN, JMN ARE WRITTEN OUT.
C223              WRITE(6,9216)SSMNPG(IMN,JMN),IMN,JMN
C224            9216 FORMAT(1H ,1F20.8,2I10)
C225            9122 CONTINUE
C226            9121 CONTINUE
C227            1909 CONTINUE
                C       THE POSSIBLE LOCAL FIELDS AT PARTICULAR ORIENTATIONS ARE
                C       CALCULATED NEXT.
                C       THE ORIENTATIONS ARE SPECIFIED   NT = 0   AND ARE WRITTEN OUT
                C       UNDER THE HEADING 'ANGLE'.
C228              DO 7578 NT = 0,90,30
C229              TN=NT
C230              WRITE(6,7354)
C231            7354 FORMAT (' ANGLE')
C232              WRITE(6,7355) NT
C233            7355 FORMAT (1H ,I15)
C234              TX=TN*3.14159/180.0
                C       THE LOCAL MAGNETIC FIELDS ARE CALCULATED BY FIRSTLY
                C       OBTAINING THE LOCAL FIELD WITH ALL SPINS UP AND SUBSEQUENTLY
                C       SUBTRACTING THE RELEVANT AMOUNT.
                C       NCN SPECIFIES THE COMPONENTS IN A CARTESIAN SYSTEM
C235              DO 4002 NCN=1,3,2
C236              SUM(NCN)=0.0
C237              M(NCN)=0.0
                C       K  SPECIFIES THE ION
```

```
C238            DO 4004 K=1,14
0239            BC(NCN,K)=0.0
C240        4004 CONTINUE
C241        4002 CONTINUE
C242            WRITE(6,7935)
C243        7935 FORMAT (' GOPROCL')
C               M(1) = (μg SIN0)/2
0244            M(1) = AM*(0.100/2.0)*SIN(TX)
C               M(3) = (μg Cos0)/2.
C245            M(3) = AM*(1.035/2.0)*COS(TX)
C
0246            DO 250 NCN=1,3,2
C247            PRESM(NCN)=0.0
C248            DO 500 K=1,14
C                   THE DISTANCE TO ATOM K IS CALCULATED . SA(K) = |r_k|
0249            SA(K)=SQRT(X(1,K)**2+X(2,K)**2+X(3,K)**2)
C                   S3(K) = |r_k|^3
C250            S3(K)=SA(K)**3
C                   S5(K) = |r_k|^5
C251            S5(K)=SA(K)**5
C252            VECOFA(K)=3.0*(M(1)*X(1,K)+M(3)*X(3,K))/S5(K)
C253            VECOFB(K)=1.0/S3(K)
C254          500 CONTINUE
C255            DO 601 K=1,8
C256            BC(NCN,K)=X(NCN,K)*VECOFA(K)-M(NCN)*VECOFB(K)
C                   PRESM(NCN) IS THE LOCAL FIELD WITH ALL SPINS UP AND IS
C                   CALCULATED FOR 14 NEIGHBOURS.
C257            PRESM(NCN)=PRESM(NCN)+BC(NCN,K)
C258          601 CONTINUE
C259            DO 600 K=9,14
C260            BC(NCN,K)=(X(NCN,K)*VECOFA(K)-M(NCN)*VECOFB(K))
C261            PRESM(NCN)=PRESM(NCN)+BC(NC,K)
C262          600 CONTINUE
0263          250 CONTINUE
C                   THE AMOUNTS TO BE SUBTRACTED ARE CALCULATED IN A SET OF
C                   NESTED 'DO LOOPS'. THE NEST CAN BE ENTERED AT ANY POINT, AND
C                   LEFT AFTER THE LOOPS INTERIOR TO THE ONE AT WHICH IT WAS
C                   ENTERED HAVE BEEN EXECUTED. THE NUMBER OF INTERIOR LOOPS IS
C                   EQUAL TO THE NUMBER OF SPINS DOWN.
C                   ENTERING THE INNERMOST LOOP TURNS DOWN EACH OF THE 14 SPINS
C                   IN SUCCESSSION. ENTERING THE SECOND  TO INNERMOST LOOP TURNS
C                   DOWN ALL COMBINATIONS OF TWO SPINS, AND SO ON FOR GREATER
C                   NUMBERS OF LOOPS.
0264            DO 700 J=1,13
0265            DO 89 IIH=1,3000
C266            A(IIH,J)=0.0
C267          89 CONTINUE
0268            DO 5456 JJJJ=1,300
0269            BB(JJJJ,J) = 0.0
C270        5456 CONTINUE
0271            DO 92 NCN=1,3,2
C272            SUM7(NCN)=0.0
C273            SUM8(NCN)=0.0
C274            SUM9(NCN)=0.0
C275            SUM10(NCN)=0.0
C276            SUM11(NCN)=0.0
C277            SUM12(NCN)=0.0
C278            SUM13(NCN)=0.0
C279            SUM14(NCN)=0.0
C280            SUM15(NCN)=0.0
C281            SUM16(NCN)=0.0
0282            SUM17(NCN)=0.0
0283            SUM18(NCN)=0.0
0284            SUM19(NCN)=0.0
0285            SUM20(NCN)=0.0
0286          92 CONTINUE
0287            DO 101 N=1,13
0288            IF(J.EQ.N) GO TO 100
0289            IF(J.NE.N) GO TO 101
0290        100 CONTINUE
0291            NA=N+1
0292            R(J,NA)=1
0293            GO TO (502,503,504,505,506,507,508,509,510,511,512,513,514) ,N
C294        514 CONTINUE
C                   THE SPINS WHICH ARE DOWN ARE LABELLED BY THE QI AND IN EACH
C                   LOOP THERE ARE TWO SUBLOOPS BY WHICH EACH OF THE CONTRIBUTING
C                   IONS IS TESTED TO SEE IF IT IS QI AND IF SO THE COMPONENTS OF
C                   ITS DIPOLAR INTERACTION BC(NCN,K) ARE DOUBLED AND ADDED TO THE
C                   SUM (RUNNING ADJACENT TO THE LOOPS) SUMJ(NCN) WHICH IS SUBTRACTED
C                   FROM PRESM(NCN) OBTAINING H_loc    SUM(NCN) = H_loc
0295          53 DO 13 Q13=1,2
0296            DO 423 K=1,14
0297            DO 222 NCN=1,3,2
0298            IF(K.EQ.Q13)SUM19(NCN)=SUM20(NCN)+BC(NCN,K)*2.0
0299        222 CONTINUE
0300        423 CONTINUE
0301            R(J,13)=Q13+1
0302        513 I13=R(J,13)
0303         52 DO 12 Q12=I13,3
0304            DO 422 K=1,14
0305            DO 221 NCN=1,3,2
0306            IF(K.EQ.Q12) SUM18(NCN)=SUM19(NCN)+BC(NCN,K)*2.0
0307        221 CONTINUE
0308        422 CONTINUE
0309            R(J,12)=Q12+1
0310        512 I12=R(J,12)
0311         51 DO 11 Q11=I12,4
C312            DO 421 K=1,14
```

```
0313              DO 220 NCN=1,3,2
0314              IF(K.EQ.Q11)SUM17(NCN)=SUM18(NCN)+BC(NCN,K)*2.0
0315            220 CONTINUE
0316            421 CONTINUE
0317              R(J,11)=Q11+1
0318            511 I11=R(J,11)
0319             50 DO 10 Q10=I11,5
0320              DO 420 K=1,14
0321              DO 219 NCN=1,3,2
0322              IF(K.EQ.Q10)SUM16(NCN)=SUM17(NCN)+BC(NCN,K)*2.0
0323            219 CONTINUE
0324            420 CONTINUE
0325              R(J,10)=Q10+1
0326            510 I10=R(J,10)
0327             49 DO 9 Q9=I10,6
0328              DO 419 K=1,14
0329              DO 218 NCN=1,3,2
0330              IF(K.EQ.Q9) SUM15(NCN)=SUM16(NCN)+BC(NCN,K)*2.0
0331            218 CONTINUE
0332            419 CONTINUE
0333              R(J,9)=Q9+1
0334            509 I9=R(J,9)
0335             48 DO 8 Q8=I9,7
0336              DO 418 K=1,14
0337              DO 217 NCN=1,3,2
0338              IF(K.EQ.Q8)SUM14(NCN)=SUM15(NCN)+BC(NCN,K)*2.0
0339            217 CONTINUE
0340            418 CONTINUE
0341              R(J,8)=Q8+1
0342            508 I8=R(J,8)
0343             47 DO 7 Q7=I8,8
0344              DO 417 K=1,14
0345              DO 216 NCN=1,3,2
0346              IF(K.EQ.Q7) SUM13(NCN)=SUM14(NCN)+BC(NCN,K)*2.0
0347            216 CONTINUE
0348            417 CONTINUE
0349              R(J,7)=Q7+1
0350            507 I7=R(J,7)
0351             46 DO 6 Q6=I7,9
0352              DO 416 K=1,14
0353              DO 215 NCN=1,3,2
0354              IF(K.EQ.Q6) SUM12(NCN)=SUM13(NCN)+BC(NCN,K)*2.0
0355            215 CONTINUE
0356            416 CONTINUE
0357              R(J,6)=Q6+1
0358            506 I6=R(J,6)
0359             45 DO 5 Q5=I6,10
0360              DO 415 K=1,14
0361              DO 214 NCN=1,3,2
0362              IF(K.EQ.Q5) SUM11(NCN)=SUM12(NCN)+BC(NCN,K)*2.0
0363            214 CONTINUE
0364            415 CONTINUE
0365              R(J,5)=Q5+1
0366            505 I5=R(J,5)
0367             44 DO 4 Q4=I5,11
0368              DO 414 K=1,14
0369              DO 213 NCN=1,3,2
0370              IF(K.EQ.Q4) SUM10(NCN)=SUM11(NCN)+BC(NCN,K)*2.0
0371            213 CONTINUE
0372            414 CONTINUE
0373              R(J,4)=Q4+1
0374            504 I4=R(J,4)
0375             43 DO 3 Q3=I4,12
0376              DO 413 K=1,14
0377              DO 212 NCN=1,3,2
0378              IF(K.EQ.Q3)SUM9(NCN)=SUM10(NCN)+BC(NCN,K)*2.0
0379            212 CONTINUE
0380            413 CONTINUE
0381              R(J,3)=Q3+1
0382            503 I3=R(J,3)
0383             42 DO 2 Q2=I3,13
0384              DO 412 K=1,14
0385              DO 211 NCN=1,3,2
0386              IF(K.EQ.Q2) SUM8(NCN)=SUM9(NCN)+BC(NCN,K)*2.0
0387            211 CONTINUE
0388            412 CONTINUE
0389              R(J,2)=Q2+1
0390            502 I2=R(J,2)
0391             41 DO 1 Q1=I2,14
0392              DO 411 K=1,14
0393              DO 210 NCN=1,3, 2
0394              IF (K .EQ.Q1) SUM7(NCN) = SUM8(NCN) + BC(NCN,K)*2.0
0395              IF(K.NE.Q1) GO TO 1000
0396            210 CONTINUE
0397              DO 900 NCN=1,3,2
0398              SUM(NCN)=PRESM(NCN)-SUM7(NCN)
0399            900 CONTINUE
                C          THE LOCAL MAGNETIC FIELD CONTRIBUTION PARALLEL TO THE EXTERNAL
                C          MAGNETIC FIELD IS CALCULATED    CONMG = H loc||
0400              CONMG=SUM(3)*COS(TX)+SUM(1)*SIN(TX)
                C          1500.5 IS ADDED TO H loc|| SO THAT IT CAN BE STORED WITHIN AN
                C          ARRAY OF POSITIVE INTEGERS A(IIH,J) J = NO. OF SPINS DOWN
                C          IIH = CONMG + 1500.5
0401              IIH=CONMG+1500.5
                C          THE OCCURRENCE OF EACH FIELD IIH IS THE QUANTITY STORED IN THE
                C          ARRAY A. IN OTHER WORDS A(IIH,J) IS THE DISTRIBUTION OF POSSIBLE
                C          LOCAL FIELDS FOR A GIVEN VALUE OF J (J BEING THE NUMBER OF
                C          SPINS TURNED DOWN)
```

```
0402              A(IIH,J)=A(IIH,J)+1
0403            1000 CONTINUE
0404             411 CONTINUE
0405               1 CONTINUE
0406                 IF(J.EQ.1) GO TO 200
0407               2 CONTINUE
0408                 IF(J.EQ.2) GO TO 200
0409               3 CONTINUE
0410                 IF(J.EQ.3) GO TO 200
0411               4 CONTINUE
0412                 IF(J.EQ.4) GO TO 200
0413               5 CONTINUE
0414                 IF(J.EQ.5) GO TO 200
0415               6 CONTINUE
0416                 IF(J.EQ.6) GO TO 200
0417               7 CONTINUE
0418                 IF(J.EQ.7) GO TO 200
0419               8 CONTINUE
0420                 IF(J.EQ.8) GO TO 200
0421               9 CONTINUE
0422                 IF(J.EQ.9) GO TO 200
0423              10 CONTINUE
0424                 IF(J.EQ.10) GO TO 200
0425              11 CONTINUE
0426                 IF(J.EQ.11) GO TO 200
0427              12 CONTINUE
0428                 IF(J.EQ.12) GO TO 200
0429              13 CONTINUE
0430                 IF(J.EQ.13) GO TO 200
0431             200 CONTINUE
0432                 DO 995 KBB=1,2991,10
                C        A(IHH,J) CAN BE SUMMED OVER J AT THIS POINT TO PRODUCE THE
                C        STATIC DIPOLAR BROADENED LOCAL MAGNETIC FIELD DISTRIBUTION.
                C        IN ORDER TO SHORTEN THE COMPUTATION TIME IN THE AVERAGING OF THE
                C        LOCAL FIELDS WHICH FOLLOWS THE 3000G DOMAIN OF VALUES IS REDUCED
                C        TO 300 VALUES BY SUMMING OVER INTERVALS OF 10G FOR EACH
                C        VALUE OF J.    BB(KAA,J) =    A(KBB+α,J)
                C                  KBB = 1,2991,10   =0
                C                  KAA = (KBB+9)/10
0433                 K1=KBB+1
0434                 K2=KBB+2
0435                 K3=KBB+3
0436                 K4=KBB+4
0437                 K5=KBB+5
0438                 K6=KBB+6
0439                 K7=KBB+7
0440                 K8=KBB+8
0441                 K9=KBB+9
0442                 KAA=(KBB+9)/10
0443                 BB(KAA,J)=A(KBB,J)+A(K1,J)+A(K2,J)+A(K3,J)+A(K4,J)
                    *+A(K5,J)+A(K6,J)+A(K7,J)+A(K8,J)+A(K9,J)
0444             995 CONTINUE
0445             101 CONTINUE
0446                 WRITE(6,992)
                C        THE SYMBOL 'AB' IS WRITTEN EACH TIME THIS IS CARRIED OUT, AS
                C        A MARKER.
0447             992 FORMAT (' AB')
0448             700 CONTINUE
                C        FINALLY THE AVERAGING FOR THE MOTIINAL NARROWING IS CALCULATED.
0449                 DO 913 IIIHH=1,3000
0450                 EMN(IIIHH)=0.0
0451             913 CONTINUE
0452                 DO 931 IMN=1,13
0453                 DO 932 JMN=1,13
0454                 DO 919 IH=1,300
                C        THE CENTRE OF THE DISTRIBUTION IS SHIFTED FROM 150 BACK TO 0
                C        HI = IH - 150 , HHI = IHH - 150
0455                 HI = IH - 150
0456                 IF(BB(IH,IMN).EQ.0.0) GO TO 919
0457                 DO 912 IHH=1,300
0458                 HHI = IHH - 150
0459                 IF(BB(IHH,JMN).EQ.0.0) GO TO 912
0460                 IF(JMN.LT.IMN) GO TO 9164
                C        THE AVERAGE FIELD IS CALCULATED AND THE CENTRE OF THE
                C        DISTRIBUTION PLACED AT 150 AGAIN (AS NEGATIVE INDICES ARE NOT
                C        ALLOWED IN THE COMPUTING)  IHHH = H     + 150
0461                 IHHH = (HI + HHI*SMNPG(IMN,JMN))/SSMNPG(IMN,JMN) +150
0462                 GO TO 9165
0463              9164 IHHH = (HI + HHI*SMNPG(JMN,IMN))/SSMNPG(JMN,IMN) +150
0464              9165 CONTINUE
                C        THE CONTRIBUTION TO THE DISTRIBUTION IS CALCULATED AND ADDED
                C        TO THE RUNNING TOTAL
                C        EMN(IHHH) = BB(IH,IMN)*BB(IHH,JMN) + EMN(IHHH)
0465                 EMN(IHHH) = BB(IH,IMN)*BB(IHH,JMN)+EMN(IHHH)
0466             912 CONTINUE
0467             919 CONTINUE
0468             932 CONTINUE
0469             931 CONTINUE
0470                 DO 996 IHHH=1,300
                C        THE DISTRIBUTION IS DIVIDED BY 16382 SO THAT ITS AREA IS THE
                C        SAME AS THE STATIC ONE.  EEMN = EMN/16382.0
0471                 EEMN(IHHH)=EMN(IHHH)/16382.0
                C        THE VALUES OF THE DISTRIBUTION EEMN(IHHH), IHHH ARE WRITTEN OUT
0472                 WRITE(6,989)EEMN(IHHH),IHHH
0473             989 FORMAT(1H ,1F20.8,1I20)
0474             996 CONTINUE
0475            8889 CONTINUE
0476            7570 CONTINUE
0477                 STOP
0478                 END
```

A3 Line Broadening Program

Summary

This program calculates all the possible local magnetic fields due to 14 neighbouring ions thereby producing the distribution of local fields for static dipolar broadening. It also calculates the distribution when motional narrowing is taken into consideration using the fields calculated in the first part as a basis for this further calculation.

The program begins by specifying the crystal lattice dimensions, ion positions and calculates the interionic distances required.

AR = a_0

DR = c_0

X(I,J) = the Ith component of the Jth neighbour

The parameters for narrowing are specified here.

PMN = p

WDTFAC = N

The factorials 1! → 14! are calculated

ZFF(NNNNM) = FACTORIAL OF NNNNM (1 → 14)

As 0 is an invalid index it is necessary to manipulate k in order that it is represented as non-zero in all instances and also to define 0! as 1

JMN = j

IMN = i

KMN = k

NMN = n

IMK = i-k

JMIPK = (j-i)+k

NMJPK = n - (j+k)

NMI = n-i

MN(IMN,JMN,KMNA) = $N_{ij}(k)$

This section calculates the probabilities for configuration type changes. The calculation of MN is done in two parts as K has two restrictions applying to it. The summation over k is next carried out in two steps:

1. IMN $\leqslant$ JMN,
2. IMN > JMN.

$$SMNK(IMN,JMN) = \sum_{KMNA} MN(IMN,JMN,KMNA)$$

$$= \Sigma\ N_{ij}(k)$$

The next calculation is that of GMN(IMN,JMN,KMNA) and again is done in two parts KMNA being subject to the two conditions $k \leqslant i$, $k \leqslant n-j$.

$$= \frac{N_{ij}(k)}{\sum_{k} N_{ij}(k)}$$

The next section calculates the average probability. The values of

$$SMNPG(IMN,JMN) = P_{ij}$$

are calculated for all i,j ($1 \leqslant i \leqslant j \leqslant n$).

$$= \sum_{k} p_{ij}(k) \times GMN$$

Finally the divisor in the average probability is calculated and also multiplied by N.

$$SSMNPG(IMN,JMN) = (1.0 + P_{ij})N$$

The values of

$$SMNPG(IMN,JMN),IMN,JMN$$

are written out.

The possible local fields at particular orientations are calculated next.

The orientations are specified and are written out under the heading NT = θ ANGLE.

The local magnetic fields are calculated by firstly obtaining the local field with all spins up and subsequently subtracting suitable amounts.

NCN specifies component

K specifies atom

$M(1) = \mu\frac{g_\perp}{2} \sin\theta$

$M(3) = \mu\frac{g_\parallel}{2} \cos\theta$

The distance to atom k is calculated

$SA(K) = |r_k|$

$S3(K) = |r_k|^3$

$S5(K) = |r_k|^5$

PRESM(NCN) is the local field with all spins up and is calculated for 14 neighbours.

The amounts to be subtracted are calculated in a set of nexted 'do loops'. The nest can be entered at any point, and exits after the loops interior to the one at which it was entered, have been executed. The number of interior loops is equal to the number of spins down.

Entering the innermost loop turns down each of the 14 spins in succession. Entering the second to innermost loop turns down all combinations of two spins, and so on for greater numbers of loops.

The spins which are down are labelled by the QI and in each loop there are two subloops by which each of the possible contributing ions is tested to see if it is QI and if so the components of its dipolar interaction BC(NCN,K) are doubled and added to the sum (nearing adjacent to the loops) SUMJ(NCN) which is subtracted from PRESM(NCN) obtaining H_{loc}.

$$SUM(NCN) = H_{loc}.$$

The local field contribution parallel to the magnetic field is calculated. 1500.5 is added to $H_{loc_{||}}$ so that it can be stored within an array of positive integers

$$CONMG = H_{loc_{||}}.$$

$$IIH = CONMG + 1500.5$$

$$A(IIH,J) \quad J = \text{No. of spins down.}$$

The occurrence of each field IIH is the quantity stored in the array A. In other words A(IIH,J) is the distribution of possible local fields for a given value of J (J being the number of spins turned down). H(IIH,J) can be summed over J at this point to produce the static dipolar broadened local magnetic field distribution. In order to shorten the computing time in the averaging of the local fields which follows the 3000G domain of values is reduced to 300 values by summing over intervals of 10 for each value of J.

$$BB(KAA,J) = \sum_{\alpha=0}^{9} A(KBB+\alpha,J)$$

$$KBB = 1,2991,10$$

$$KAA = (KBB+9)/10$$

The symbols AB are written each time. This is carried out to act as a marker.

Finally the averaging for the motional narrowing is calculated.

The centre of the distribution is shifted from 150 back to 0

$$HI = IH - 150$$

$$HHI = IHH - 150$$

The average field is calculated and the centre of the distribution placed at 150 again (as negative indices are not allowed in the computing).

$$IHHH = H_{av_{ij}} + 150$$

The contribution to the distribution is calculated and added to a running total.

$$EMN(IHHH) = BB(IH,IMN)*BB(IHH,JMN) + EMN(IHHH)$$

The distribution is divided by 16382 so that its area is the same as that of the static one.

$$EEMN = \frac{EMN}{16382.0}$$

The values of the distribution are written out.

EEMN(IHHHH), IHHH

APPENDIX B1

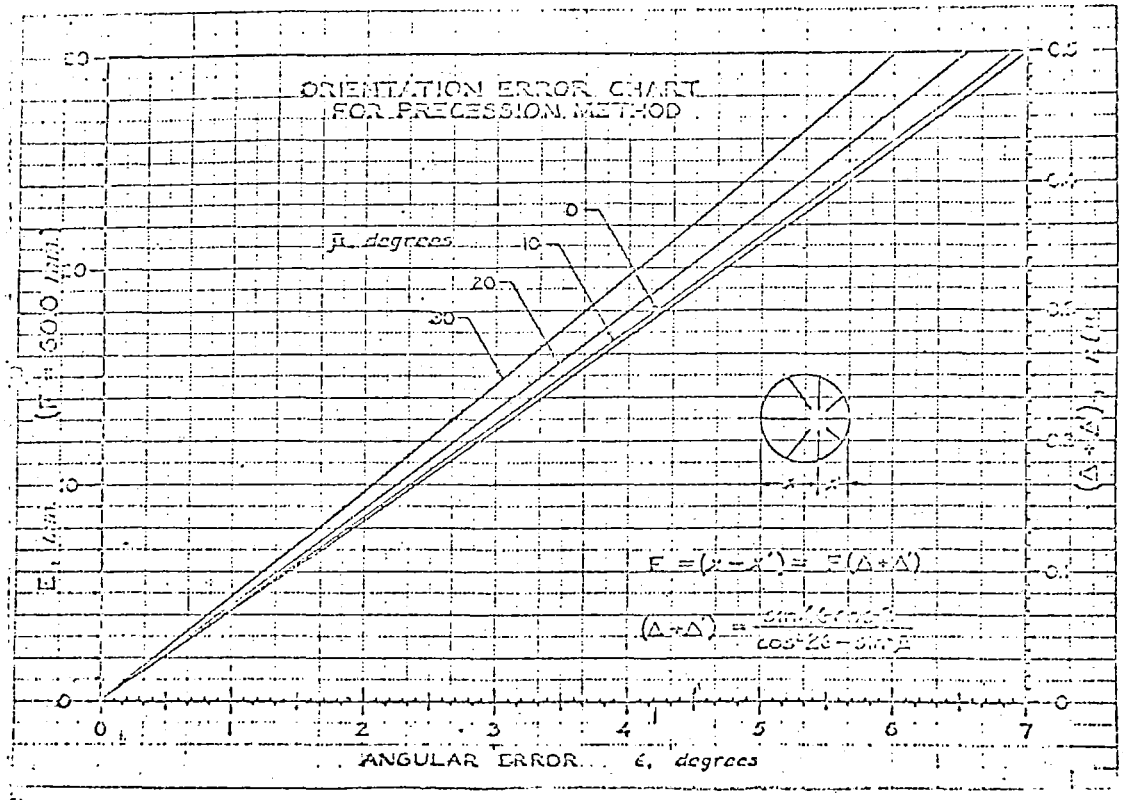

PRECESSION PHOTOGRAPHS – Correcting orientation errors

Setting photographs should be taken of zero reciprocal lattice layers with unfiltered radiation and an angle of tilt equal to 7°. It is useful to have the goniometer axes perpend. ular and parallel to the film when the angle of tilt is set equal to zero degrees. All corrections to the spindle dial setting MUST be made with zero angle of tilt.

Errors in the spindle dial setting are indicated by 2 x vertical displacement (= E_V) of the edge of the circular field from the central position.

Errors in the goniometer axe perpendicular to the film are indicated by 2x horizontal displacement (=$E_{||}$) of the edge of the circular field from the central position.

Correction angles ϵ_{sp} and $\epsilon_{\perp}$ are determined graphically from E_V and $E_{||}$.

Directions for the different correction rotations according to field centre positions are given below. The film is viewed from the collimator side of the instrument so that these diagrams are equally applicable to wet film and polaroid films.

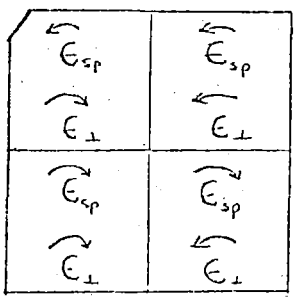

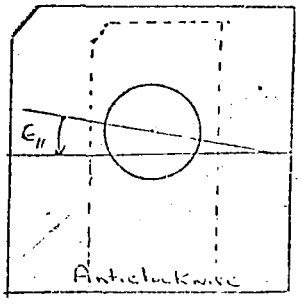

Errors in the goniometer axe parallel to the film ($\epsilon_{||}$) are measured directly on the angle bar horizontal axis (marked minute direction) and the row line it is desired [illegible] axis direction. An example is given in the right hand diagram above. [illegible] it is best to turn the spindle through 90° so that it becomes the [illegible]

APPENDIX B2

$PrCl_3$ - Hexagonal crystal

Direct Cell Parameters

A	B	C	α	β	γ	VOLUME
7.423	4.272	4.272	90.0°	90.0°	120.0°	203.855

Reciprocal Cell Parameters

A*	B*	C*	α*	β*	γ*	VOLUME
0.1555	0.1555	0.2341	90.0°	90.0°	60.0°	0.004905

Linear Absorption Coefficients

Z	DENSITY	CU K(α)	MO K(α)	CO K(α)	F(000)
1	2.01	508.35	68.25	708.25	110
2	4.03	1016.70	136.50	1416.50	220
3	6.04	1525.06	204.75	2124.75	330
4	8.06	2033.41	273.00	2833.00	440
6	12.08	3050.11	409.50	4249.50	660
8	16.11	4066.82	546.00	5666.00	880

Bragg Angles and FD* Distances for Films from precession cameras with F = 60 mm

		CU K(α)		MD K(α)	
NO.	PLANE	FD*(MM)	θ	FD*(MM)	θ
1	(1 0 0)	14.4	6.89	6.6	3.17
2	(0 1 0)	14.4	6.89	6.6	3.17
3	(0 0 1)	21.7	10.40	10.0	4.77
4	(0 1 1)	26.0	12.51	12.0	5.73